REDUCING THE ENERGY DEMAND OF BIOETHANOL THROUGH SALT EXTRACTIVE
DISTILLATION ENABLED BY ELECTRODIALYSIS

by

MOHAMMED HUSSAIN

B.Tech., Madurai Kamaraj University, 2002
M.S., University of North Dakota, 2007

AN ABSTRACT OF A DISSERTATION

submitted in partial fulfillment of the requirements for the degree

DOCTOR OF PHILOSOPHY

Department of Chemical Engineering
College of Engineering

KANSAS STATE UNIVERSITY
Manhattan, Kansas

2011

Abstract

The expanded Renewable Fuel Standard (RFS2), established under the Energy Independence and Security Act (EISA) of 2007, mandates the production of 136.3 GL/year of renewable fuels in the U.S. in 2022: 56.8 GL/year of corn-ethanol, 60.6 GL/year of second generation biofuels such as cellulosic ethanol, and 18.9 GL/year of advanced biofuels such as biomass-based diesel. One of the several challenges when a biochemical conversion technique is used to produce bioethanol from corn and cellulosic feedstock is the high energy demand for recovering and purifying ethanol, which is mainly due to the low concentration of ethanol in the fermentation broth and the challenging water-ethanol vapor liquid equilibrium.

Dilute ethanol from the fermentation broth can be separated and concentrated aided by salt extractive distillation to directly produce fuel ethanol leading to significant energy savings. Techniques other than highly energy intensive evaporative salt concentration/crystallization and solids drying for recovering salt, which is used to facilitate distillation, have rarely been considered. In this study, a novel combination of electrodialysis and spray drying was investigated to recover the salt. Salt extractive distillation – with salt recovery enabled by electrodialysis – was conceptually integrated in the fermentation broth-ethanol separation trains of corn and cellulosic ethanol facilities and investigated through process simulation with Aspen Plus® 2006.5 to reduce the recovery and purification energy demand of bioethanol.

Experiments for the electrodialytic concentration of calcium chloride from high diluate concentrations, prevalent in the salt recovery process when calcium chloride is used as the salt separating agent in the salt extractive distillation of bioethanol, were carried out to determine the fundamental transport properties of an ion exchange membrane pair comprising commercially available membranes for implementation in the conceptual process designs. The maximum calcium chloride concentration achievable through electrodialytic concentration is 34.6 wt%, which is mainly limited by the water transport number.

In case of corn-ethanol, retrofitted salt extractive distillation resulted in an energy demand reduction of about 20% and total annual cost savings on the order of MM$0.5 per year when compared with the state-of-the-art rectification/adsorption process for producing fuel ethanol from the beer column distillate. In case of cellulosic ethanol, salt extractive distillation with direct vapor recompression provided the highest energy savings of about 22% and total

annual cost savings on the order of MM$2.4 per year when compared with the base case comprising conventional distillation and adsorption for recovering and purifying ethanol from the fermentation broth.

Based on the conceptual process design studies, an overall maximum energy savings potential of $1.5*10^{17}$ J or about 0.14 Quad (as natural gas higher heating value) per year could be estimated for the targeted 56.8 GL of corn-ethanol and 60.6 GL of cellulosic ethanol to be produced in the U.S in 2022 when salt extractive distillation enabled by electrodialysis is implemented in the fermentation broth-ethanol separation trains of the corn and cellulosic ethanol facilities.

REDUCING THE ENERGY DEMAND OF BIOETHANOL THROUGH SALT EXTRACTIVE
DISTILLATION ENABLED BY ELECTRODIALYSIS

by

MOHAMMED HUSSAIN

B.Tech., Madurai Kamaraj University, 2002
M.S., University of North Dakota, 2007

A DISSERTATION

submitted in partial fulfillment of the requirements for the degree

DOCTOR OF PHILOSOPHY

Department of Chemical Engineering
College of Engineering

KANSAS STATE UNIVERSITY
Manhattan, Kansas

2011

Approved by:

Major Professor
Dr. Peter H. Pfromm

Copyright

MOHAMMED HUSSAIN

2011

Abstract

The expanded Renewable Fuel Standard (RFS2), established under the Energy Independence and Security Act (EISA) of 2007, mandates the production of 136.3 GL/year of renewable fuels in the U.S. in 2022: 56.8 GL/year of corn-ethanol, 60.6 GL/year of second generation biofuels such as cellulosic ethanol, and 18.9 GL/year of advanced biofuels such as biomass-based diesel. One of the several challenges when a biochemical conversion technique is used to produce bioethanol is the high energy demand for recovering and purifying ethanol, which is mainly due to the low concentration of ethanol in the fermentation broth and the challenging water-ethanol vapor liquid equilibrium.

Dilute ethanol from the fermentation broth can be separated and concentrated aided by salt extractive distillation to directly produce fuel ethanol leading to significant energy savings. Techniques other than highly energy intensive evaporative salt concentration/crystallization and solids drying for recovering salt, which is used to facilitate distillation, have rarely been considered. In this study, a novel combination of electrodialysis and spray drying was investigated to recover the salt. Salt extractive distillation – with salt recovery enabled by electrodialysis – was conceptually integrated in the fermentation broth-ethanol separation trains of corn and cellulosic ethanol facilities and investigated through process simulation with Aspen Plus® 2006.5 to reduce the recovery and purification energy demand of bioethanol.

Experiments for the electrodialytic concentration of calcium chloride from high diluate concentrations, prevalent in the salt recovery process when calcium chloride is used as the salt separating agent in the salt extractive distillation of bioethanol, were carried out to determine the fundamental transport properties of an ion exchange membrane pair comprising commercially available membranes for implementation in the conceptual process designs. The maximum calcium chloride concentration achievable through electrodialytic concentration is 34.6 wt%, which is mainly limited by the water transport number.

In case of corn-ethanol, retrofitted salt extractive distillation resulted in an energy demand reduction of about 20% and total annual cost savings on the order of MM$0.5 per year when compared with the state-of-the-art rectification/adsorption process for producing fuel ethanol from the beer column distillate. In case of cellulosic ethanol, salt extractive distillation with direct vapor recompression provided the highest energy savings of about 22% and total

annual cost savings on the order of MM\$2.4 per year when compared with the base case comprising conventional distillation and adsorption for recovering and purifying ethanol from the fermentation broth.

Based on the conceptual process design studies, an overall maximum energy savings potential of $1.5*10^{17}$ J or about 0.14 Quad (as natural gas higher heating value) per year could be estimated for the targeted 56.8 GL of corn-ethanol and 60.6 GL of cellulosic ethanol to be produced in the U.S in 2022 when salt extractive distillation enabled by electrodialysis is implemented in the fermentation broth-ethanol separation trains of the corn and cellulosic ethanol facilities.

Table of Contents

List of Figures

List of Tables

Acknowledgements

I would like to take this opportunity to express my deepest thankfulness to my advisor, Dr. Peter Pfromm, for his invaluable guidance, support, and patience during my doctoral study. I would also like to thank the members of my advisory committee, Dr. John Schlup, Dr. Stefan Bossmann, Dr Jennifer Anthony, and Dr. Richard Nelson for their valuable suggestions and guidance, and for taking time to serve on the committee. I am also grateful to Dr. Mary Rezac for her support and guidance.

I would like to thank the former and current members of the research group especially Devinder Singh, Juan Cruz, Mandeep Kular, and Neha Dhiman for their support and pleasant time spent at the lab.

I also like to express my deepest gratitude to my father, Mahaboob Hussain; my mother, Rahamathunisa; and my brothers, Kadar and Rahman for their endless appreciation and support during my studies.

No words will suffice to express my gratitude to the love of my life, Shirin Naderipour, for her endless love, encouragement, and patience which helped me tide over tough times.

Finally, I would like to thank the Almighty Lord for making this work possible by giving me the strength and passion.

Chapter 1 - Introduction and background

1.1 Research motivation

Currently, corn-ethanol is the most widely produced biofuel in the U.S.[1] The expanded Renewable Fuel Standard (RFS2), established under the Energy Independence and Security Act (EISA) of 2007, mandates the production of 136.3 GL/year of renewable fuels in the U.S. in 2022: 56.8 GL/year of corn-ethanol, 60.6 GL/year of second generation biofuels such as cellulosic ethanol, and 18.9 GL/year of advanced biofuels such as biomass-based diesel.[1] Dry milling is currently the most widely used process in the U.S for producing fuel ethanol from corn by fermentation. Similar to corn-ethanol, fermentation can be used to produce fuel ethanol from cellulosic feedstock.[2-9] Recovering ethanol from fermentation broth and purifying it to fuel grade is difficult and energy intensive because of the dilute nature of the fermentation broth and the challenging water-ethanol vapor liquid equilibrium (VLE) with an azeotrope at about 96 wt% ethanol. Simple distillation cannot be used to distill ethanol above the azeotropic composition. The state-of-the-art technique used in the fuel ethanol industry to produce fuel ethanol is distillation close to the azeotropic composition followed by dehydration in a molecular sieve-based adsorption unit.[10-13] The ethanol concentration in the fermentation broth varies from about 10 to 15 wt% for corn-ethanol[10, 11, 14-16] compared to about 3 to 6 wt% for cellulosic ethanol.[2-9] In case of corn-ethanol, recovering and purifying ethanol from fermentation broth requires about 70 % of the total steam generated in the dry milling plant.[17] While the separation energy demand for corn-ethanol is high, the separation energy demand for cellulosic ethanol is even higher due to the drastic increase in the distillation energy demand with the decrease in the concentration of ethanol in the fermentation broth: 4.2 MJ/liter for 15 wt% ethanol (corn-ethanol) and 7 MJ/liter for 5 wt% ethanol (cellulosic ethanol) has been reported.[14] The lower heating value of pure ethanol is 21.2 MJ/liter.[18] Hence, it is essential to reduce the separation and purification energy demand to improve the possible economical and environmental advantages of bioethanol over fossil fuels.

Salt extractive distillation can be used to recover ethanol from the fermentation broth and directly purify it to fuel grade leading to significant energy savings.[14, 19-25]

Evaporation and drying are the most widely investigated techniques for recovering salt, which is used to facilitate the distillation.[19-22, 26-29] Since evaporative salt concentration/crystallization and solids drying techniques are energy intensive, reducing the energy demand for the salt recovery step becomes essential for reducing the overall energy demand. In this study, a novel scheme of electrodialysis and spray drying was investigated for recovering salt. The salt extractive column bottoms stream is pre-concentrated by electrodialysis followed by spray drying. In electrodialysis, the dilute salt solution is concentrated by selectively removing the salt ions from the solution rather than evaporating water; therefore, requiring less energy than an evaporative process. Final recovery of dry salt is achieved in a spray dryer.

1.2 Research objectives

This study focuses on the conceptual integration of salt extractive distillation, enabled by a novel scheme of electrodialysis and spray drying for salt recovery, in the water-ethanol separation trains of fermentation-based corn and cellulosic ethanol facilities for reducing the recovery and purification energy demand of bioethanol. This study will also focus on the experimental evaluation of electrodialysis to concentrate calcium chloride, which is used as the salt separating agent, at process conditions expected in the salt extractive distillation of bioethanol.

1.2.1 Conceptual process design

Initial conceptual process designs for the fermentation broth-ethanol separation train were developed and investigated for energy demand reduction and economic viability through process simulation and economic analysis with Aspen Plus® 2006.5 and Aspen Icarus Process Evaluator® 2006.5, respectively. Since there is already a large amount of installed capital for corn-ethanol facilities, improving the already existing process through retrofitting with salt extractive distillation was considered. Commercial development of cellulosic ethanol is in its incipient stages; hence, completely new design schemes implementing salt extractive distillation along with energy saving heat-integrated distillation operations were considered.

1.2.2 Electrodialysis experiments

The electrodialytic concentration of calcium chloride was experimentally studied to characterize the fundamental transport properties of an ion exchange membrane pair comprised of commercially available ion exchange membranes in high calcium chloride concentration conditions prevalent in the salt recovery process of salt extractive distillation. Finally, the experimentally derived features of electrodialysis were incorporated in the conceptual process designs to carry out the final economic analysis

1.3 Recovery and purification of ethanol from fermentation broth

1.3.1 Limitations of conventional distillation

Recovering ethanol from fermentation broth and purifying it to fuel grade is a difficult and energy intensive process. The recovery and purification energy demand is high mainly due to the dilute nature of the fermentation broth and the challenging water-ethanol vapor liquid equilibrium (VLE) with an azeotrope at about 96 wt% ethanol and tangential approach of the water-ethanol equilibrium curve to the 45° line at high ethanol concentrations in the y-x VLE diagram representation (Figure 1-1). Ethanol is more volatile than water, when the ethanol concentration in the liquid phase is below 96 wt%; therefore, ethanol gets concentrated in the vapor phase in this concentration range. However, when the ethanol concentration in the liquid phase increases to about 96 wt%, the relative volatility of ethanol decreases and finally becomes identical with that of water, and at this point further separation cannot be achieved. The azeotropic point can be shifted to higher compositions of ethanol by decreasing the pressure, and at about 10.6 kPa the azeotrope eventually disappears enabling the production of fuel grade ethanol (99.5 wt%) directly in a single distillation column.[30] However, low pressure distillation is not economical due to the high energy requirement.[30] The state of the art technique used in the fuel ethanol industry to produce fuel ethanol is distillation close to the azeotropic composition followed by dehydration in a molecular sieve-based adsorption unit.[10-13]
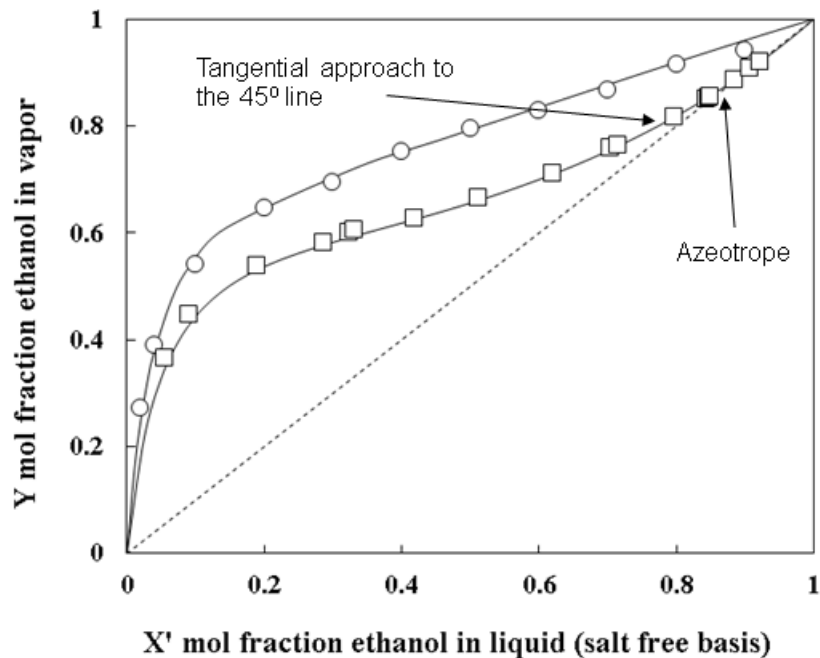
Figure 1-1. VLE curves for the water-ethanol-CaCl$_2$ and water-ethanol systems: (○) experimental data[31] with 16.7 wt% CaCl$_2$ liquid phase concentration (salt free basis) at 101.3 kPa, (solid line) calculated using Electrolyte Non-Random Two Liquid-Redlich Kwong (ENRTL-RK) property method; (□) experimental data[32] without salt at 101.3 kPa, (solid line) calculated using Non-Random Two Liquid-Redlich Kwong (NRTL-RK) property method.

1.3.2 "Salting out" effect

Dissolving a salt in a mixed solvent system containing two volatile and miscible solvents may alter the activities of the volatile components through liquid phase associations or through the alteration of the structure of the solvent mixture[26] When the dissolved salt associates more preferentially with one component, two different regions in the solution are formed: Ion region, enriched in the more attracted component, and the rest of the solution enriched in the less attracted component. Hence, the less attracted component is "salted out" from the ion regions. Since the volatility of the ion regions is substantially reduced by the electrostatic attraction field of the ions, the equilibrium vapor composition is mainly determined by the rest of the solution enriched in the less attracted component. Hence, the addition of salt changes the equilibrium vapor pressure,

4

even though the salt is not present in the vapor phase.[26] The VLE of the water-ethanol system can be improved towards ethanol separation by "salting out" to raise the equilibrium vapor ethanol content.[20, 26, 33, 34] In addition, this may also break the azeotrope.[20, 26, 35] Potassium acetate[21, 22, 25, 27-29, 35-37] and calcium chloride[19, 23, 24, 36, 37] have been reported for water-ethanol separation utilizing the "salting out" effect. The use of the salt separating agent in a process with tightly closed water cycles such as the bioethanol plant requires that the salt not impact other processing areas negatively. In this study, calcium chloride was selected as the salt separating agent for the following reasons: low cost, large "salting out" effect[36, 37] (Figure 1-1) and compatibility with fermentation.

1.3.3 Salt extractive distillation

Extractive distillation is used to separate azeotropes and other mixtures with low relative volatility, which are otherwise difficult to separate using regular distillation.[38] In extractive distillation, a high boiling liquid separating agent is used to alter the liquid phase activity coefficients of the mixture enabling the separation of the key components. In salt extractive distillation, a salt separating agent is used instead of the liquid separating agent. A salt separating agent is much more effective in altering the relative volatilities of the key components than the liquid separating agent; thereby requiring lower separating agent recovery and recycle capacity, and lower overall energy demand.[20] Figure 1-2 shows a typical flow sheet for salt extractive distillation. The salt is usually dissolved in the reflux stream and introduced at the top of the column. Unlike the liquid extractive agents such as ethylene glycol, salt is non volatile and always remains in the liquid phase; thereby, enabling the production of a high purity distillate free of salt. The salt moves downward in the column and is recovered and purified from the distillation column bottoms for re-use in the top of the column. Hence, there are two distinct steps involved: salt extractive distillation and salt recovery/purification. Corrosion due to aqueous ethanolic salt solutions requires consideration in regards to materials of construction.[19, 38] Other issues are related to solids handling, feeding and dissolving salt in the reflux stream, potential decrease in plate efficiency, and foaming inside the column.[20, 26, 35] In this study, the possible benefit in terms of energy demand is

established, demonstrating that the concept may be attractive enough to deal with the possible complications.
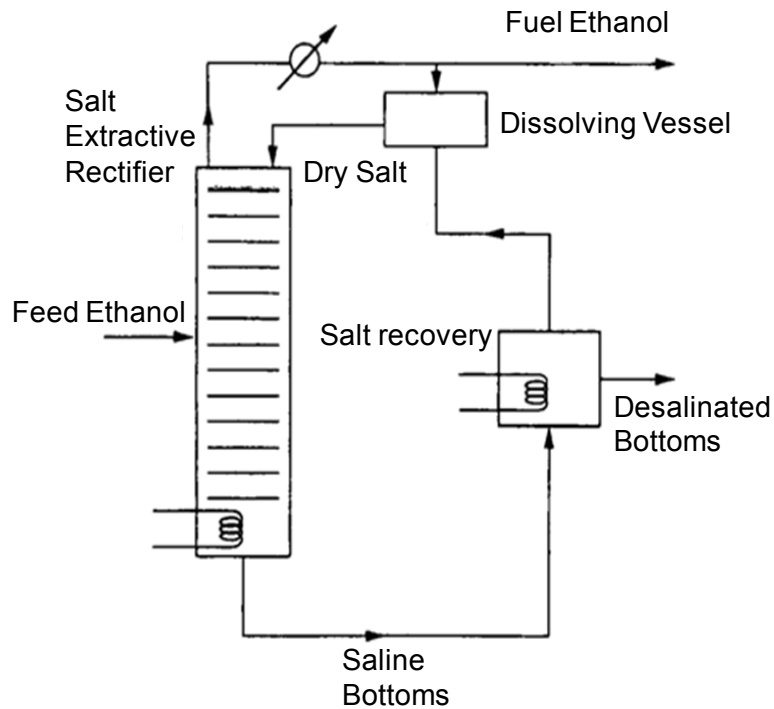
Figure 1-2. Process flow scheme for conventional salt extractive distillation. Adapted from Furter.[20]

1.3.4 Novel scheme for salt recovery

There are many experimental and theoretical studies[19, 21-25, 27-29, 35-37] on producing fuel ethanol by utilizing the "salting out" effect, but most of them focus only on the salt extractive distillation step. Moreover, the studies,[19-22, 26-29] which include both steps of salt extractive distillation and salt recovery, do not generally consider techniques other than evaporation and drying for salt recovery. Evaporative salt concentration/crystallization and solids drying techniques are energy intensive. Reducing the energy demand for the salt recovery step becomes essential to reap the benefit of salt-induced VLE improvement. Hence, a novel scheme of electrodialysis and spray drying for salt recovery is proposed in this study (Figure 1-3). The salt extractive column bottoms stream is pre-concentrated by electrodialysis and dried to an anhydrous state by spray drying. In electrodialysis, the dilute salt solution is concentrated by selectively separating the salt ions from the solution[39, 40] rather than evaporating water; therefore,

requiring less energy than that of an evaporative process. Final recovery of dry salt is achieved through spray drying, which is a widely used unit operation to convert a liquid feed containing salt into dry solid particles in a single step.[41, 42]
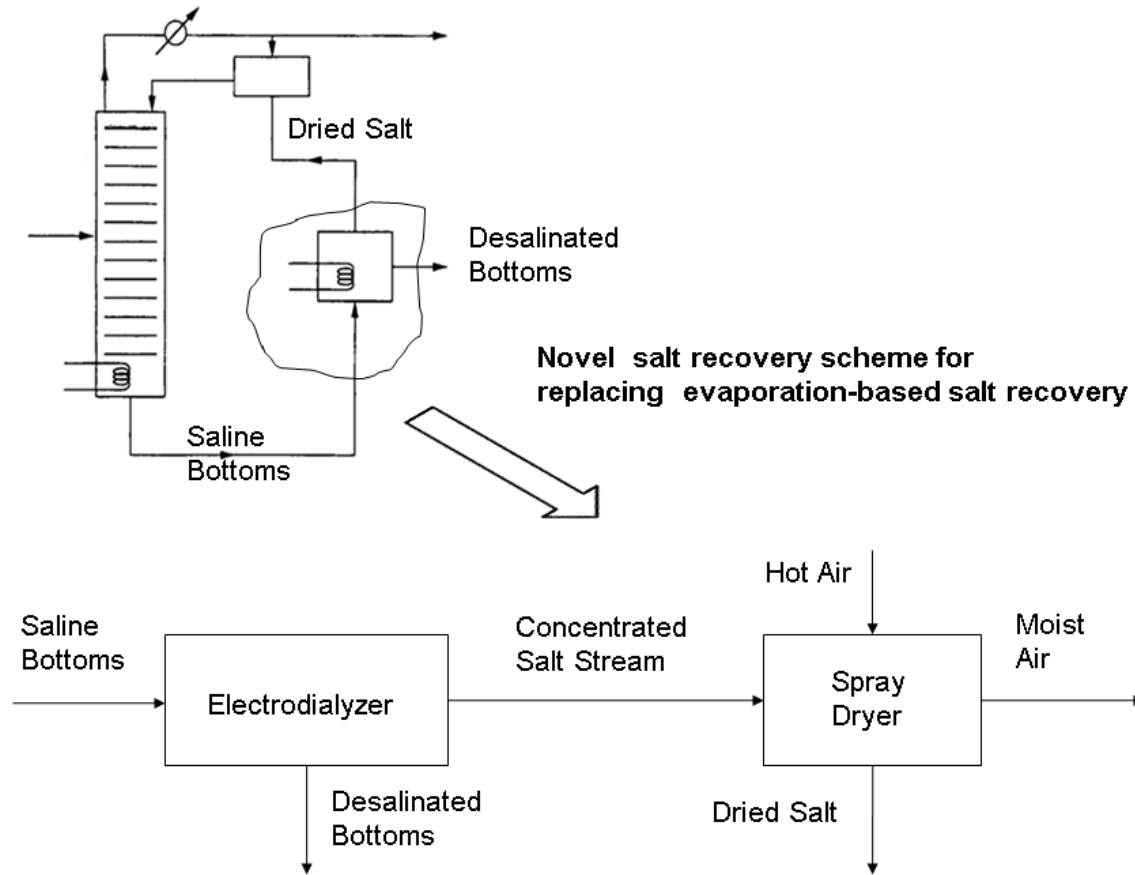
Figure 1-3. Novel process scheme of electrodialysis and spray dryer for salt recovery in salt extractive distillation.

1.4 Electrodialysis

1.4.1 Principle of operation

The working principle behind electrodialysis is illustrated in Figure 1-4. Cation exchange membranes (cem) and anion exchange membranes (aem) are arranged in an alternative fashion between the anode and cathode forming individual chambers of diluate and concentrate. When an electrolyte solution is circulated through the individual chambers and an electric potential is established, the electrolyte species in the solution migrate in the opposite directions: cations migrate towards the cathode, and anions

7

migrate towards the anode. Since the ion exchange membranes are selective to only one type of electrolyte species, cation exchange membrane is selective towards cations and anion exchange membrane is selective towards anions, there is a net transport of electrolyte species from the diluate chambers into the concentrate chambers resulting in the desalination of the diluate and concentration of the concentrate. The main industrial applications of electrodialysis include brackish water desalination, waste water treatment, sea water concentration, demineralization of food products such as cheese whey and skimmed milk, and deacidification of fruit juices.[39, 40, 43] Since electrodialysis is a separation process involving selective removal of salts rather than the energy intensive phase separation unit operations such as evaporation and crystallization, it is uniquely suited for the salt recovery in the salt extractive distillation process.
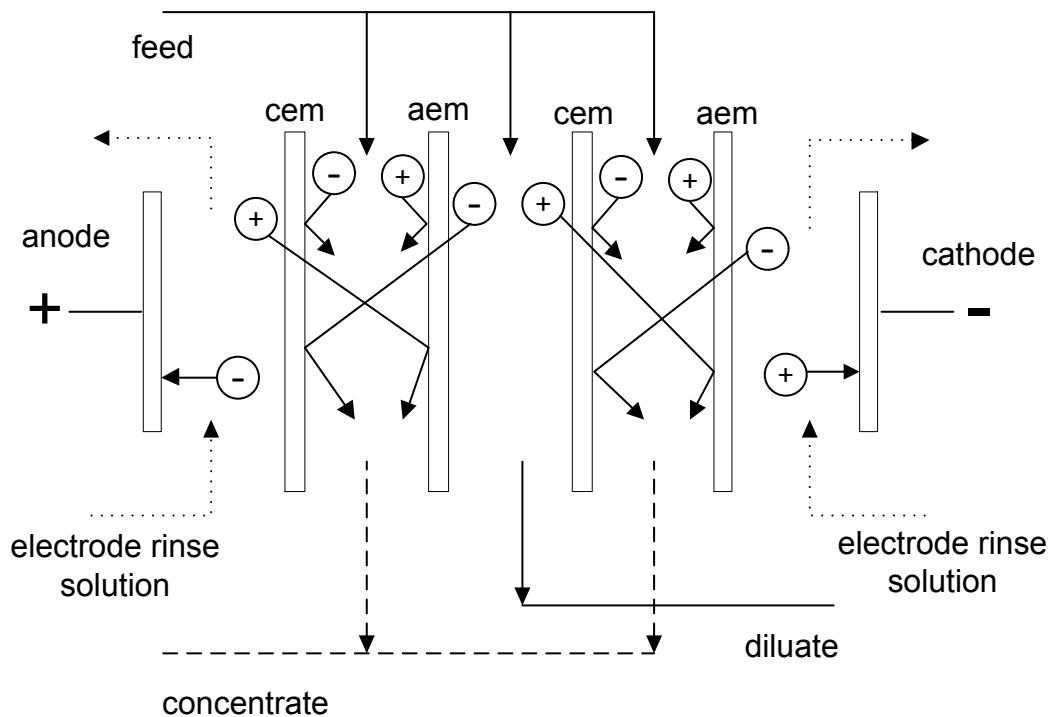
Figure 1-4. Principle of desalination in an electrodialysis stack. Adapted from Strathmann.[40]

1.4.2 Ion exchange membranes

The removal/concentration of salt in the electrodialysis process is accomplished principally through the selective nature of the ion exchange membranes. Ion exchange membrane is basically a functionalized polymer with affixed ionic groups, typically in a

8

sheet form.[39, 40] Ion exchange membranes can be classified based on their functional groups and structural properties. Based on the functional groups, ion exchange membranes can be classified mainly into two groups: cation exchange membrane and anion exchange membrane. Cation exchange membrane contains fixed anionic groups, $-SO_3^-$; $-COO^-$; $-PO_3^{2-}$; $-HPO_2^-$; $-AsO_3^{2-}$; $-SeO_3^-$, that allow the selective exchange and passage of cations from the external electrolyte, but exclude the anions. Contrarily, the anion exchange membrane contains fixed cationic groups, $-RNH_2^+$; $-R_3N^+$; $-R_2NH^+$; $-R_3P^+$; $-R_2S^+$, that allow the selective exchange and passage of anions from the external electrolyte, but exclude the cations.[40] The selective nature of the ion exchange membranes can be explained through the principle of Donnan exclusion.[40] Figure 1-5 shows the structure of a cation exchange membrane. Since the fixed charges in the polymer network are the anions, the mobile cations in the membrane matrix are referred to as counter ions, while the mobile anions in the membrane matrix are referred to as co-ions. When the ion exchange membrane is immersed in an external electrolyte solution, a perfectly selective membrane should completely exclude the co-ions. The effect of the external electrolyte solution concentration on the concentration of the different ionic species in the membrane is governed by the Donnan equilibrium. In case of a dilute solution of a monovalent electrolyte such as NaCl, the equilibrium co-ion concentration in the membrane phase can be described through the following equation:[44]

$$C^m_{co\ ion} = \left[\frac{C^2_{co\ ion}}{C^m_{fix}}\right]\left[\frac{\gamma_\pm}{\gamma^m_\pm}\right]^2 \qquad\qquad \text{Equation 1-1}$$

where C^m_{co-ion} is the concentration of co-ion in the membrane in *equivalent/cm³*; C_{co-ion}, concentration of co-ion in the electrolyte solution, *equivalent/cm³*; C^m_{fix}, concentration of fixed ions in the membrane, *equivalent/cm³*; $\gamma_\pm$, mean activity coefficient of the electrolyte in the external solution; and $\gamma^m_\pm$, mean activity coefficient of the electrolyte in the membrane phase. It can be clearly seen from Equation 1-1, that the co-ion exclusion, permselectivity of the membrane, increases with increasing fixed ion concentration in the membrane and decreasing external solution concentration. Furthermore, the other factors influencing the permselectivity of the membrane are the valence of the co-ions and the affinity of the ion exchange membrane to the counter ions.[40]
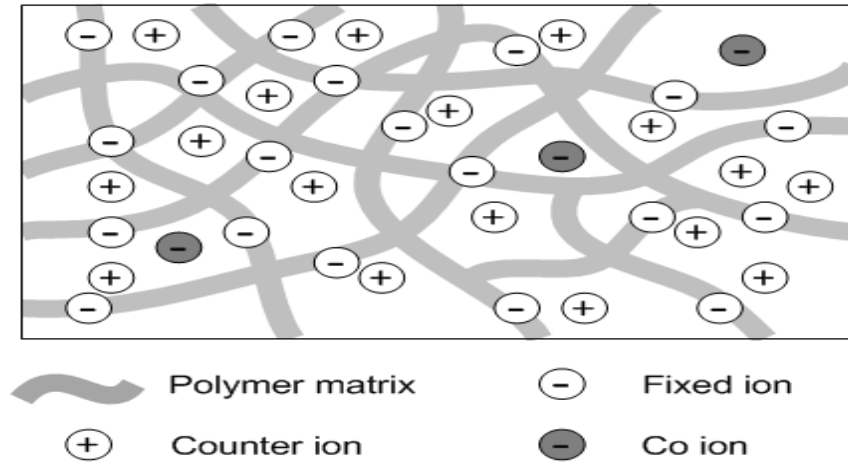
Figure 1-5. Structure of a homogeneous cation exchange membrane. Adapted from Strathmann.[40]

1.4.3 Transport processes in electrodialysis

During electrodialysis, there are several transport processes (Figure 1-6) occurring simultaneously: diffusion, osmosis, migration of counter ions and co-ions, and electroosmosis. When there is a concentration difference across the membranes, there is a diffusion of electrolyte from the concentrated stream to the dilute stream. In contrast, there is a transport of water from the dilute stream to the concentrated stream due to osmosis. Transport of the ions through the membrane is characterized by the ionic transport number, defined as follows:[40]

$$T_i \quad = \frac{z_i J_i}{\sum_i z_i J_i}$$

Equation 1-2

where T_i is the transport number; J_i, ionic flux, mol/m^2s; and z_i, valence of the ionic species i. Elecroosmosis occurs due to the transport of the water molecules along with the migrating ions through the membranes, which can be characterized by the water transport number:[40]

$$T_w \quad = \frac{J_w}{\sum_i J_i}$$

Equation 1-3

where T_w is the water transport number; J_i, ionic flux, mol/m^2s; and J_w, flux of water, mol/m^2s. Water transport number directly gives the number of water molecules

transported along with each ion through the membrane. The widely used method to study the transport phenomena in the ion exchange membranes is based on the Nernst-Planck equation, which relates the ionic flux to the local gradient of the electrochemical potential:[39, 45]

$$J_i = -C_i u_i \frac{d\mu_i}{dx} \qquad \text{Equation 1-4}$$

where C_i is the concentration of the ionic species i in mol/cm^3; u_i, ionic mobility cm^2/Vs; and μ_i, electrochemical potential, J/mol. The main advantage of the Nernst-Planck equation is the relative simplicity along with the requirement of very few parameters. However, this approach does not consider the interactions among the several permeating species through the membrane.[39, 40, 45] For instance, in a cation exchange membrane, the number of cations is higher than anions; thereby, cations while permeating through the membrane impart more momentum on the water molecules than the anions resulting in a net flow of water in the direction of the cations. This phenomenon is taken into consideration through a correction term in the extended Nernst-Planck equation:[39, 40, 45]

$$J_i = -C_i u_i \frac{d\mu_i}{dx} + C_i v \qquad \text{Equation 1-5}$$

where v is the flow velocity of the solvent in cm/s.

The coupling between the different fluxes in the membrane is described through phenomenological equations based on irreversible thermodynamics[46, 47] and frictional model of membrane transport.[48, 49] In the irreversible thermodynamics approach, for a system in which several forces and corresponding fluxes are involved, the relation between the fluxes and the forces can be expressed as a linear function when the system is near equilibrium:[45]

$$J_i = \sum_k L_{ik} X_k \qquad \text{Equation 1-6}$$

where L_{ik} are the phenomenological coefficients independent of the fluxes and forces, and X_k are the driving forces. For a system with n fluxes and forces, the number of phenomenological coefficients required equals to n^2. However, the number of coefficients required can be reduced to $n(n+1)/2$ through the Onsager's reciprocal relation. In the frictional model for membrane transport, the steady state transport processes are

described as the balances between the thermodynamic forces acting on the system and the frictional interactions between the system components as follows:[45]

$$X_i = \sum_k f_{ik} (v_i - v_k)$$

Equation 1-7

where f_{ik} are the frictional coefficients; v_i, v_k, velocity of the species, *m/s*. Similar to the phenomenological equations, the number of friction coefficients required to describe the transport properties is *n(n+1)/2*. The approaches based on phenomenological equations and frictional model provide a complete description of all the transport processes occurring in the membranes. However, they are complicated due to the requirement of a large number of transport coefficients.[40]
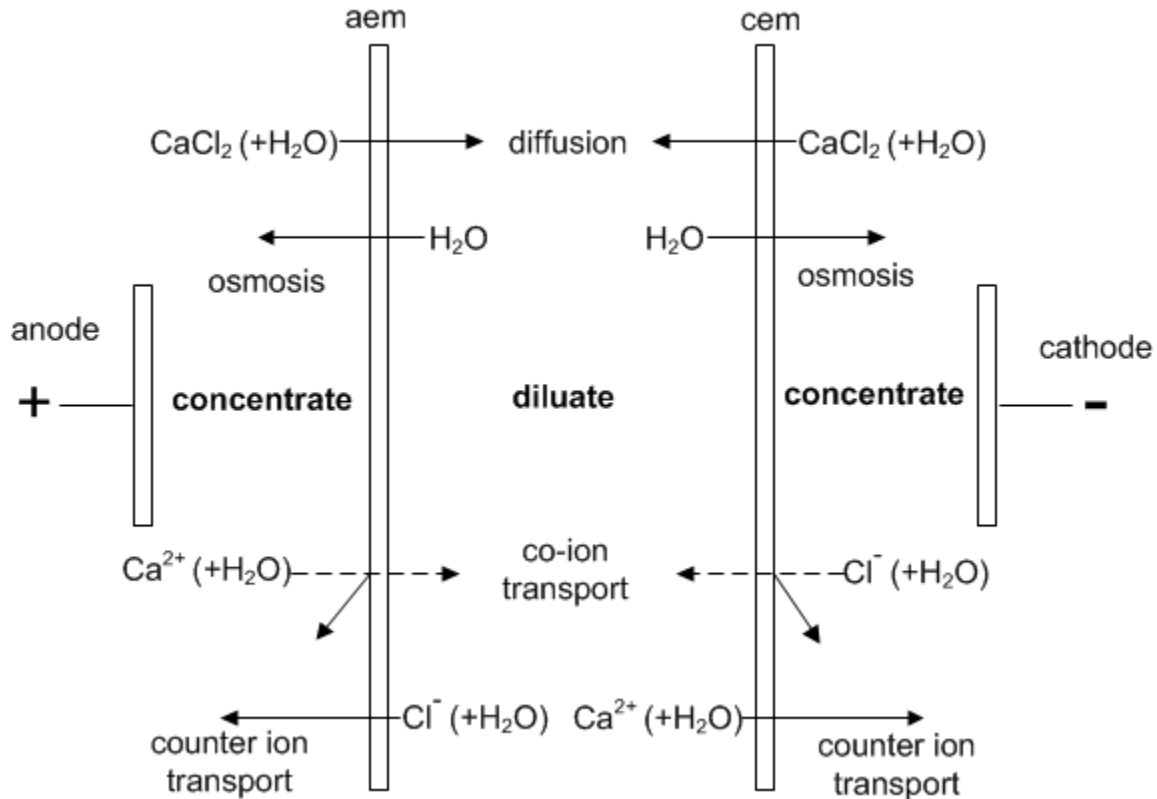
Figure 1-6. Schematic of simultaneous transport processes occurring during electrodialysis. Adapted from Mizutani et al.[50]

1.4.4 Electrodialysis for concentrating solutions

Based on the application of irreversible thermodynamics to electrodialysis,[51-55] the overall salt and water fluxes occurring through an ion exchange membrane pair during electrodialysis can be written as follows:[51, 54, 55]

$$j_s = \frac{\eta i}{ZF} - p_s \Delta C \qquad \text{Equation 1-8}$$

$$j_w = \frac{t_w i}{F} + p_w \Delta C \qquad \text{Equation 1-9}$$

$$\eta = T_c + T_a - 1 \qquad \text{Equation 1-10}$$

where j_s is the solute flux in $mol/m^2 s$; j_w, water flux, $mol/m^2 s$; η, current efficiency; T_c and T_a, cation and anion transport numbers, respectively; Z, ion valence, equivalent/mol; F, Faraday constant, 96485 *As/equivalent*; t_w, water transport number, *mol/F*; p_s, solute permeability, *m/s*; p_w, osmotic water permeability, *m/s*; and ΔC, solute concentration difference between the diluate and concentrate, mol/m^3. The above relations have been applied to describe the transport processes occurring during the electrodialytic concentration process for concentrations up to about 5M.[56-60] General conclusions can be drawn based on Equation 1-8 and Equation 1-9 regarding the factors affecting the electrodialytic concentration process. High current efficiencies can be obtained when the cation and anion transport numbers are high. However, as discussed in the earlier sections, Donnan exclusion decreases with the increase in the equilibrium electrolyte concentration which may result in lower current efficiencies. Further, the back diffusion of the solute from the concentrate to the diluate chamber increases with the increase in the solute concentration difference between the concentrate and the diluate, ΔC. The solute concentration in the concentrate can be obtained by combining Equation 1-8 and Equation 1-9:

$$C_{sc}^* = \frac{j_s}{j_s + j_w} = \frac{\frac{\eta i}{ZF} - p_s \Delta C}{\left[\frac{\eta}{Z} + t_w\right]\frac{i}{F} + [p_w - p_s]\Delta C} \qquad \text{Equation 1-11}$$

From the above equation, it can be seen that the most desirable characteristics of the ion exchange membranes to achieve high solute concentration in the concentrate are low solute and osmotic permeabilities, high ionic transport numbers, and low water

13

transport number. Ion exchange membranes with low water content and high fixed charge density can meet the above requirements.[61] In addition, the other desired general properties of the ion exchange membranes include low electrical resistance, high chemical stability, good mechanical and dimensional stability[40] at the operating conditions encountered during the electrodialytic concentration process.

One of the main industrial applications of electrodialysis is the preconcentration of sea water to produce NaCl,[39, 40, 43] and this process has been extensively studied.[57-60, 62-68] Furthermore, electrodialytic concentration of several organic and inorganic salts,[69-81] and acids[82-85] also has been investigated. However, there are only a few studies on the electrodialytic concentration of $CaCl_2$.[50, 61, 86-88] All these studies focused on concentrating $CaCl_2$ from dilute solutions, as opposed to the expected requirement of concentrating $CaCl_2$ from solutions with initial $CaCl_2$ concentrations as high as 15 wt% obtained from the bottoms stream in the salt extractive distillation of fuel ethanol. The water transport number is dependent on the concentration of the solute in the diluate. Several studies for other salts such as NaCl and LiCl[56, 60, 65, 89, 90] have reported the decrease in the water transport number with the increase in the solute concentration in the external electrolyte. Also, when the external solution concentration increases membrane deswelling occurs resulting in an increase of the membrane's fixed ion concentration.[91, 92] In general, when the external solution concentration increases, the Donnan sorption of the electrolyte increases leading to the decrease in the ionic transport numbers (current efficiency). However, an increase in ionic transport numbers with the increase in the external solution concentration has been reported[93] which is attributed to the membrane dehydration. For instance, a perfluorocarbon carboxylic acid membrane in sodium hydroxide solution, showed decreasing transport number when the concentration increased up to 5N due to the increase in the Donnan sorption of the electrolyte in the membranes. However, the transport number increases with further increase in the concentration of the electrolyte, which is attributed to the membrane dehydration leading to the increase in the fixed ion concentration. After the electrolyte concentration is increased beyond 13 N, the transport number eventually decreases due to the strong binding of the sodium ions to fixed ionic groups in the membrane.[39] Hence, the transport

14

properties of the ion exchange membrane in high external solution concentrations and gradients are expected to differ from that in dilute electrolyte solutions.

1.4.5 Limiting current density and energy demand

In addition to the transport properties of the ion exchange membranes, it is essential to evaluate the operational aspects of limiting current density and energy demand for designing the electrodialytic concentration process. With the passage of electric current, concentration gradients arise in the boundary layers along the ion exchange membrane (Figure 1-7). Since the transport number of cations is higher than anions in a cation exchange membrane, cations are transferred across the cation exchange membrane at faster rates than both the supply and removal rates in the solution at each side of the cation exchange membrane. Hence, concentration in the boundary layer in the diluate side decreases and the concentration in the boundary layer in the concentrate side increases. Finally, a steady state condition in the boundary layers is established when the combined electrical and diffusive fluxes in the solution balance the electrical flux across the membrane. When the passage of electric current across the membrane is increased, the salt concentration at the membrane interface in the diluate side eventually becomes zero. At such conditions, additional electric current through the membrane is balanced through the hydrogen ions produced by water splitting and/or through co-ion intrusion from the concentrate side.[44] The current density at which the interfacial solute concentration reaches essentially zero is known as the limiting current density. Operating above the limiting current density leads to changes in pH of the solutions and high energy demand due to the greatly increased electric resistance and reduced current efficiency. The limiting current density can be calculated using the following equation:[40]

$$i_{lim} = \frac{Fk_s}{z_c[T_c^m - T_c]} C_b \qquad\qquad \text{Equation 1-12}$$

where i_{lim} is the limiting current density in A/m^2; F, Faraday constant; k_s, mass transfer coefficient, m/s; C_b, concentration of the solute in the bulk diluate solution, mol/m^3; Z_c, valence of the cation, *equivalent/mol*; T_c^m and T_c, transport number of the cation in membrane and solution, respectively. The mass transfer coefficient, k_s, depends on the hydrodynamics of the feed solution in the cell: cell and spacer dimensions, feed velocity,

and diffusion coefficient of salt. When all the other factors in Equation 1-12 are held constant, the limiting current density is directly proportional to the concentration of the solute, C_b. In case of simultaneous salt recovery and concentration, as encountered in this study, the maximum amount of salt recovery is limited by the limiting current density.
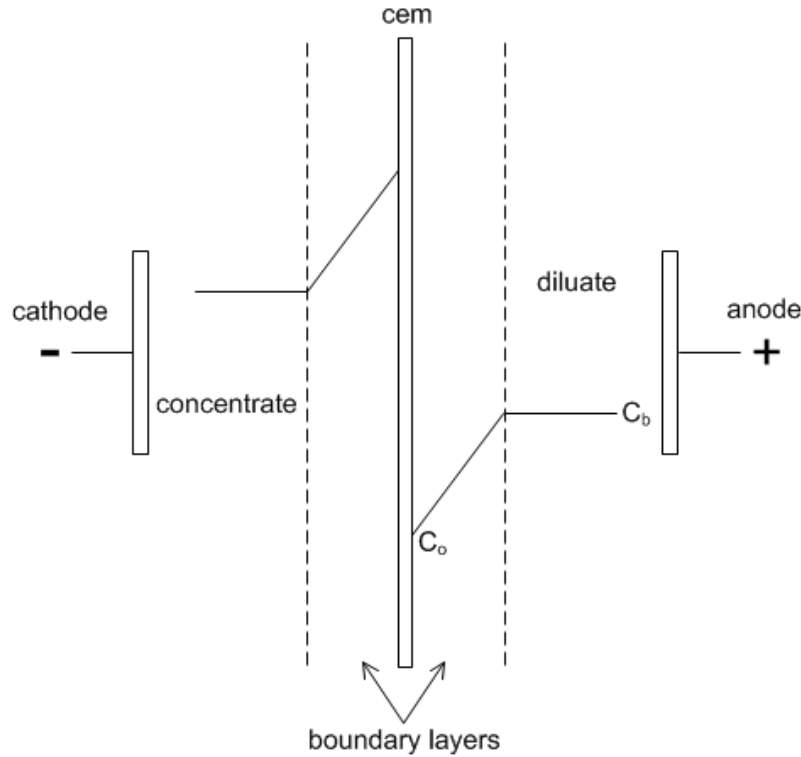
Figure 1-7. Concentration profiles of salt in the boundary layers on either side of the cation exchange membrane during electrodialysis. Adapted from Davis et al.[44]

The specific electrical energy requirement of electrodialysis for removing and concentrating the salt can be calculated as follows:

$$E = \frac{V_{cp}ZF}{3600M\eta}$$
Equation 1-13

where E is the specific energy demand in *kWh/kg*; V_{cp}, voltage drop per cell pair, *V*; and *M*, molecular weight of the salt, *g/mol*. This does not include the energy required for the electrode reactions. The voltage drop per cell pair is directly proportional to the operating current density and the electric resistance of the cell pair.[44] Overall, the increase in current efficiency decreases the energy requirement, while the increase in current density and cell pair resistance increases the energy requirement. In addition, electrical energy is required for pumping the electrolyte solutions through the electrodialysis stacks.

16

1.5 Process simulation and economics packages

Process simulation and economic analysis was carried out with Aspen Plus[®] 2006.5 and Aspen Icarus Process Evaluator[®] 2006.5, respectively. Aspen Plus[®] is a commercially available process modeling tool used to simulate steady-state processes. It is a valuable tool for conceptual process design and optimization. Simulation flowsheets can be generated using the built-in models for conventional process equipment which include distillation columns, heat exchangers, pumps, and compressors. Moreover, there are several available property methods to calculate the physical and thermodynamic properties of conventional chemical species, electrolytes, polymers, and solids. Aspen Icarus Process Evaluator[®] is an economic evaluation tool used to estimate capital cost, operating cost, and profitability of process designs. Process simulator output data can be directly mapped to built-in equipment models to determine the preliminary equipment size and cost which is used to evaluate the conceptual process designs for economic viability.

1.6 Dissertation outline

Chapter 2 – an accepted paper, published online in the AIChE Journal:[94] This paper describes a conceptual process design study which investigates the reduction of the energy demand of corn-ethanol by implementing salt extractive distillation enabled by electrodialysis through retrofitting an already existing fermentation broth-ethanol separation train. The details about the thermodynamic property method used in modeling the water/ethanol/$CaCl_2$ system and the process simulation procedure are also included.

Chapter 3 – submitted manuscript, Separation Science and Technology: The focus was on reducing the energy demand of cellulosic ethanol. Completely new separation process design schemes for fermentation broth-ethanol separation, which integrate salt extractive distillation, enabled by electrodialysis, together with energy saving heat integrated distillation techniques of double effect distillation and direct vapor recompression were evaluated.

Chapter 4 – manuscript in preparation for Journal of Membrane Science: Electrodialytic concentration of calcium chloride to enable the salt extractive distillation of bioethanol was investigated. Fundamental transport properties of an ion exchange

17

membrane comprising commercially available membranes were studied in high calcium chloride concentrations expected in the salt extractive distillation of bioethanol.

In Chapter 5, the results and important findings from the conceptual process design studies, electrodialytic concentration of calcium chloride¸ and final economic analysis are summarized along with the recommendations for future work.

1.7 Literature Cited

1. Renewable Fuels Association (RFA). Available at: http://www.ethanolrfa.org. Accessed August 4, 2011.

2. Aden, A.; Ruth, M.; Ibsen, K.; Jechura, J.; Neeves, K.; Sheehan, J.; Wallace, B.; Montague, L.; Slayton, A.; Lukas, J. *Lignocellulosic Biomass to Ethanol Process Design and Economics Utilizing Co-current Dilute Acid Prehydrolysis and Enzymatic Hydrolysis for Corn Stover.NREL/TP-510-32438*; NREL: 2002.

3. Alzate, C. A. C.; Toro, O. J. S., Energy consumption analysis of integrated flowsheets for production of fuel ethanol from lignocellulosic biomass. *Energy* 2006**,** 31, (13), 2447-2459.

4. Hamelinck, C. N.; van Hooijdonk, G.; Faaij, A. P. C., Ethanol from lignocellulosic biomass: techno-economic performance in short-, middle- and long-term. *Biomass Bioenergy* 2005**,** 28, (4), 384-410.

5. Lynd, L. R., Overview and evaluation of fuel ethanol from cellulosic biomass: Technology, economics, the environment, and policy. *Annu. Rev. Energy Env.* 1996**,** 21, 403-465.

6. McAloon, A.; Taylor, F.; Yee, W.; Ibsen, K.; Wooley, R. *Determining the Cost of Producing Ethanol from Corn Starch and Lignocellulosic Feedstocks. NREL/TP-580-28893*; NREL: 2000.

7. Wingren, A.; Galbe, M.; Zacchi, G., Energy considerations for a SSF-based softwood ethanol plant. *Bioresour. Technol.* 2008**,** 99, (7), 2121-2131.

8. Zacchi, G.; Ohgren, K.; Rudolf, A.; Galbe, M., Fuel ethanol production from steam-pretreated corn stover using SSF at higher dry matter content. *Biomass Bioenergy* 2006**,** 30, (10), 863-869.

9. Zhang, S. P.; Marechal, F.; Gassner, M.; Perin-Levasseur, Z.; Qi, W.; Ren, Z. W.; Yan, Y. J.; Favrat, D., Process Modeling and Integration of Fuel Ethanol Production from Lignocellulosic Biomass Based on Double Acid Hydrolysis. *Energy Fuels* 2009**,** 23, 1759-1765.

10. Griend, D. L. V. Ethanol Distillation Process. U.S. Patent 7,297,236 B1, 2007.

11. Kwiatkowski, J. R.; McAloon, A. J.; Taylor, F.; Johnston, D. B., Modeling the process and costs of fuel ethanol production by the corn dry-grind process. *Ind. Crops Prod.* 2006**,** 23, (3), 288-296.

12. Swain, R. L. B., Molecular Sieve Dehydrators: Why They Became the Industry Standard and How They Work. In *The Alcohol Textbook*, Fifth ed.; Ingeldew, W. M.; Kelsall, D. R.; Austin, G. D.; Kluhspies, C., Eds. Nottingham University Press: Thrumpton, U.K., 2009; pp 379-384.

13. Vane, L. M., Separation technologies for the recovery and dehydration of alcohols from fermentation broths. *Biofuels, Bioprod. Biorefin.* 2008**,** 2, (6), 553-588.

14. Côté, P.; Noël, G.; Moore, S., The Chatham demonstration: From design to operation of a 20 m^3/d membrane-based ethanol dewatering system. *Desalination* 2010**,** 250, (3), 1060-1066.

15. Shapouri, H.; Gallagher, P. *USDA's 2002 Ethanol Cost-of-Production Survey. Agricultural Economic Report Number 841*; United States Department of Agriculture: Washington DC, July 2005.

16. Summers, D. R.; Ehmann, D. Enhanced V-Grid Trays Increase Column Performance. Presented at the AIChE Annual Meeting, Indianapolis, IN, November 2002.

17. Meredith, J., Understanding Energy Use and Energy Users in Contemporary Ethanol Plants. In *The Alcohol Textbook*, Fourth ed.; Jacques, K. A.; Lyons, T. P.; Kelsall, D. R., Eds. Nottingham University Press: Thrumpton, U.K., 2003; pp 355-361.

18. Jackson, M. D.; Moyer, C. B., Alcohol Fuels. In *Kirk-Othmer Encyclopedia of Chemical Technology: [e-book]*, NY: Wiley; 2000. Available from: Wiley online library. Accessed May 4, 2010.

19. Barba, D.; Brandani, V.; Digiacomo, G., Hyperazeotropic ethanol salted-out by extractive distillation - theoretical evaluation and experimental check. *Chem. Eng. Sci.* 1985**,** 40, (12), 2287-2292.

20. Furter, W. F., Production of fuel-grade ethanol by extractive distillation employing the salt effect. *Sep. Purif. Methods* 1993**,** 22, (1), 1-21.

21. Ligero, E. L.; Ravagnani, T. M. K., Simulation of salt extractive distillation with spray dryer salt recovery for anhydrous ethanol production. *J. Chem. Eng. Jpn.* 2002**,** 35, (6), 557-563.

22. Ligero, E. L.; Ravagnani, T. M. K., Dehydration of ethanol with salt extractive distillation - A comparative analysis between processes with salt recovery. *Chem. Eng. Process.* 2003**,** 42, 543-552.

23. Llano-Restrepo, M.; Aguilar-Arias, J., Modeling and simulation of saline extractive distillation columns for the production of absolute ethanol. *Comput. Chem. Eng.* 2003**,** 27, (4), 527-549.

24. Pinto, R. T. P.; Wolf-Maciel, M. R.; Lintomen, L., Saline extractive distillation process for ethanol purification. *Comput. Chem. Eng.* 2000**,** 24, (2-7), 1689-1694.

25. Siklós, J.; Timár, L.; Ország, I.; Ratkovics, F., A simulation of the distillation of ethanol-water mixtures containing salts. *Hung. J. Ind. Chem.* 1982**,** 10, 309-316.

26. Furter, W. F., Salt effect in distillation : A technical review. *Chem. Eng. (Rugby, U. K.)* 1968**,** 46, (5), CE173-CE177.

27. Lynd, L. R.; Grethlein, H. E., IHOSR/Extractive distillation for ethanol separation. *Chem. Eng. Prog.* 1984, 59-62.

28. Schmitt, D.; Vogelpohl, A., Distillation of ethanol - water solutions in the presence of potassium acetate. *Sep. Sci. Technol.* 1983**,** 18, (6), 547-554.

29. Torres, J. L.; Grethlein, H. E.; Lynd, L. R., Computer simulation of the Dartmouth process for separation of dilute ethanol water mixtures. *Appl. Biochem. Biotechnol.* 1989**,** 20-1, 621-633.

30. Maiorella, B.; Wilke, C. R.; Blanch, H. W., Alcohol Production and Recovery. In *Advances in Biochemical Engineering*, Fiechter, A., Ed. Springer-Verlag: Berlin, 1981; Vol. 20, pp 43-92.

31. Nishi, Y., Vapor-liquid equilibrium relations for the system accompanied by hypothetical chemical reaction containing salt. *J. Chem. Eng. Jpn.* 1975**,** 8, (3), 187-191.

32. Kurihara, K.; Nakamichi, M.; Kojima, K., Isobaric vapor-liquid-equilibria for methanol+ethanol+water and the 3 constituent binary-systems. *J. Chem. Eng. Data* 1993**,** 38, (3), 446-449.

33. Furter, W. F., Salt effect in distillation : A literature-review II. *Can. J. Chem. Eng.* 1977**,** 55, (3), 229-239.

34. Furter, W. F.; Cook, R. A., Salt effect in distillation - a literature review. *Int. J. Heat Mass Transfer* 1967**,** 10, (1), 23-36.

35. Cook, R. A.; Furter, W. F., Extractive distillation employing a dissolved salt as separating agent. *Can. J. Chem. Eng.* 1968**,** 46, (2), 119-123.

36. Cespedes, A. P.; Ravagnani, S. P., Modelado y simulación del proceso de destilacion extractiva salina de etanol. *Inf. Tecnol.* 1995**,** 6, (5), 17-20.

37. Ravagnani, S. P.; Reis, P. R., Modelo de orden reducido aplicado a una columna de destilacion extractiva salina. *Inf. Tecnol.* 2000**,** 11, (2), 43-50.

38. Seader, J. D.; Henley, E. J., *Separation Process Principles*. Second ed.; Wiley: New York, 2006.

39. Sata, T., *Ion Exchange Membranes: Preparation, Characterization, Modification and Application*. Royal Society of Chemistry: Cambridge, 2004.

40. Strathmann, H., *Ion-Exchange Membrane Separation Processes*. First ed.; Elsevier: Amsterdam, The Netherlands, 2004.

41. Masters, K., *Spray Drying Handbook*. Fourth ed.; George Godwin: London, 1985.

42. Oakley, D. E., Spray dryer modeling in theory and practice. *Drying Technol.* 2004**,** 22, (6), 1371-1402.

43. Strathmann, H., Electrodialysis, a mature technology with a multitude of new applications. *Desalination* 2010**,** 264, (3), 268-288.

44. Davis, T. A.; Brockman, G. F., Physiochemical Aspects of Electromembrane Processes. In *Industrial Processing with Membranes*, Lacey, R. E.; Loeb, S., Eds. Wiley: New York, 1972.

45. Meares, P.; Thain, J. F.; Dawson, D. G., Transport across ion-exchange resin membranes: The frictional model of transport. In *Membranes: A series of advances. Macroscopic systems and models*, Eisenmann, G., Ed. Marcel Dekker: New York, 1972; Vol. 1.

46. Katchalsky, A.; Curran, P. F., *Nonequilibrium thermodynamics in biophysics*. Harvard University Press: Cambridge, 1965.

47. Kedem, O.; Katchalsky, A., Permeability of composite membranes. Part 1.—Electric current, volume flow and flow of solute through membranes. *Trans. Faraday Soc.,* 1963**,** 59, 1918-1930.

48. Spiegler, K. S., Transport processes in ionic membranes. *Trans. Faraday Soc.,* 1958**,** 54, 1408-1428.

49. Wesselingh, J. A.; Vonk, P.; Kraaijeveld, G., Exploring the Maxwell-Stefan Description of Ion-Exchange. *Chemical Engineering Journal and the Biochemical Engineering Journal* 1995**,** 57, (2), 75-89.

50. Hirayama, K.; Hanada, F.; Sata, T.; Mizutani, Y. In *Analysis of Properties of Advanced Ion-Exchange Membranes: Neosepta CIMS and ACS-2*, Seventh Symposium on Salt, 1993; 1993; pp 53-58.

51. Garrido, J., Transport coefficients in desalting processes by electrodialysis. *Desalination* 2011**,** 265, (1-3), 274-278.

52. Hwang, S. T., Nonequilibrium thermodynamics of membrane transport. *AlChE J.* 2004**,** 50, (4), 862-870.

53. Kedem, O., The role of volume flow in electrodialysis. *Journal of Membrane Science* 2002**,** 206, (1-2), 333-340.

54. Tanaka, Y., Irreversible thermodynamics and overall mass transport in ion-exchange membrane electrodialysis. *Journal of Membrane Science* 2006**,** 281, (1-2), 517-531.

55. Zabolotskii, V. I.; Shudrenko, A. A.; Gnusin, N. P., Transport characteristics of ion-exchange membranes during concentration of electrolytes by electrodialysis. *Elektrokhimiya* 1988**,** 24, (6), 744-750.

56. Demin, A. V.; Zabolotskii, V. I., Model verification of limiting concentration by electrodialysis of an electrolyte solution. *Russ. J. Electrochem.* 2008**,** 44, (9), 1058-1064.

57. Shkirskaya, S. A.; Protasov, K. V.; Berezina, N. P.; Zabolotskii, V. I., Composite Sulfonated Cation-Exchange Membranes Modified with Polyaniline and Applied to Salt Solution Concentration by Electrodialysis. *Russ. J. Electrochem.* 2010**,** 46, (10), 1131-1140.

58. Tanaka, Y., Ion-Exchange Membrane Electrodialysis for Saline Water Desalination and Its Application to Seawater Concentration. *Ind. Eng. Chem. Res.* 2011**,** 50, (12), 7494-7503.

59. Tanaka, Y.; Ehara, R.; Itoi, S.; Goto, T., Ion-exchange membrane electrodialytic salt production using brine discharged from a reverse osmosis seawater desalination plant. *Journal of Membrane Science* 2003**,** 222, (1-2), 71-86.

60. Zabolotskii, V. I.; Protasov, K. V.; Sharafan, M. V., Sodium chloride concentration by electrodialysis with hybrid organic-inorganic ion-exchange membranes: An investigation of the process. *Russ. J. Electrochem.* 2010**,** 46, (9), 979-986.

61. Nishiwaki, T., Concentration of Electrolytes with an Electromembrane Process Prior to Evaporation. In *Industrial Processing with Membranes*, Lacey, R. E.; Loeb, S., Eds. Wiley: New York, 1972.

62. Casas, S.; Bonet, N.; Aladjem, C.; Cortina, J. L.; Larrotcha, E.; Cremades, L. V., Modelling Sodium Chloride Concentration from Seawater Reverse Osmosis Brine by Electrodialysis: Preliminary Results. *Solvent Extr. Ion Exch.* 2011**,** 29, (3), 488-508.

63. Kobuchi, Y.; Terada, Y.; Tani, Y. In *The first salt plant in the middle east using electrodialysis and ion exchange membranes*, Sixth International Symposium on Salt, Toronto, Canada, 1983; Toronto, Canada, 1983; pp 541-555.

64. Moresi, M.; Fidaleo, M., Optimal strategy to model the electrodialytic recovery of a strong electrolyte. *Journal of Membrane Science* 2005**,** 260, (1-2), 90-111.

65. Schoeman, J. J.; vanStaden, J. F., Electro-osmotic pumping of sodium chloride solutions. *Journal of Membrane Science* 1997**,** 132, (1), 1-21.

66. Sreenivasarao, K.; Patsiogiannis, F.; Hryn, J. N. In *Concentration and precipitation of NaCl and KCl from salt cake leach solutions by electrodialysis*, Light metals, Warrendale, PA, 1997; Warrendale, PA, 1997; pp 1153-1158.

67. Tanaka, Y., Regularity in ion-exchange membrane characteristics and concentration of sea water. *Journal of Membrane Science* 1999**,** 163, (2), 277-287.

68. Yamane, R.; Ichikawa, M.; Mizutani, Y.; Onoue, Y., Concentrated Brine Production from Sea Water by Electrodialysis Using Ion Exchange Membranes. *Industrial & Engineering Chemistry Process Design and Development* 1969**,** 8, (2), 159-&.

69. Audinos, R., Optimization of Solution Concentration by Electrodialysis - Application to Zinc-Sulfate Solutions. *Chem. Eng. Sci.* 1983**,** 38, (3), 431-439.

70. Audinos, R.; Paci, S., Water Transport during the Concentration of Waste Zinc-Sulfate Solutions by Electrodialysis. *Desalination* 1987**,** 67, 523-545.

71. Boniardi, N.; Rota, R.; Nano, G.; Mazza, B., Analysis of the sodium lactate concentration process by electrodialysis. *Separations Technology* 1996**,** 6, (1), 43-54.

72. Cheryan, M.; Chukwu, U. N., Electrodialysis of acetate fermentation broths. *Appl. Biochem. Biotechnol.* 1999**,** 77-9, 485-499.

73. de Groot, M. T.; Bos, A. A. C. M.; Lazaro, A. P.; de Rooij, R. M.; Bargeman, G., Electrodialysis for the concentration of ethanolamine salts. *Journal of Membrane Science* 2011**,** 371, (1-2), 75-83.

74. Fidaleo, M.; Moresi, M., Modelling the electrodialytic recovery of sodium lactate. *Biotechnol. Appl. Biochem.* 2004**,** 40, 123-131.

75. Fidaleo, M.; Moresi, M., Modeling of sodium acetate recovery from aqueous solutions by electrodialysis. *Biotechnol. Bioeng.* 2005**,** 91, (5), 556-568.

76. Fidaleo, M.; Moresi, M., Assessment of the main engineering parameters controlling the electrodialytic recovery of sodium propionate from aqueous solutions. *J. Food Eng.* 2006**,** 76, (2), 218-231.

77. Moresi, M.; Fidaleo, M., Application of the Nernst-Planck approach to model the electrodialytic recovery of disodium itaconate. *Journal of Membrane Science* 2010**,** 349, (1-2), 393-404.

78. Rockstraw, D. A.; Scamehorn, J. F.; Orear, E. A., An Integrated Electrodialysis Evaporation Process for the Treatment of Aqueous Process Streams Containing Electrolytes. *Journal of Membrane Science* 1990**,** 52, (1), 43-56.

79. Thampy, S. K.; Narayanan, P. K.; Chauhan, D. K.; Trivedi, J. J.; Indusekhar, V. K.; Ramasamy, T.; Prasad, B. G. S.; Rao, J. R., Concentration of Sodium-Sulfate from Pickle Liquor of Tannery Effluent by Electrodialysis. *Sep. Sci. Technol.* 1995**,** 30, (19), 3715-3722.

80. Hakushi, T.; Azumi, T.; Takashima, S., Studies on ion exchange membranes (VI). Measurement of the dynamic transport of ion-exchange membranes by the electrodialytic concentration method. *Himeji Kogyo Daigaku Kenkyu Hokoku* 1965**,** 18, 69-75.

81. Grebenyuk, V. D.; Penkalo, I. I.; Fedorova, I. A., Effect of certain factors on the process of extreme concentration of salts during electrodialysis. *Khimiya i Tekhnologiya Vody* 1984**,** 6, (5), 399-401.

82. Andres, L. J.; Riera, F. A.; Alvarez, R., Recovery and concentration by electrodialysis of tartaric acid from fruit juice industries waste waters. *J. Chem. Technol. Biotechnol.* 1997**,** 70, (3), 247-252.

83. Aziz, N.; Rohman, F. S.; Othman, M. R., Modeling of batch electrodialysis for hydrochloric acid recovery. *Chem. Eng. J.* 2010**,** 162, (2), 466-479.

84. Habe, H.; Shimada, Y.; Fukuoka, T.; Kitamoto, D.; Itagaki, M.; Watanabe, K.; Yanagishita, H.; Sakaki, K., Two-stage electrodialytic concentration of glyceric acid from fermentation broth. *Journal of Bioscience and Bioengineering* 2010**,** 110, (6), 690-695.

85. Luo, G. S.; Pan, S.; Liu, J. G., Use of the electrodialysis process to concentrate a formic acid solution. *Desalination* 2002**,** 150, (3), 227-234.

86. Bobrinskaya, G. A.; Lebedinskaya, G. A.; Tolov, Y. A., Electrolytic desalting of water after lime coagulation purification. *Khimiya i Tekhnologiya Vody* 1981**,** 3, (4), 349-351.

87. Hakushi, T.; Dohno, R.; Azumi, T.; Takashima, S., Studies on ion exchange membranes. XXIII. The electrodialytic concentration of various chloride solutions using ion exchange membranes. *Himeji Kogyo Daigaku Kenkyu Hokoku* 1973**,** 26, 75-79.

88. Smagin, V. N.; Chukhin, V. A.; Kharchuck, V. A., Technological Account of Electrodialysis Apparatus for Concentration. *Desalination* 1983**,** 46, (May), 283-290.

89. Berezina, N.; Gnusin, N.; Dyomina, O.; Timofeyev, S., Water Electrotransport in Membrane Systems - Experiment and Model Description. *Journal of Membrane Science* 1994**,** 86, (3), 207-229.

90. Berezina, N. P.; Kononenko, N. A.; Dyomina, O. A.; Gnusin, N. P., Characterization of ion-exchange membrane materials: Properties vs structure. *Adv. Colloid Interface Sci.* 2008**,** 139, (1-2), 3-28.

91. Narebska, A.; Wodzki, R., Swelling Equilibria and Structure Variations of Nafion and Polyethylene-Poly (Styrene Sulfonic-Acid) Membranes at High Electrolyte

Concentrations and Increased Temperature. *Angew. Makromol. Chem.* 1982**,** 107, (Sep), 51-60.

92. Narebska, A.; Wodzki, R.; Erdmann, K., Properties of Perfluorosulfonic Acid Membranes in Concentrated Sodium-Chloride and Sodium-Hydroxide Solutions. *Angew. Makromol. Chem.* 1983**,** 111, (Jan), 85-95.

93. Sata, T.; Onoue, Y., Perfluorinated ion exchange membranes. In *Perfluorinated Ionomer Membranes, ACS Symposium Series 180*, Eisenberg, A.; Yeager, H. L., Eds. American Chemical Society: 1982; Vol. 180, pp 411-415.

94. Hussain, M. A. M.; Anthony, J. L.; Pfromm, P. H., Reducing the energy demand of corn-based fuel ethanol through salt extractive distillation enabled by electrodialysis. *AlChE J.* 2011**,** doi:10.1002/aic.12577.

Chapter 2 - Reducing the energy demand of corn-based ethanol through salt extractive distillation enabled by electrodialysis

2.1 Abstract

The thermal energy demand for producing fuel ethanol from the fermentation broth of a contemporary corn-to-fuel ethanol plant in the U.S. is largely satisfied by combustion of fossil fuels, which impacts the possible economical and environmental advantages of bio-ethanol over fossil fuels. To reduce the thermal energy demand for producing fuel ethanol, a process integrating salt extractive distillation – enabled by a new scheme of electrodialysis and spray drying for salt recovery – in the water-ethanol separation train of a contemporary corn-to-fuel ethanol plant is investigated. Process simulation using Aspen Plus® 2006.5, with the electrolyte nonrandom two liquid Redlich-Kwong property method to model the vapor liquid equilibrium of the water-ethanol-salt system, was carried out. The integrated salt extractive distillation process may provide a thermal energy savings of about 30%, when compared with the contemporary process for separating fuel ethanol from the beer column distillate.[a]

2.2 Introduction

Currently, the annual production capacity for fuel ethanol, mostly corn-ethanol, in the U.S. is about 55.7 GL, including about 4.5 GL capacity in new construction or expansion.[1] The Renewable Fuels Standard (RFS2), established under the Energy Independence and Security Act (EISA) of 2007, mandates the production of 136.3 GL/year of renewable fuels in 2022: 56.8 GL/year of corn-ethanol, 60.6 GL/year of second-generation bio-fuels such as cellulosic ethanol, and 18.9 GL/year of advanced bio-fuels such as biomass based diesel.[1] Dry milling is currently the most widely used process in the U.S for producing fuel ethanol from corn by fermentation. The energy demand of old dry mill facilities[2-8] was high. Contemporary dry mill facilities have higher energy efficiency, and require about 9.8 MJ (generally from natural gas) of thermal energy and 0.7 MJ (0.19 kWh) of electrical energy to produce 1 liter of non-denatured fuel grade ethanol. The energy demand includes drying of non-fermentables to produce distillers' dried grain with solubles (DDGS).[9-12] The lower heating value of pure ethanol is 21.2 MJ per liter.[13] About 70% of the thermal energy is expended to generate steam which is used for recovering ethanol from fermentation broth, purifying ethanol to fuel grade (99.5 wt%), cooking and liquefying corn mash, and concentrating thin stillage. Recovering and purifying ethanol from fermentation broth is energy intensive and requires about 70 % of the total steam generated in the dry milling plant.[14] Fuel ethanol plants mainly use natural gas boilers to generate steam. Reducing the steam demand for recovering and purifying ethanol is essential to improve the energy balance of bio-ethanol, even if non-fermentable biomass components would be burned instead of natural gas to produce steam. The vast amounts of bio-ethanol produced by fermentation worldwide would similarly benefit from reducing the energy demand of the water (fermentation broth)-ethanol separation.

The ethanol concentration in the fermentation broth may vary from about 10 to 15 wt% for different facilities.[10, 15-18] The fermentation broth contains many components besides water and ethanol: unfermented biomass, microorganisms, proteins, oils, and volatile organics. Recovering ethanol from fermentation broth and purifying it to fuel grade is difficult and energy intensive because of the dilute nature of the fermentation

broth and the challenging water-ethanol vapor liquid equilibrium (VLE) with an azeotrope at about 96 wt% ethanol and tangential approach of the water-ethanol equilibrium curve to the 45° line at high ethanol concentrations in the familiar y-x VLE diagram representation. Simple distillation cannot be used to distill ethanol above the azeotropic composition. The state of the art technique used in the fuel ethanol industry to produce fuel ethanol is distillation close to the azeotropic composition followed by dehydration in a molecular sieve based adsorption unit[10, 16, 19, 20] or, in some cases, distillation followed by dehydration with membrane vapor permeation.[15, 21] Membrane-assisted vapor stripping was tested at the pilot scale level for producing fuel ethanol from a dilute ethanol feed (5 wt%), representing fermentation broth obtained from lignocellulosic feedstocks.[22, 23] Green field facilities for producing fuel ethanol from lignocellulosic feedstocks are expected to be built to meet the requirements of EISA. Our study focuses on the significant installed capital equipment for corn-based fuel ethanol facilities where the ethanol concentration in the fermentation broth is much higher than is expected for the cellulosic case. The technology proposed here would offer retrofit opportunities for existing facilities, while the above mentioned membrane technology would be targeted towards new construction, not making use of the conventional equipment beyond the beer column. Membrane technology will, for example, require specialized ethanol vapor compressors. Heat integrated distillation operations such as multi-effect distillation and vapor recompression can reduce distillation energy demand. In particular, multi-effect distillation can lead to significant energy savings; 45% energy savings has been reported for a heat integrated dry mill process using multi-effect distillation, compared to a heat integrated dry mill process using standard distillation.[24] Nevertheless, multi-effect distillation is not considered in our study, as it requires a complete re-design of the distillation train of the existing dry mill corn-ethanol facilities.

The VLE of the water-ethanol system can be improved by employing a salt dissolved in the liquid phase to raise the equilibrium vapor ethanol content.[25-28] Adding a suitable salt can specifically improve the relative volatility of ethanol ("salting out") as well as break the azeotrope.[25, 27, 29] For example, 99.6 wt % ethanol was distilled using potassium acetate as the salt with only a quarter of the energy required for salt-free distillation to obtain lower quality 93 wt% ethanol directly from a feed containing 70

wt% ethanol.[30] Efficient recovery and reuse of the salt used as the separating agent is, however, crucial.

Potassium acetate[29-37] and calcium chloride[31, 36, 38-40] have been reported for water-ethanol separation utilizing the "salting out" effect. The use of the salt separating agent in a process with tightly closed water cycles such as the state of the art dry mill corn-to-fuel ethanol plant requires that the salt not impact other processing areas negatively. In this study, calcium chloride was selected for the following reasons: low cost, large "salting out" effect of calcium chloride,[31, 36] and process compatibility. Calcium ion stabilizes the α-amylase enzyme,[41, 42] used in the cooking process, and (at low levels) acts as a co-nutrient for yeast used in fermentation.[43]

In a salt extractive distillation column, the salt is usually dissolved in the reflux stream and introduced at the top of the column. Unlike the liquid extractive agents such as ethylene glycol, salt is non-volatile and always remains in the liquid phase; thereby, enabling the production of a high purity distillate free of salt. The salt moves downward in the column and is recovered and purified from the distillation column bottoms for re-use in the top of the column. Hence, there are two distinct steps involved: salt extractive distillation and salt recovery/purification. Corrosion due to aqueous ethanolic salt solutions is an issue and special construction materials may be necessary or increased corrosion rates may be planned for.[38, 44] Other issues are related to solids handling, feeding and dissolving salt in the reflux stream, potential decrease in plate efficiency, and foaming inside the column.[25, 27, 29] In the study presented here, the possible benefit in terms of energy demand is established, which will determine if the concept is attractive enough to deal with the possible complications.

There are many experimental and theoretical studies[29-40] on producing fuel ethanol by utilizing the "salting out" effect, but most of them focus only on the salt extractive distillation step. Moreover, the studies[25, 27, 32-35, 37, 38] which include both steps of salt extractive distillation and salt recovery do not consider techniques other than evaporation and drying for salt recovery. Evaporative salt concentration/crystallization and solids drying techniques are energy intensive. Reducing the energy demand for the salt recovery step becomes essential to reap the benefit of salt-induced VLE improvement. In this study, a combination of electrodialysis and spray drying is

investigated. The salt extractive column bottoms stream is pre-concentrated by electrodialysis and dried to an anhydrous state by spray drying. In electrodialysis, the dilute salt solution is concentrated by selectively separating the salt ions from the solution[45, 46] rather than evaporating water; therefore, requiring less energy than that of an evaporative process. Moreover, electrodialysis is rugged and can be operated at high ionic strengths.[47] Final recovery of dry salt is achieved in a spray dryer. This approach is widely used to convert a liquid feed containing salt into dry solid particles in a single step.[48, 49] Integrating salt extractive distillation, with salt recovery enabled by electrodialysis and spray drying, in the water-ethanol separation train of a state of the art corn-to-fuel ethanol plant was found to yield significant energy savings through process simulation using Aspen Plus® 2006.5.

2.3 Design Cases

2.3.1 Benchmark process: Case I

The target fuel ethanol production rate was set at 151.4 ML ($1.17*10^5$ tonne) per year with an ethanol concentration of 99.5 wt%. In a standard U.S. corn-to-fuel ethanol plant based on fermentation using yeast, recovery of ethanol from the fermentation broth and further purification to fuel grade is achieved by three distillation columns (beer column, rectifier, and side stripper) and final water removal by molecular sieve based adsorption[10, 20] as shown in Figure 2-1. Beer from the fermentation process is fed to the beer column operated as a stripper (no reflux) to produce a vapor distillate with an ethanol concentration of about 55 wt% and a bottom aqueous stream, termed whole stillage, consisting of water, dissolved matter, unfermented solids, oils, and trace amounts of ethanol. Then, the vapor distillate from the beer column is enriched to about 92 wt% ethanol in the rectifier. In the adsorption cycle of the molecular sieve unit, superheated moist ethanol vapor from the rectifier overhead is dehydrated to fuel grade ethanol by the selective adsorption of water, while in the desorption cycle, the adsorbent bed is depressurized and purged with dry product ethanol vapors for regeneration. The regeneration stream from the adsorbers is recycled to the rectifier. The side stripper strips residual ethanol from the rectifier bottoms stream and the stripped ethanol vapor stream

is returned to the rectifier bottoms while the water from the side stripper bottoms is available for recycling to mash preparation and fermentation.

The rectifier and the side stripper essentially operate as a single column, but they are physically separated to minimize capital cost through the opportunity to have the side stripper with a reduced column diameter compared to the rectifier. In this study, a separation train consisting of a beer column, a rectifier (representing both the rectifier and the side stripper in the state of art installations), and a molecular sieve unit is considered as the benchmark process (Figure 2-2). Further, the beer column and rectifier are assumed to operate under sub atmospheric pressure conditions, enhancing the relative volatility of ethanol at high ethanol concentration.[50] Since the molecular sieve unit requires a superheated vapor feed under pressure (172 kPa) in the adsorption cycle, the rectifier overhead condenser is operated as a total condenser producing a liquid distillate which is pressurized with a pump, and then evaporated and superheated for dehydration in the molecular sieve unit.

2.3.2 Salt extractive process: salt in rectifier only, Case II

The efficient recovery and re-use of salt in salt extractive distillation is of paramount importance in regard to the energy demand, capital cost and process requirements. Since separation and recovery of salt from the highly complex beer column bottoms stream would be a formidable challenge, no salt should be added to the beer column. The rectifier deals with a relatively clean feed stream (the beer column distillate) without solids which facilitates salt recovery from the rectifier bottoms stream. Due to the above reason we opted to purify the beer column distillate in a salt extractive rectifier to fuel grade ethanol, eliminating the need for the molecular sieve unit (Figure 2-3). The salt extractive rectifier bottoms stream is divided into diluate and concentrate for the electrodialysis process. After receiving the salt from the diluate, the salt enriched in the concentrate stream is recovered by evaporating the remaining water with hot natural gas combustion gases in a co-current spray dryer before recycling to the salt extractive rectifier reflux.
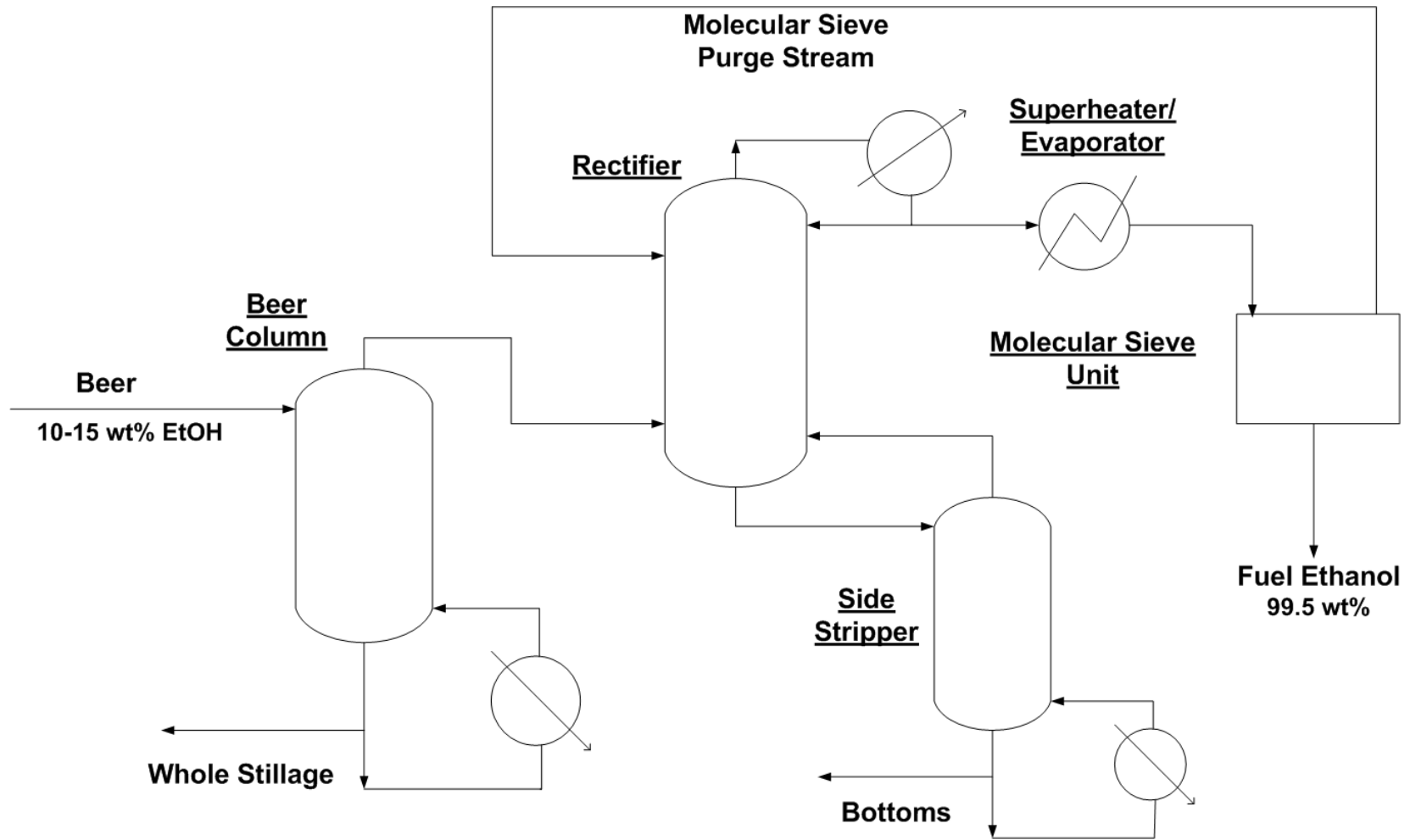
Figure 2-1. Process flow scheme for ethanol recovery and purification in a state of the art fermentation based corn-to-fuel ethanol plant.
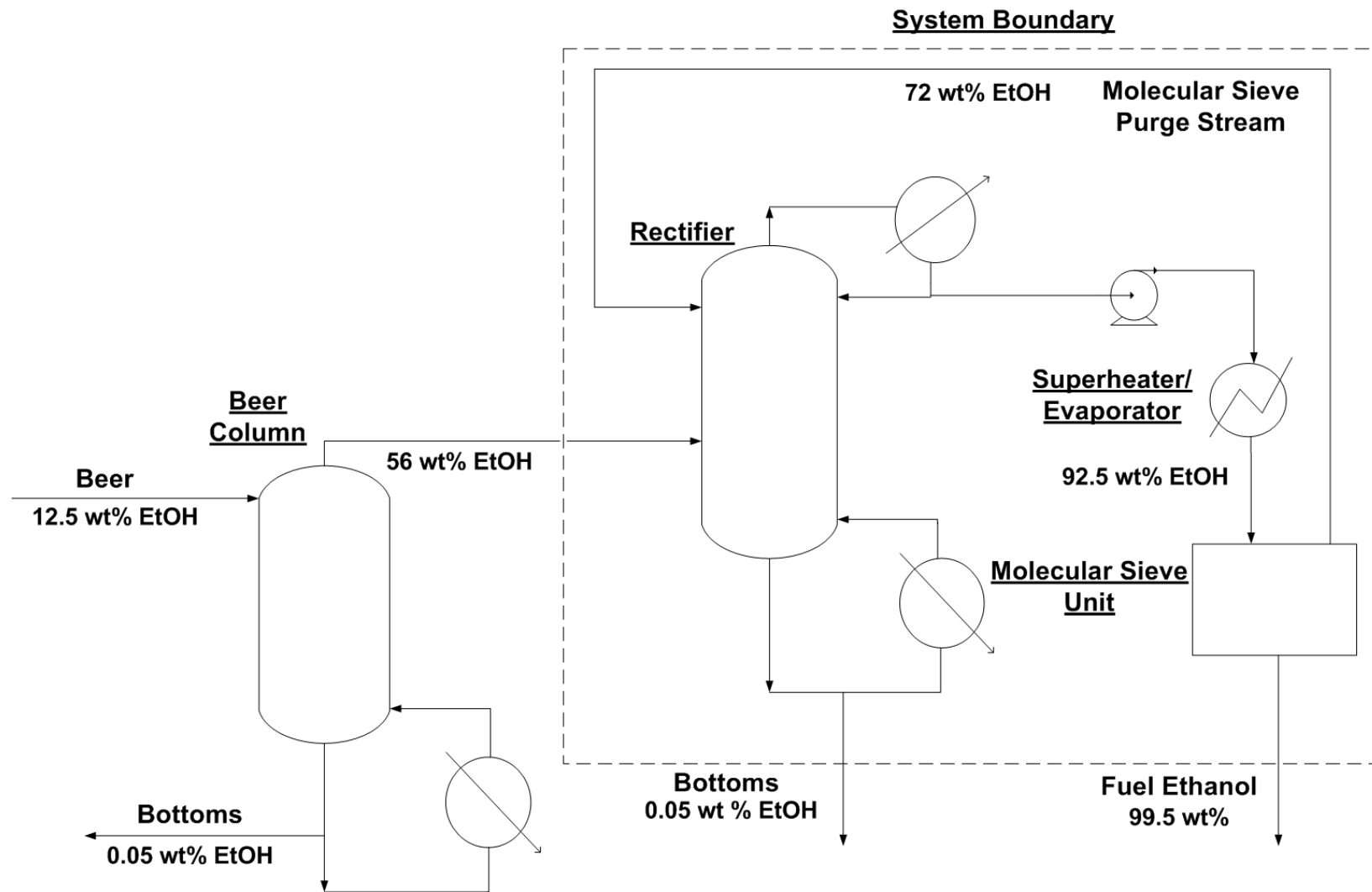
Figure 2-2. Process flow scheme for Case I – benchmark process.
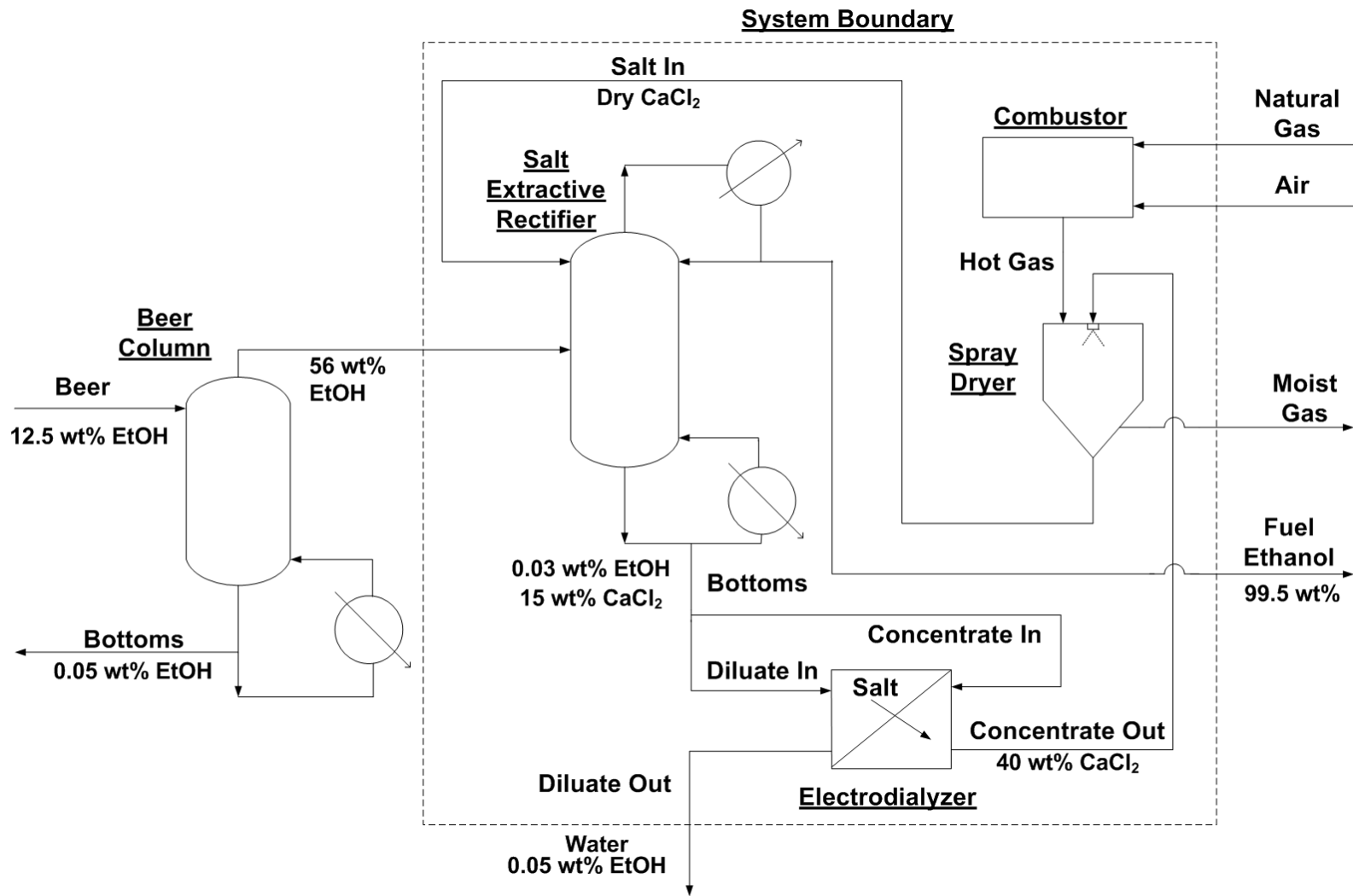
Figure 2-3. Process flow scheme for Case II –salt extractive process.

2.3.3 Summary of energy demand comparison approach

Comparing energy demands for different processing schemes is complex. Heat integration interconnects unit operations, and different qualities of energy (2nd law of thermodynamics based balance, for example, thermal vs. electrical) besides the simple quantity of energy (1st law of thermodynamics based balance) impact both economics and environmental issues such as green house gas emissions.

The input data and specified parameters for the system boundaries for Case I (benchmark process, Figure 2-2) and Case II (salt extractive process, Figure 2-3) are given, respectively, in Table 2-1 and Table 2-2. Input in Case I and Case II is an identical stream of 26.2 tonne/h (vapor distillate containing 56 wt% ethanol and balance water) from a beer column operating as a stripping column at a pressure of 44.8 kPa with 13 stages and a beer feed concentration of 12.5 wt% ethanol, an average of the typical fermentation broth ethanol concentrations (about 10 to 15 wt%) prevalent in contemporary dry mill corn-ethanol facilities. Identical streams of fuel ethanol are produced in Case I and II. As an aside, the liquid water output streams from the design cases are not identical since water vapor is lost in the spray dryer with the moist air stream in Case II.

Table 2-1. Input data and specified parameters for Case I – benchmark process

Input Data and Specified Parameters	Benchmark Process
Rectifier	
Number of Stages	37
Operating Pressure (kPa)	34.5
Distillate Ethanol Concentration (wt%)	92.5
Bottoms Ethanol Concentration (wt%)	0.05
Molecular Sieve Unit [a]	
Operating Temperature (K)	389.15
Adsorption Pressure (kPa)	172.2
Desorption Pressure (kPa)	14.2
Purge Stream Ethanol Concentration (wt%)	72.3
Fuel Ethanol Concentration(wt%)	99.5

[a] Data taken from Aden et al.[58]

The comparison of the energy demand of Case I and II is based on calculating natural gas energy equivalents (HHV) for electrical energy or steam that is needed. The

thermal energy as steam is converted back to natural gas energy equivalents by using a boiler efficiency of 80%, while for electrical energy, a natural gas-to-electrical energy conversion efficiency of 33% was assumed. The thermal energy demand of the spray dryer is directly calculated from the natural gas usage.

Table 2-2. Input data and specified parameters for Case II – salt extractive process

Input Data and Specified Parameters	Salt Extractive Process
Salt extractive rectifier	
Number of Stages	37
Operating Pressure (kPa)	34.5
Distillate Ethanol Concentration (wt%)	99.5
Bottoms Ethanol Concentration (wt%)	0.03
Electrodialysis	
Operating Temperature (K)	313.15
Concentration of $CaCl_2$ in Concentrate (wt%)	40
Current Efficiency (%)	90
Spray Dryer	
Hot Gas Temperature (K)	923.15
Moist Gas Temperature (K)	473.15

2.4 Methods

2.4.1 Thermodynamic modeling of the water-ethanol and water-ethanol-CaCl₂ systems

The VLE of the water-ethanol system is described by the following equation[51]:

$$y_i \varphi_i P = x_i \gamma_i P_i^* \varphi_i^* \exp\left[\frac{1}{RT} \int_{P_i^*}^{p} v_i^* dp \right]$$

Equation 3-1

where y_i and x_i represent, respectively, vapor and liquid phase mole fractions, φ_i and φ_i^* represent, respectively, partial and pure component fugacity coefficients, P and P_i^* represent, respectively, system pressure and pure component vapor pressure in kPa, γ_i represents the liquid phase activity coefficient, v_i^* represents the saturated liquid molar volume in $m^3/kmol$ at system temperature T in K, and R represents the gas constant in $kJ/K.kmol$. In case of the water-ethanol system, vapor phase fugacity coefficients were

calculated using the Redlich-Kwong (RK) equation[52], whereas liquid phase activity coefficients were calculated using the Non-Random Two Liquid (NRTL) model.[53] VLE calculations for water–ethanol were performed using default binary parameters (Table 2-3) in Aspen Properties® 2006.5 for the NRTL-RK property method. The NRTL-RK VLE data shows good agreement with experimental data (Table 2-4, Figure 2-4).

Table 2-3. Binary parameters of NRTL-RK property method for water(i)-ethanol(j) system[a]

a_{ij}	3.622
a_{ji}	-0.922
b_{ij}	-636.726
b_{ji}	284.286
α_{ij}	0.3

[a] Molecule-molecule binary parameters were retrieved from Aspen Properties® 2006.5. The energy interaction parameter (τ) was considered as temperature dependent: $\tau_{ij} = a_{ij} + b_{ij}/T$ where T is the system temperature. α_{ij} is the nonrandomness factor.

Table 2-4. Deviation between experimental data and NRTL-RK property method calculations for system temperature (T) and pressure (P), and vapor phase mole fraction of ethanol (y) in water-ethanol system

Isobaric VLE			
Pressure (kPa)	*$\Delta T\ (K)^a$*	*Δy^a*	*Reference*
287.5	0.89	0.011	59
101.3	0.11	0.005	60
25.3	- -	0.008	61
Isothermal VLE			
Temperature (K)	*$\Delta P\ (\%)^b$*	*Δy^a*	*Reference*
343.15	0.43	0.004	62
363.15	0.38	0.004	62

$$^a\ AAD = \sum_{i=1}^{k} \frac{|Z_i - ZM_i|}{k}$$

$$^b\ AADP = \frac{100}{k} \sum_{i=1}^{k} \left|\frac{Z_i - ZM_i}{ZM_i}\right|$$

where *AAD* is the average absolute deviation, *AADP* is the average absolute deviation in percentage, Z_i is the regressed property value, ZM_i is the corresponding experimental value, and k is the number of data points.

In case of the water-ethanol-CaCl$_2$ system, the VLE relationship for the volatile components was determined using Equation 3-1. The Redlich-Kwong equation was used to calculate vapor phase fugacity coefficients, and the Electrolyte Non-Random Two Liquid (ENRTL) model[54-56] was used to calculate liquid phase activity coefficients. The ENRTL model assumes that the total excess Gibbs energy (G^{ex}) of the mixed solvent electrolyte system can be represented as a sum of three contributions:

$$G^{ex} = G^{ex}_{PDH} + G^{ex}_{lc} + G^{ex}_{Born} \hspace{3cm} \text{Equation 3-2}$$

where G^{ex}_{PDH} represents the long range interaction contribution from the Pitzer-Debye Huckel equation, accounting for the electrostatic interactions among the ions. G^{ex}_{lc} represents the short range interactions among the solution species. These interaction forces are described based on the local composition concept, and on the assumptions of local electroneutrality and like-ion repulsion. G^{ex}_{Born} represents the Born contribution, accounting for the change in Gibbs energy due to the transfer of ionic species from the infinite dilution mixed solvent reference state to the infinite dilution aqueous reference

state. The adjustable ENRTL parameters required for water-ethanol-$CaCl_2$ are molecule-molecule (water-ethanol) and molecule-electrolyte (water-$CaCl_2$/ethanol-$CaCl_2$) pair interaction parameters. In the absence of electrolyte components, the ENRTL model reduces to the NRTL model; hence, molecule-molecule pair parameters used in the NRTL model were retained in the ENRTL model. The molecule-electrolyte pair parameters were regressed from experimental data covering the entire range of the process conditions studied (least squares method based on the maximum likelihood principle, DRS module of Aspen Properties[®] 2006.5). The Britt-Luecke algorithm[57] along with the Deming initialization method was used to regress the pair parameters shown along with other parameters in Table 2-5. The approach described above showed good agreement with experimental data (Table 2-6, Figure 2-4).

Table 2-5. Parameters of ENRTL-RK property method for water(i)-ethanol(j)-CaCl$_2$(k) system

Dielectric Constant of Solvents[a]			
Solvent	**A**	**B**	**C**
Ethanol	24.11	12601.63	298.15
Water	78.54	31989.38	298.15

Born Radius of Ionic Species[b]	
Ionic Species	**Born Radius (10^{-10} m)**
Ca^{2+}	1.862
Cl$^-$	1.937

Molecule-Electrolyte Binary Parameters Regressed from Experimental Data

Interaction Pair	Energy Parameter (τ)	Nonrandomness Factor (α)
i,k	10.262	0.2
k,i	-5.160	0.2
j,k	29.571	0.0396
k,j	-16.093	0.0396

[a] Values were retrieved from Aspen Properties® 2006.5. The temperature dependency of the dielectric constant (ε) is given by:
$\varepsilon = A + B\ (1/T-1/C)$, where T is the system temperature.
[b] Values were taken from Rashin et al.[63]
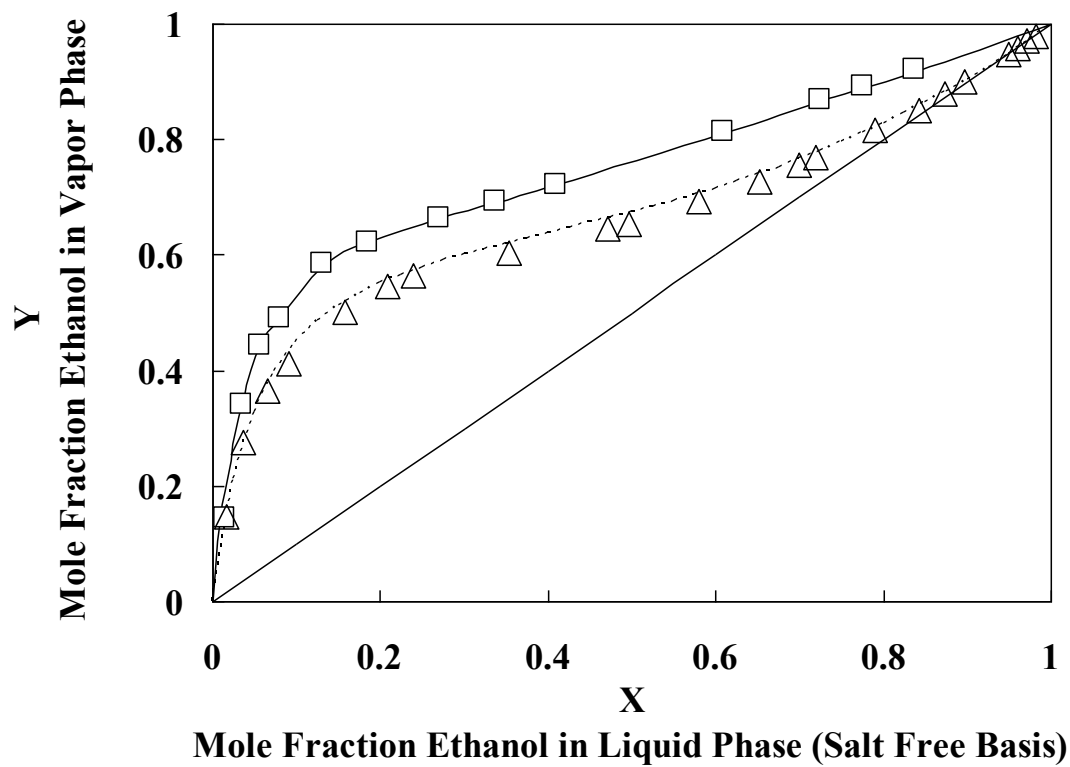
Figure 2-4. VLE curves for the water-ethanol-$CaCl_2$ and water-ethanol systems: (□) experimental data[67] with 10.8 wt% $CaCl_2$ liquid phase concentration (salt free basis) at 12.3 kPa, (solid line) calculated using ENRTL-RK property method; (Δ) experimental data[61] without salt at 25.3 kPa, (dotted line) calculated using NRTL-RK property method.

Table 2-6. Deviation between experimental data and ENRTL-RK property method calculations for osmotic coefficient (Φ), system temperature (T) and pressure (P), and vapor phase mole fraction of ethanol (y) in water-ethanol-CaCl$_2$ system

Osmotic Coefficients in Water-CaCl$_2$ System			
Temperature (K)	*Salt concentration (mol/kg solvent)*	*$\Delta\Phi^a$*	*Reference*
298.15	0.1 - 4	0.058	64

Vapor Pressures of Water-CaCl$_2$ System			
Temperature (K)	*Salt Concentration (mol/kg solvent)*	*ΔP (%)^b*	*Reference*
322.7 - 398.5	0.957 - 4.086	0.27	65

Isobaric VLE for Water-Ethanol-CaCl$_2$ System				
Pressure (kPa)	*Salt Concentration (mol/kg solvent)*	*ΔT (K)^a*	*Δy^a*	*Reference*
101.3	1.505	0.419	0.004	66
12.3	0.974	0.508	0.001	67

Isothermal VLE for Water-Ethanol-CaCl$_2$ System				
Temperature (K)	*Salt Concentration (mol/kg solvent)*	*ΔP (%)^b*	*Δy^a*	*Reference*
298.15	0.474	0.16	0.007	68

$$^a\ AAD = \sum_{i=1}^{k} \frac{|Z_i - ZM_i|}{k}$$

$$^b\ AADP = \frac{100}{k} \sum_{i=1}^{k} \left| \frac{Z_i - ZM_i}{ZM_i} \right|$$

where *AAD* is the average absolute deviation, *AADP* is the average absolute deviation in percentage, Z_i is the regressed property value, ZM_i is the corresponding experimental value, and *k* is the number of data points.

2.4.2 Simulation procedure

The distillation columns were rigorously simulated using the MESH equations implemented in the RadFrac module of Aspen Plus® 2006.5. For the rectifier and the salt extractive rectifier, the Newton algorithm was used, which solves the MESH equations using the Naphtali-Sandholm procedure. Optimum feed stages for the rectifier and the salt extractive rectifier were determined by sensitivity analyses. In Case II, the CaCl$_2$ concentration profile in the salt extractive rectifier is an important parameter. Increasing the CaCl$_2$ concentration in the salt extractive rectifier can decrease the reboiler duty because of the improvement in the VLE, but can lead to an increase in salt recovery energy demand because of the increased CaCl$_2$ mass

flow. The CaCl$_2$ concentration in the salt extractive rectifier was optimized to achieve a minimum of the sum of the energy requirements for the system shown in Figure 2-3. The mass and energy balance calculations for the molecular sieve unit, electrodialyzer, and the spray dryer were separately performed using Microsoft Excel® 2003 and Mathcad® 13. The results were later incorporated in the overall simulation using the User Model feature of Aspen Plus® 2006.5.

2.5 Results and Discussion

The target mass flow of fuel grade ethanol to be produced has been fixed (see above) which essentially determines the bottoms mass flow of water from the salt extractive rectifier (Case II), provided there is a negligible ethanol loss with the bottoms. The main parameters are then the reflux (mass flow) in the salt extractive rectifier and the concentration of salt in this reflux stream.

It is necessary to at least eliminate the azeotrope so that fuel grade ethanol can be produced at all in a single salt extractive rectifier. This already occurs at about 2.9 wt% of CaCl$_2$ in the reflux. Above this concentration, the thermal energy demand of the salt extractive rectifier steeply declines with increasing CaCl$_2$ concentration in the reflux but this benefit levels out above about 5 wt% (Figure 2-5). The reason is that the distillation pinch point, the point of contact between the operating line and the VLE curve in a McCabe-Thiele diagram, shifts from the location at high ethanol content (tangent pinch) to the feed stage (feed pinch) which is at about 56 wt% of ethanol. This shift yields the principal benefit of the salt extractive approach above and beyond eliminating the azeotrope. Further increase in the CaCl$_2$ concentration in the reflux causes an increase in CaCl$_2$ mass flow (Figure 2-6) along with increasing energy demand for salt recovery (Figure 2-7) without significant added benefit. The overall combined energy demand, therefore, shows a minimum at about 5.6 wt% CaCl$_2$ in the reflux due to the competition between energy savings due to facilitated distillation, and energy demand for salt recovery (Figure 2-8). Since there is already a large amount of installed capital for corn-based fuel ethanol facilities, the opportunity to improve the already existing process (rectifier and side stripper) by salt extractive distillation is attractive. Matching the salt extractive distillation column diameter, and the reboiler and condenser heat transfer areas with that of the corresponding process equipments from Case I is necessary for retrofit purposes. Based on the reflux salt concentrations showing potential energy savings, design calculations indicated salt

extractive distillation columns operating with salt concentrations greater than about 5.6 wt% $CaCl_2$ in the reflux satisfy the capacity requirements. An economic analysis (see Appendix A) shows at about 6.1 wt% $CaCl_2$ in the reflux, maximal cost savings on the order of 500,000$ per year (Figure 2-9) can be achieved. Case I, requires 1778 kJ/L (6378 Btu/gal) for producing fuel ethanol from the beer column distillate. Retrofitted Case II – salt extractive process, requires 1270 kJ/L (4555 Btu/gal, Figure 2-10), reducing the thermal energy demand, based on the system boundaries selected here, by 28.5%, which translates to 4.3% thermal energy demand reduction on an overall plant level, considering a fermentation based dry corn mill facility producing both fuel ethanol and DDGS.
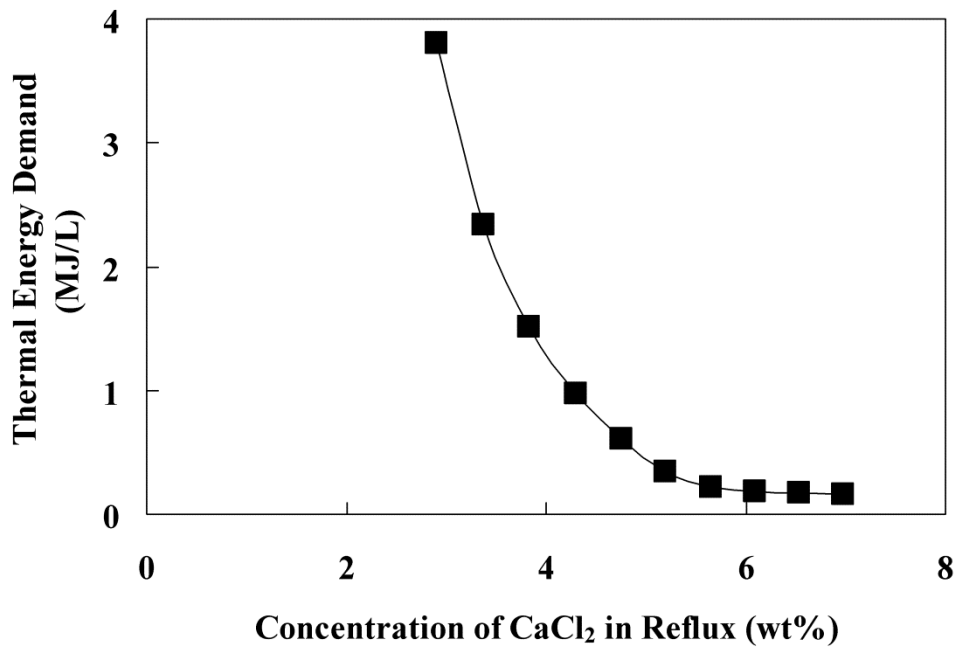
Figure 2-5. Influence of concentration of $CaCl_2$ in reflux on the thermal energy demand of the salt extractive rectifier.
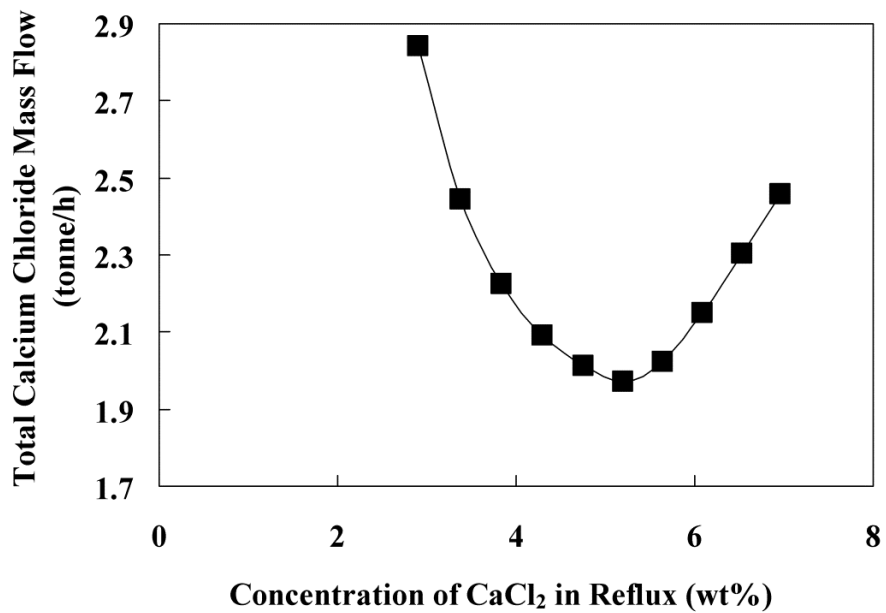
Figure 2-6. Influence of concentration of CaCl$_2$ in reflux on the total CaCl$_2$ mass flow to the salt extractive rectifier.
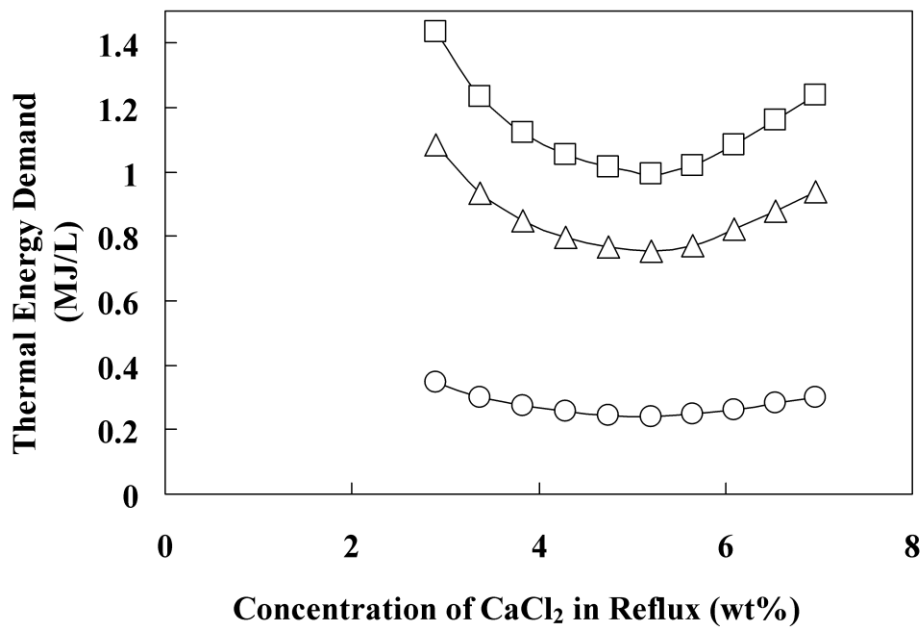
Figure 2-7. Influence of concentration of CaCl$_2$ in reflux on the thermal energy demand of the salt recovery units: (□) total energy demand; (Δ) spray dryer energy demand; (O) electrodialyzer energy demand.
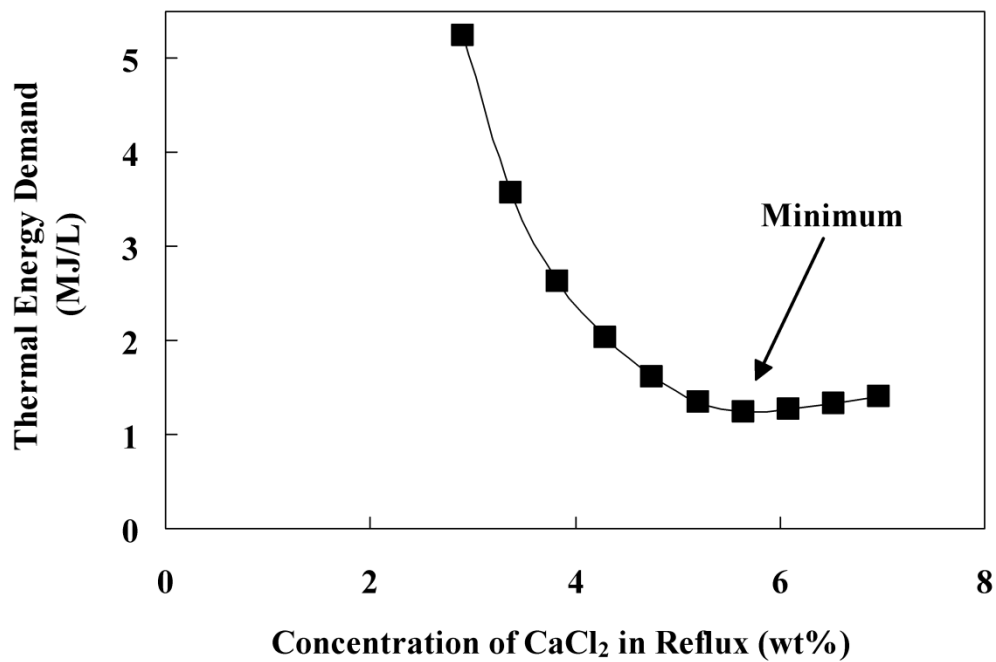
Figure 2-8. Influence of concentration of $CaCl_2$ in reflux on the total thermal energy demand of the salt extractive rectifier and salt recovery units.
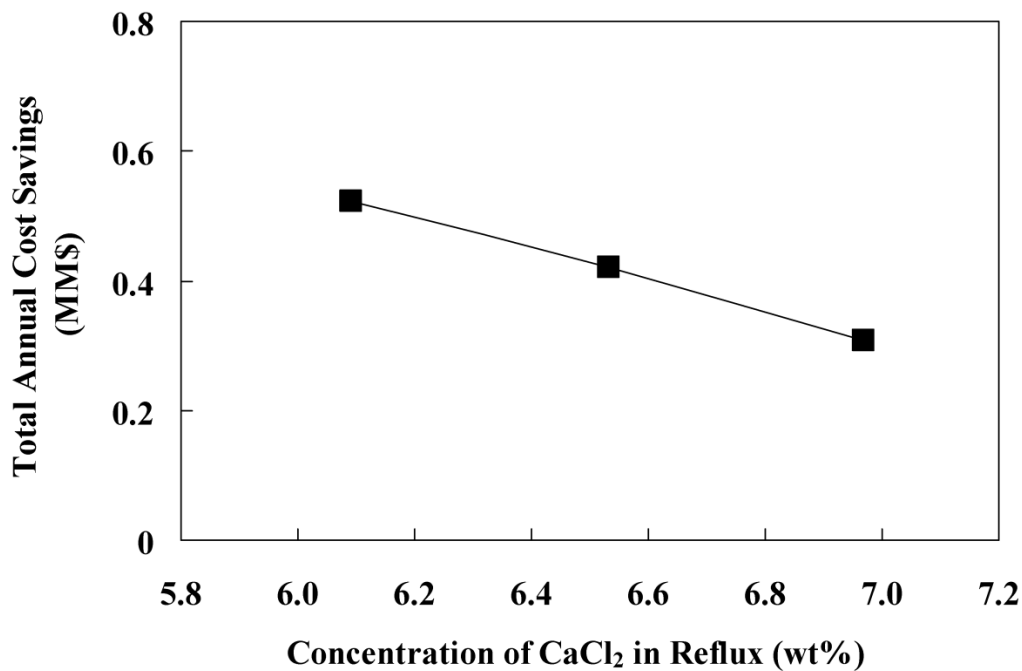
Figure 2-9. Influence of concentration of $CaCl_2$ in reflux on the total annual cost savings.
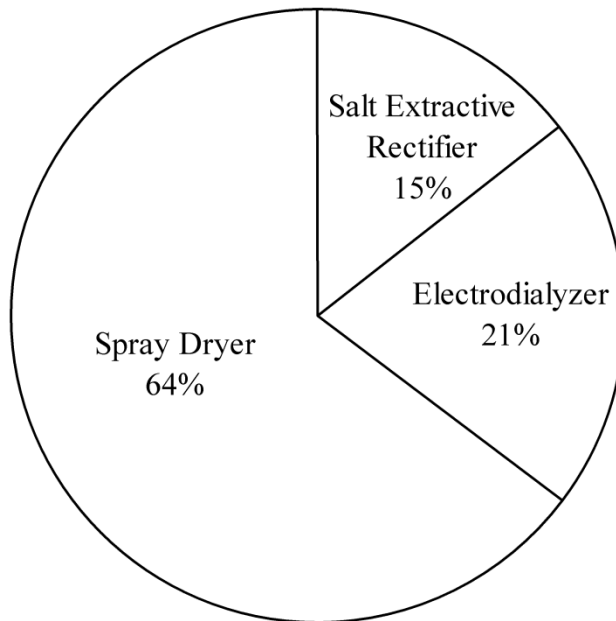
Figure 2-10. Thermal energy demand distribution of individual process units in retrofitted Case II – salt extractive process (total energy demand: 1270 kJ/L).

2.6 Conclusions and Outlook

The approach of fundamentally changing the vapor liquid equilibrium of water-ethanol mixtures by adding a salt was investigated by process simulation towards energy savings for fermentative fuel ethanol production from corn in a dry mill with DDGS production. Salt extractive distillation, with salt recovery enabled by a new scheme of electrodialysis and spray drying, was conceptually integrated in the water-ethanol separation train of a contemporary fermentation based corn-to-fuel ethanol plant for reducing the thermal energy demand. The vapor liquid equilibrium of the water-ethanol-CaCl$_2$ system predicted by the ENRTL-RK property method, with the regressed pair parameters, showed good agreement with experimental data covering the entire range of process conditions. Retrofitted salt extractive distillation resulted in a thermal energy reduction of 28.5% for producing fuel ethanol from an assumed beer column distillate, if the state of the art rectification/adsorption process (Case I) is compared to the salt extractive rectification with salt recovery (Case II). A thermal energy savings potential of 7.7*10^{13} J (as natural gas HHV) per year with a total annual cost savings potential on the order

of $500,000 per year can be estimated for producing 151.4 ML of fuel ethanol (99.5 wt%) per year. An overall maximum energy savings potential of $5.8*10^{16}$ J or about 0.06 Quad (as natural gas HHV) per year could be realized for the targeted 117.4 GL of fuel ethanol to be produced in the U.S in 2022, if fermentation is the process of choice.

2.7 Literature Cited

1. Renewable Fuels Association (RFA). Available at: http://www.ethanolrfa.org. Accessed May 4, 2010.

2. Graboski MS. *Fossil Energy Use in the Manufacture of Corn Ethanol. Prepared for the National Corn Growers Association.* Denver, CO.: Colorado School of Mines; 2002.

3. Keeney DR, DeLuca TH. Biomass as an energy source for the midwestern U.S. *Am. J. Alternate. Agr.* 1992;7:137-144.

4. Lorenz D, Morris D. *How Much Energy Does It Take to Make a Gallon of Ethanol?* Minneapolis, MN.: Institute for Local Self-Reliance; 1995.

5. Pimentel D. Limits of Biomass Utilization. In: Meyers RA, ed. *Encyclopedia of physical science and technology.* Vol 2. 3 ed. San Diego, U.S.: Academic Press; 2002:159-171.

6. Pimentel D. Ethanol fuels: energy balance, economics, and environmental impacts are negative. *Natural Resources Research.* 2003;12:127-134.

7. Shapouri H, Duffield JA, Graboski MS. *Estimating the Net Energy Balance of Corn Ethanol. Agricultural Economic Report Number 721.* Washington DC: United States Department of Agriculture; July 1995.

8. Shapouri H, Duffield JA, Wang M. *The Energy Balance of Corn Ethanol: An Update. Agricultural Economic Report Number 813.* Washington DC: United States Department of Agriculture; July 2002.

9. Eidman VR. Ethanol Economics of Dry Mill Plants: Chapter 3 in Corn-Based Ethanol in Illinois and the U.S.; A Report from the Department of Agricultural and Consumer Economics, University of Illinois, November 2007. Available at: http://www.farmdoc.illinois.edu/policy/research_reports/ethanol_report/index.html. Accessed May 4, 2010.

10. Kwiatkowski JR, McAloon AJ, Taylor F, Johnston DB. Modeling the process and costs of fuel ethanol production by the corn dry-grind process. *Ind. Crops Prod.* 2006;23:288-296.

11. Mueller S, Cuttica J. Research Investigation for the Potential Use of Illinois Coal in Dry Mill Ethanol Plants. Energy Resources Center, University of Illinois at Chicago, October 2006. Available at: http://www.chpcentermw.org/12-00_library.html. Accessed May 4, 2010.

12. Wang M, Hong MW, Huo H. Life-cycle energy and greenhouse gas emission impacts of different corn ethanol plant types. *Environ. Res. Lett.* 2007;2:1-13.

13. Jackson MD, Moyer CB. Alcohol Fuels. *Kirk-Othmer Encyclopedia of Chemical Technology: [e-book]*: NY: Wiley; 2000. Available from: Wiley online library. Accessed May 4, 2010.

14. Meredith J. Understanding Energy Use and Energy Users in Contemporary Ethanol Plants. In: Jacques KA, Lyons TP, Kelsall DR, eds. *The Alcohol Textbook*. Fourth ed. Thrumpton, U.K.: Nottingham University Press; 2003:355-361.

15. Côté P, Noël G, Moore S. The Chatham demonstration: From design to operation of a 20 m^3/d membrane-based ethanol dewatering system. *Desalination.* 2010;250:1060-1066.

16. Griend DLV. Ethanol Distillation Process. U.S. Patent 7,297,236 B1. Nov 20, 2007.

17. Shapouri H, Gallagher P. *USDA's 2002 Ethanol Cost-of-Production Survey. Agricultural Economic Report Number 841.* Washington DC: United States Department of Agriculture; July 2005.

18. Summers DR, Ehmann D. Enhanced V-Grid Trays Increase Column Performance. Presented at the AIChE Annual Meeting, Indianapolis, IN, November 2002.

19. Swain RLB. Molecular Sieve Dehydrators: Why They Became the Industry Standard and How They Work. In: Ingeldew WM, Kelsall DR, Austin GD, Kluhspies C, eds. *The Alcohol Textbook*. Fifth ed. Thrumpton, U.K.: Nottingham University Press; 2009:379-384.

20. Vane LM. Separation technologies for the recovery and dehydration of alcohols from fermentation broths. *Biofuels, Bioprod. Biorefin.* 2008;2:553-588.

21. Côté P, Roy C, Bernier N. Energy reduction in the production of ethanol by membrane dehydration. *Sep. Sci. Technol.* 2009;44:110-120.

22. Vane LM, Alvarez FR. Membrane-assisted vapor stripping: energy efficient hybrid distillation-vapor permeation process for alcohol-water separation. *Journal of Chemical Technology and Biotechnology*. 2008;83:1275-1287.

23. Vane LM, Alvarez FR, Huang Y, Baker RW. Experimental validation of hybrid distillation-vapor permeation process for energy efficient ethanol-water separation. *Journal of Chemical Technology and Biotechnology*. 2010;85:502-511.

24. Karuppiah R, Peschel A, Grossmann IE, Martin M, Martinson W, Zullo L. Energy optimization for the design of corn-based ethanol plants. *AIChE J.* 2008;54:1499-1525.

25. Furter WF. Salt effect in distillation : A technical review. *Chem. Eng. (Rugby, U. K.).* 1968;46:CE173-CE177.

26. Furter WF. Salt effect in distillation : A literature-review II. *Can. J. Chem. Eng.* 1977;55:229-239.

27. Furter WF. Production of fuel-grade ethanol by extractive distillation employing the salt effect. *Sep. Purif. Methods.* 1993;22:1-21.

28. Furter WF, Cook RA. Salt effect in distillation - a literature review. *Int. J. Heat Mass Transfer.* 1967;10:23-36.

29. Cook RA, Furter WF. Extractive distillation employing a dissolved salt as separating agent. *Can. J. Chem. Eng.* 1968;46:119-123.

30. Siklós J, Timár L, Ország I, Ratkovics F. A simulation of the distillation of ethanol-water mixtures containing salts. *Hung. J. Ind. Chem.* 1982;10:309-316.

31. Cespedes AP, Ravagnani SP. Modelado y simulación del proceso de destilacion extractiva salina de etanol. *Inf. Tecnol.* 1995;6:17-20.

32. Ligero EL, Ravagnani TMK. Simulation of salt extractive distillation with spray dryer salt recovery for anhydrous ethanol production. *J. Chem. Eng. Jpn.* 2002;35:557-563.

33. Ligero EL, Ravagnani TMK. Dehydration of ethanol with salt extractive distillation - A comparative analysis between processes with salt recovery. *Chem. Eng. Process.* 2003;42:543-552.

34. Lynd LR, Grethlein HE. IHOSR/Extractive distillation for ethanol separation. *Chem. Eng. Prog.* 1984:59-62.

35. Schmitt D, Vogelpohl A. Distillation of ethanol - water solutions in the presence of potassium acetate. *Sep. Sci. Technol.* 1983;18:547-554.

36. Ravagnani SP, Reis PR. Modelo de orden reducido aplicado a una columna de destilacion extractiva salina. *Inf. Tecnol.* 2000;11:43-50.

37. Torres JL, Grethlein HE, Lynd LR. Computer simulation of the Dartmouth process for separation of dilute ethanol water mixtures. *Appl. Biochem. Biotechnol.* 1989;20-1:621-633.

38. Barba D, Brandani V, Digiacomo G. Hyperazeotropic ethanol salted-out by extractive distillation - theoretical evaluation and experimental check. *Chem. Eng. Sci.* 1985;40:2287-2292.

39. Llano-Restrepo M, Aguilar-Arias J. Modeling and simulation of saline extractive distillation columns for the production of absolute ethanol. *Comput. Chem. Eng.* 2003;27:527-549.

40. Pinto RTP, Wolf-Maciel MR, Lintomen L. Saline extractive distillation process for ethanol purification. *Comput. Chem. Eng.* 2000;24:1689-1694.

41. Elander RT, Putsche VL. Ethanol from Corn: Technology and Economics. In: Wyman CE, ed. *Handbook on Bioethanol: Production and Utilization*. Washington, DC: Taylor & Francis; 1996:329-349.

42. Kelsall DR, Piggot R. Grain Milling and Cooking for Alcohol Production: Designing for the Options in Dry Milling. In: Ingeldew WM, Kelsall DR, Austin GD, Kluhspies C, eds. *The Alcohol Textbook*. Fifth ed. Thrumpton, U.K.: Nottingham University Press; 2009:161-175.

43. Russell I. Understanding Yeast Fundamentals. In: Jacques KA, Lyons TP, Kelsall DR, eds. *The Alcohol Textbook*. Fourth ed. Thrumpton, U.K.: Nottingham University Press; 2003:85-119.

44. Seader JD, Henley EJ. *Separation Process Principles*. Second ed. New York: Wiley; 2006.

45. Sata T. *Ion Exchange Membranes: Preparation, Characterization, Modification and Application*. Cambridge, U.K.: Royal Society of Chemistry; 2004.

46. Strathmann H. *Ion-Exchange Membrane Separation Processes*. First ed. Amsterdam, The Netherlands: Elsevier; 2004.

47. Pfromm PH. Low effluent processing in the pulp and paper industry: Electrodialysis for continuous selective chloride removal. *Sep. Sci. Technol.* 1997;32:2913-2926.

48. Masters K. *Spray Drying Handbook*. Fourth ed. London: George Godwin; 1985.

49. Oakley DE. Spray dryer modeling in theory and practice. *Drying Technol.* 2004;22:1371-1402.

50. Maiorella B, Wilke CR, Blanch HW. Alcohol Production and Recovery. In: Fiechter A, ed. *Advances in Biochemical Engineering.* Vol 20. Berlin: Springer-Verlag; 1981:43-92.

51. Aspen Physical Property System - Physical Property Methods ver. 2006.5. Aspen Technology, Inc., Cambridge, MA.

52. Redlich O, Kwong JNS. On the thermodynamics of solutions. V. An equation of state. Fugacities of gaseous solutions. *Chem. Rev. (Washington, DC, U. S.)*. 1949;44:233-244.

53. Renon H, Prausnitz JM. Local compositions in thermodynamic excess functions for liquid mixtures. *AIChE J.* 1968;14:135-144.

54. Chau-Chyun C, Britt HI, Boston JF, Evans LB. Local composition model for excess Gibbs energy of electrolyte systems. Part I: Single solvent, single completely dissociated electrolyte systems. *AIChE J.* 1982;28:588-596.

55. Chen CC, Evans LB. A local composition model for the excess Gibbs energy of aqueous-electrolyte systems. *AIChE J.* 1986;32:444-454.

56. Mock B, Evans LB, Chen CC. Thermodynamic representation of phase-equilibria of mixed-solvent electrolyte systems. *AIChE J.* 1986;32:1655-1664.

57. Britt IH, Luecke RH. The estimation of parameters in nonlinear, implicit models. *Technometrics.* 1973;15:233-247.

58. Aden A, Ruth M, Ibsen K, et al. *Lignocellulosic Biomass to Ethanol Process Design and Economics Utilizing Co-current Dilute Acid Prehydrolysis and Enzymatic Hydrolysis for Corn Stover.NREL/TP-510-32438*: NREL; 2002.

59. Othmer DF, Moeller WP, Englund SW, Christopher RG. Composition of vapors from boiling binary solutions - recirculation-type still and equilibria under pressure for ethyl alcohol-water system. *Ind. Eng. Chem.* 1951;43:707-711.

60. Kurihara K, Nakamichi M, Kojima K. Isobaric vapor-liquid-equilibria for methanol+ethanol+water and the 3 constituent binary-systems. *J. Chem. Eng. Data.* 1993;38:446-449.

61. Beebe AH, Jr. C, K.E., Lindsay RA, Baker EM. Equilibria in ethanol-water system at pressures less than atmospheric. *Ind. Eng. Chem.* 1942;34:1501-1504.

62. Pemberton RC, Mash CJ. Thermodynamic properties of aqueous non-electrolyte mixtures .2. Vapor-pressures and excess Gibbs energies for water+ethanol at 303.15-K to 363.15-K determined by an accurate static method. *J. Chem. Thermodyn.* 1978;10:867-888.

63. Rashin AA, Honig B. Reevaluation of the Born model of ion hydration. *J. Phys. Chem.* 1985;89:5588-5593.

64. Robinson RA, Stokes RH. *Electrolyte Solutions*. 2nd ed. London: Butterworths; 1970.

65. Sako T, Hakuta T, Yoshitome H. Vapor-pressures of binary (H_2O-Hcl, H_2O-$MgCl_2$, and H_2O-$CaCl_2$) and ternary (H_2O-$MgCl_2$-$CaCl_2$) aqueous-solutions. *J. Chem. Eng. Data.* 1985;30:224-228.

66. Nishi Y. Vapor-liquid equilibrium relations for the system accompanied by hypothetical chemical reaction containing salt. *J. Chem. Eng. Jpn.* 1975;8:187-191.

67. Meyer T, Polka HM, Gmehling J. Low-pressure isobaric vapor-viquid-equilibria of ethanol water mixtures containing electrolytes. *J. Chem. Eng. Data.* 1991;36:340-342.

68. Mishima K, Iwai Y, Yamaguchi S, Isonaga H, Arai Y, Hongo M. Correlation of vapor - liquid equilibria of ethanol-water-calcium chloride and methanol-ethanol-calcium chloride systems at 25° C. *Mem. Fac. Eng., Kyushu Univ. (1943-1999).* 1986;46:407-433.

Chapter 3 - Reducing the energy demand of cellulosic ethanol through salt extractive distillation enabled by electrodialysis

3.1 Abstract

One of the main challenges when a biochemical conversion technique is employed to produce cellulosic ethanol is the low concentration of ethanol in the fermentation broth, which increases the energy demand for recovering and purifying ethanol to fuel grade. In this study, two design cases implementing salt extractive distillation – with salt recovery enabled by a novel scheme of electrodialysis and spray drying – along with heat integrated distillation techniques of double-effect distillation and direct vapor recompression are investigated through process simulation with Aspen Plus$^{®}$ 2006.5 for reducing the thermal energy demand. Conventional distillation along with molecular sieve based dehydration is considered as the base case. Salt extractive distillation along with direct vapor recompression is found to be the most economical ethanol recovery approach for cellulosic ethanol with a thermal energy demand of 7.1 MJ/L (natural gas energy equivalents, higher heating value), which corresponds to a thermal energy savings of 23% and cost savings of 12% relative to the base case separation train thermal energy demand and total annual cost.[b]

---

[b] Submitted manuscript to Separation Science and Technology (2011), by Hussain, M. A. M.; and Pfromm, P. H.

3.2 Introduction

Currently, corn-ethanol is the most widely produced biofuel in the U.S.[1] The expanded Renewable Fuel Standard (RFS2), established under the Energy Independence and Security Act (EISA) of 2007, mandates the production of 136.3 GL/year of renewable fuels in 2022: 56.8 GL/year of corn-ethanol, 60.6 GL/year of second generation biofuels such as cellulosic ethanol, and 18.9 GL/year of advanced biofuels such as biomass-based diesel.[1] In order to meet the specific renewable fuel production volume and green house gas emission reduction requirements of RFS2, transitioning of the feedstock from corn to cellulosic sources for future production of bioethanol is essential. Cellulosic ethanol can be produced through biochemical and thermochemical conversion processes.[2-15] In a biochemical conversion process, the cellulosic feedstock is chemically or enzymatically hydrolyzed to sugars for subsequent microbial fermentation to ethanol. While in a thermochemical process, the cellulosic feedstock is gasified to produce syngas which is converted into ethanol through microbial fermentation or catalytic reactions. The principal advantages of the biochemical conversion process include relatively low capital costs, less dependence on economy of scale for profitability, high selectivity and conversion efficiencies.[15-18] However, there are several key challenges in various areas of the biochemical conversion process that need to be addressed.[3, 8, 9, 11, 19] In the product recovery area, the main disadvantage is the dilute nature of the fermentation broth with ethanol concentration varying from about 3 to 6 wt%,[2, 9, 10, 14, 20-23] compared to about 10 to 15 wt% for corn-ethanol.[24-28] Recovering ethanol from fermentation broth and purifying to fuel grade is difficult and energy intensive because of the dilute nature of the fermentation broth and the challenging water-ethanol vapor liquid equilibrium (VLE) with an azeotrope at about 96 wt% ethanol and tangential approach of the water-ethanol equilibrium curve to the 45° line at high ethanol concentrations in the familiar y-x VLE diagram representation. Simple distillation cannot be used to distill ethanol above the azeotropic composition. The state of the art technique used in the corn-ethanol industry to produce fuel ethanol is distillation close to the azeotropic composition followed by dehydration in a molecular sieve based adsorption unit.[25, 26, 29, 30] A similar technique can be used for recovering and purifying ethanol from the fermentation broth obtained from cellulosic feedstock. However, there is a drastic increase in the distillation energy demand as the ethanol concentration in the fermentation broth decreases.[24, 31-33]

Heat integrated distillation operations such as multi-effect distillation and vapor recompression can reduce distillation energy demand. These energy saving techniques have been shown to significantly reduce the distillation energy demand for the water-ethanol system;[34-44] for instance, distillation energy demand reduction on the order of 42% has been reported for double-effect distillation with a split feed compared to conventional distillation with a single column for distilling 93 wt% ethanol from a feed containing 7 wt% ethanol.[37] Conversely, the VLE of the water-ethanol system can be improved towards ethanol separation by dissolving a salt in the liquid phase to raise the equilibrium vapor ethanol content.[45-48] In addition to "salting out" ethanol this may also break the azeotrope.[45, 47, 49] For example, starting with 70 wt% ethanol in water, 99.6 wt % ethanol was distilled using potassium acetate as the salt requiring only a quarter of the energy needed to obtain an inferior 93 wt% ethanol by conventional distillation.[50] Efficient recovery and reuse of the salt used as the separating agent is, however, crucial. Potassium acetate[34, 49-56] and calcium chloride[51, 55, 57-59] have been reported for water-ethanol separation utilizing the "salting out" effect. The use of the salt separating agent in a process with tightly closed water cycles such as the cellulosic bioethanol plant requires that the salt not impact other processing areas negatively. In this study, calcium chloride was selected for the following reasons: low cost, large "salting out" effect [51, 55] and compatibility with fermentation.

In a salt extractive distillation column, the salt is usually dissolved in the reflux stream and introduced at the top of the column. Unlike the liquid extractive agents such as ethylene glycol, salt is non-volatile and always remains in the liquid phase; thereby, enabling the production of a high purity distillate free of salt. The salt moves downward in the column and is recovered and purified from the distillation column bottoms for re-use in the top of the column. Hence, there are two distinct steps involved: salt extractive distillation and salt recovery/purification. Corrosion due to aqueous ethanolic salt solutions requires consideration in regards to materials of construction.[57, 60] Other issues are related to solids handling, feeding and dissolving salt in the reflux stream, potential decrease in plate efficiency, and foaming inside the column.[45, 47, 49] In the study presented here, the possible benefit in terms of energy demand is established, demonstrating that the concept may be attractive enough to deal with the possible complications.

There are many experimental and theoretical studies[34, 49-59] on producing fuel ethanol by utilizing the "salting out" effect, but most of them focus only on the salt extractive distillation

step. Moreover, the studies[34, 45, 47, 52-54, 56, 57] which include both steps of salt extractive distillation and salt recovery do not generally consider techniques other than evaporation and drying for salt recovery. Evaporative salt concentration/crystallization and solids drying techniques are energy intensive. Reducing the energy demand for the salt recovery step becomes essential to reap the benefit of salt-induced VLE improvement. In this study, a combination of electrodialysis and spray drying is investigated. The salt extractive column bottoms stream is pre-concentrated by electrodialysis and dried to an anhydrous state by spray drying. In electrodialysis, the dilute salt solution is concentrated by selectively separating the salt ions from the solution[61, 62] rather than evaporating water; therefore, requiring less energy than that of an evaporative process. Moreover, electrodialysis is rugged and can be operated at high ionic strengths.[63] Final recovery of dry salt is achieved through spray drying, which is a widely used unit operation to convert a liquid feed containing salt into dry solid particles in a single step.[64, 65]

The main goal of this study is to combine the relative advantages of heat-integrated distillation and salt extractive distillation towards reducing the overall energy demand for recovering and purifying ethanol from the fermentation broth of a cellulosic ethanol facility. Two different design cases implementing heat integrated distillation techniques of double-effect distillation with split feed and direct vapor recompression for stripping ethanol from the fermentation broth, and salt extractive distillation for rectifying the stripped ethanol vapors to fuel grade are considered. For base case, a design scheme comprising conventional distillation and molecular sieve based adsorption for recovering and purifying ethanol from the fermentation broth is adapted from the National Renewable Energy Laboratory (NREL) process design for cellulosic ethanol production.[2] The design cases are investigated for energy demand reduction and economic viability through process simulation and economic analysis with Aspen Plus® 2006.5 and Aspen Icarus Process Evaluator® 2006.5 respectively.

3.3 Design Cases

3.3.1 Base Case: Conventional distillation with molecular sieve based dehydration, Case I

The target fuel ethanol production rate was set at 270 ML (2.1 $*10^5$ tonne) per year with an ethanol concentration of 99.5 wt%. Recovery of ethanol from the fermentation broth and further purification to fuel grade is achieved by two distillation columns (beer column and

rectifier) and final water removal by molecular sieve based adsorption as shown in Figure 3-1. Fermentation broth from the beer well with an ethanol concentration of about 5.5 wt% is preheated and fed to the beer column operated as a stripper to remove the dissolved carbon dioxide and to produce a vapor distillate with an ethanol concentration of about 44 wt% and a bottom aqueous stream (stillage), consisting of water, dissolved matter, unfermented solids, proteins, and trace amounts of ethanol. The stripped carbon dioxide stream from the beer column is treated along with the fermenter offgas in a scrubber for recovering and recycling the residual ethanol to the beer well. The vapor distillate from the beer column is fed to the rectifier, producing an enriched overhead product of about 92 wt% ethanol and a bottoms aqueous product with trace amounts of ethanol, which is used as recycle water. In the adsorption cycle of the molecular sieve unit, superheated moist ethanol vapor from the rectifier overhead is dehydrated to fuel grade ethanol by the selective adsorption of water, while in the desorption cycle, the molecular sieve adsorber bed is depressurized and purged with dry product ethanol vapors for regeneration. The regeneration stream from the adsorbers is recycled to the rectifier.
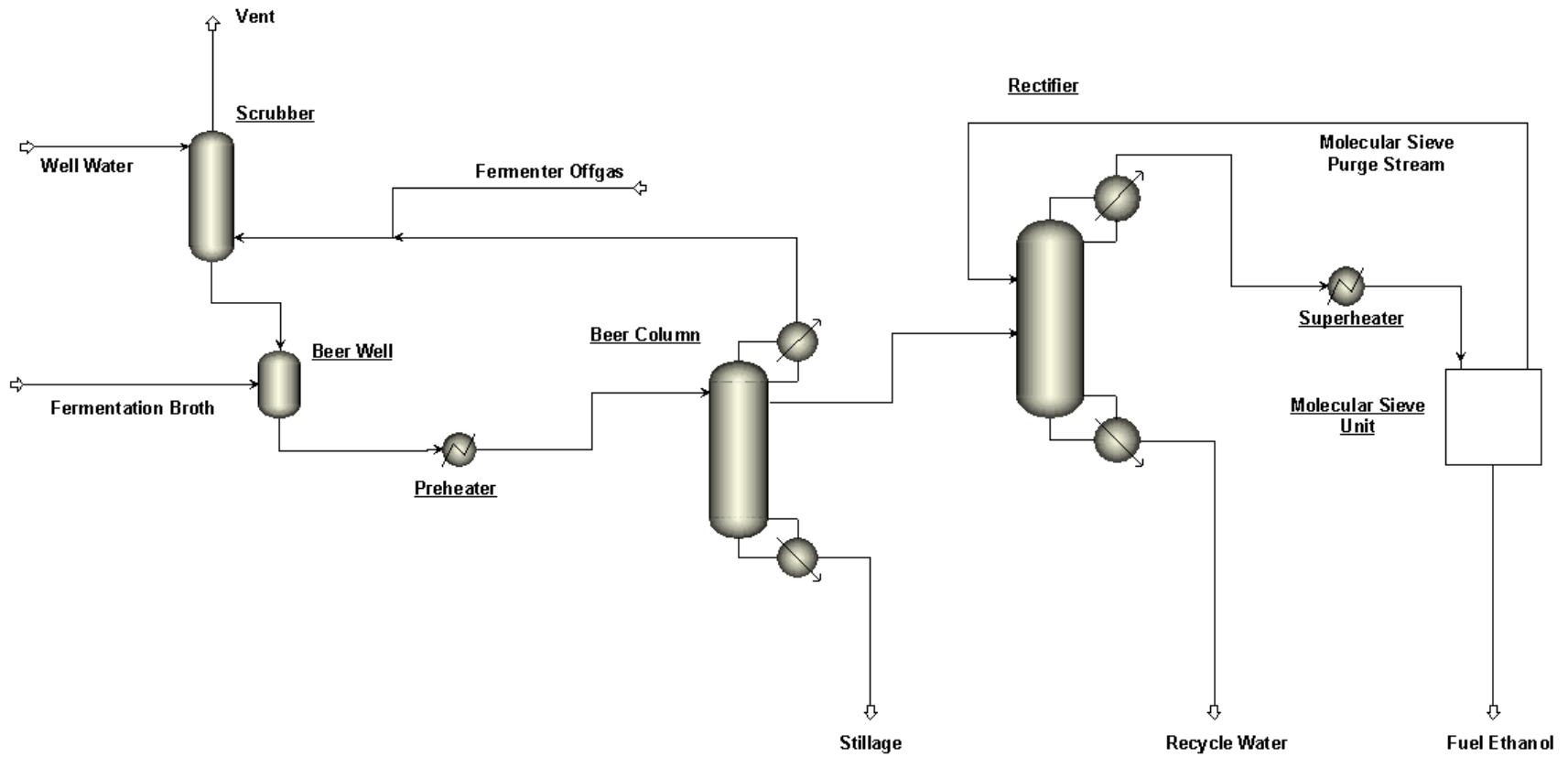
Figure 3-1. Process flow scheme for Case I – base case, conventional distillation with molecular sieve based dehydration.

3.3.2 Salt extractive process with double-effect beer columns, Case II

The efficient recovery and re-use of salt in salt extractive distillation is of paramount importance in regard to the energy demand, capital cost, and process requirements. Since separation and recovery of salt from the highly complex beer column bottoms stream would be a formidable challenge, no salt should be added to the beer column. The rectifier deals with a relatively clean feed stream (the beer column distillate) without solids which facilitates salt recovery from the rectifier bottoms stream. In addition, the VLE of the ethanol-water system is very favorable at the dilute feed conditions. Due to the above reasons, we opted to separately strip the fermentation broth, producing a distillate free of solids for subsequent purification in a salt extractive rectifier to fuel grade ethanol. This eliminates the molecular sieve unit. Double-effect distillation with split feed for stripping ethanol from the fermentation broth is used to reduce the significant energy demand by conventional means. Salt extractive distillation for final purification to fuel grade ethanol is considered (Figure 3-2). After initial preheating, fermentation broth from the beer well is treated in a degasser and cooler arrangement to remove the dissolved carbon dioxide, which is sent to the scrubber to recover and recycle the residual ethanol to the beer well. After carbon dioxide removal, the liquid stream from the flash tank is split into two streams and fed to two beer columns (BC1 and BC2) operating in parallel. Overhead vapor distillate from BC2 is condensed to provide the reboiling duty of BC1. The operating pressures of BC1 and BC2, and the feed split ratio between them has to be adjusted, respectively, to provide sufficient temperature driving force (weighted average LMTD = 10 K) in the reboiler-condenser and to balance the reboiling duty of BC1 with the condensing duty of BC2. Then, the overhead streams from BC1 and BC2 are purified in the salt extractive rectifier directly to fuel grade ethanol. The salt extractive rectifier bottoms stream is divided into diluate and concentrate for the electrodialysis process. After receiving the salt from the diluate, the salt enriched in the concentrate stream is recovered by evaporating the remaining water with hot natural gas combustion gases in a co-current spray dryer before recycling to the salt extractive rectifier reflux.
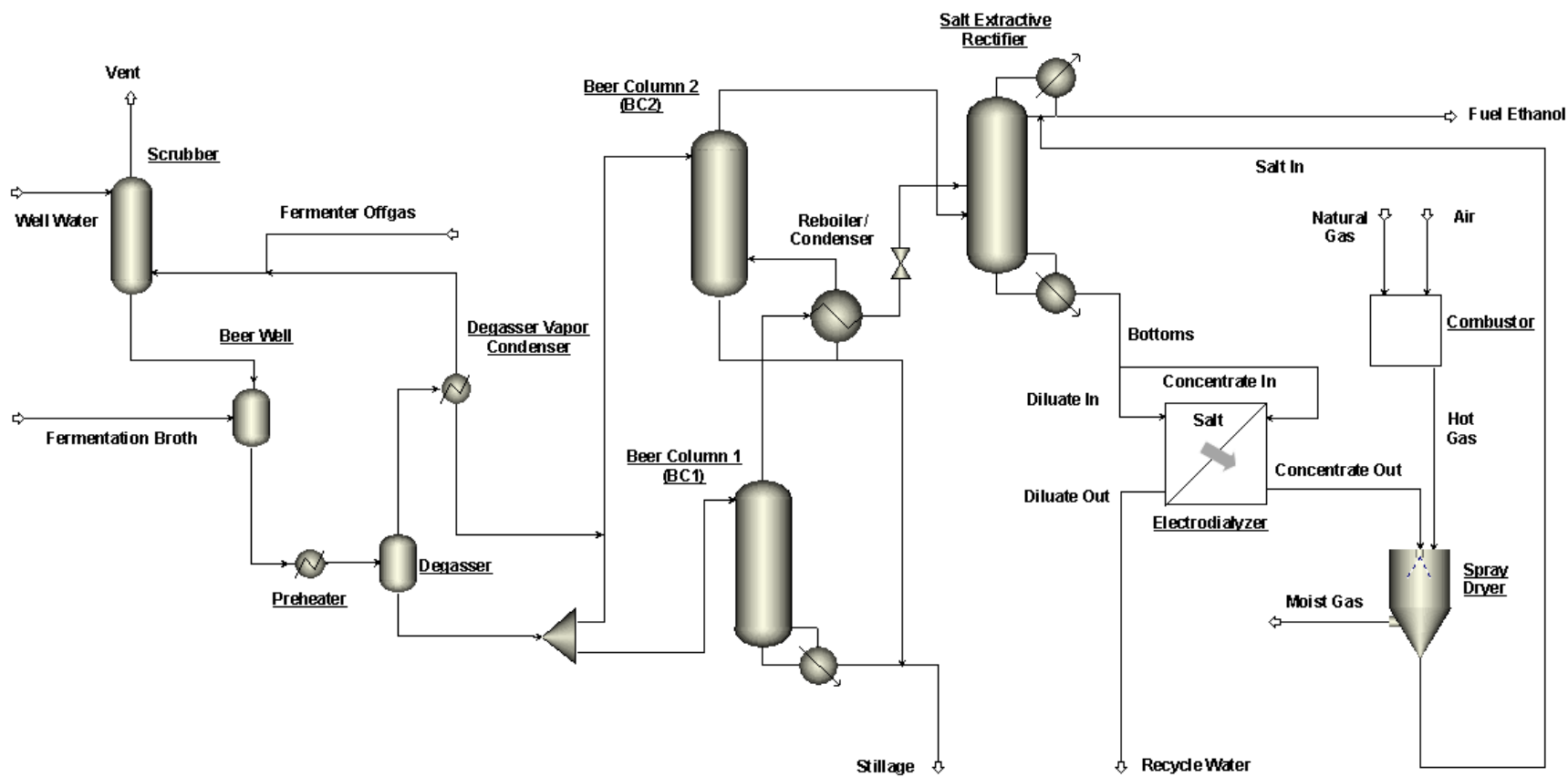
Figure 3-2. Process flow scheme for Case II – salt extractive process with double-effect beer columns.

3.3.3 Salt extractive process with direct vapor recompression for beer column, Case III

In Case III (Figure 3-3), direct vapor recompression reduces the energy demand for stripping the fermentation broth. After removal of carbon dioxide and preheating to essentially saturated liquid conditions, fermentation broth is fed to the beer column. The overhead vapor distillate from the beer column is compressed and then condensed in the reboiler-condenser at the bottom of the beer column; thereby, providing the reboiling duty. Sufficient temperature driving force (weighted average LMTD = 10 K) in the reboiler–condenser is maintained by adjusting the compressor outlet pressure. Afterwards, the beer column distillate is purified to the fuel grade level in the salt extractive rectifier as in Case II.

3.3.4 Summary of energy demand comparison approach

Comparing energy demands for different processing schemes is complex. Heat integration interconnects unit operations, and different qualities of energy (2nd law of thermodynamics based balance, for example, thermal vs. electrical) besides the simple quantity of energy (1st law of thermodynamics based balance) impact both economics and environmental issues such as green house gas emissions.

The input data and specified parameters for Case I (base case, Figure 3-1), Case II (salt extractive process with double-effect beer columns, Figure 3-2) and Case III (salt extractive process with direct vapor recompression for beer column, Figure 3-3) are given, respectively, in Table 3-1, Table 3-2, and Table 3-3. Input in all design cases is an identical stream of 412 tonne/h (fermentation broth). Identical streams of fuel ethanol are produced in all of the design cases. The liquid water output streams from the design cases are not identical since water vapor is lost in the spray dryer with the moist air stream in Cases II and III.

The comparison of the energy demand is based on converting all steam and electrical energy to natural gas energy equivalents (HHV) using 80% boiler efficiency to raise steam and 33% efficiency for natural gas to electricity. The thermal energy demand of the spray dryer is directly calculated from the natural gas usage.

Table 3-1.Input data and specified parameters for Case I – base case, conventional distillation with molecular sieve based dehydration

Input Data and Specified Parameters	Base Case
Beer Column	
Number of Stages	16
Operating Pressure (kPa)	193.5
Bottoms Ethanol Concentration (wt%)	0.05
Rectifier	
Number of Stages	36
Operating Pressure (kPa)	172.3
Distillate Ethanol Concentration (wt%)	92.5
Bottoms Ethanol Concentration (wt%)	0.05
Molecular Sieve Unit [a]	
Operating Temperature (K)	389.15
Purge Stream Ethanol Concentration (wt%)	72.3
Fuel Ethanol Concentration(wt%)	99.5

[a] Data taken from Aden et al.[2]

3.4 Methods

Process simulation and economic analysis (see Appendix A) for the design cases are carried out, respectively, with Aspen Plus® 2006.5 and Aspen Icarus Process Evaluator® 2006.5. The thermodynamic property method used in modeling the VLE included the Non-Random Two Liquid model (NRTL)[66] for the liquid phase without electrolytes, the Electrolyte Non-Random Two Liquid model (ENRTL)[67-69] for the liquid phase with electrolytes, the Redlich-Kwong (R-K) equation of state for the vapor phase[70], and the Henry's law for the dissolved gases. The default property parameters in Aspen Properties® 2006.5 are used for all the thermodynamic models except for the ENRTL model. In case of the ENRTL model, the molecule-electrolyte pair parameters and other property parameters are taken from a previous study by the authors.[71] The distillation columns are rigorously simulated with the RadFrac module of Aspen Plus® 2006.5 using the Newton algorithm. Optimum feed stages for the distillation columns are determined by sensitivity analyses. For modeling the compressor, the Comp block, assuming a centrifugal compressor with a polytropic efficiency of 72 %, is used.

Table 3-2. Input data and specified parameters for Case II – salt extractive process with double-effect beer columns

Input Data and Specified Parameters	Case II
Beer Column 1 (BC1)	
Number of Stages	15
Operating Pressure (kPa)	294.4
Bottoms Ethanol Concentration (wt%)	0.05
Beer Column 2 (BC2)	
Number of Stages	15
Operating Pressure (kPa)	121.6
Bottoms Ethanol Concentration (wt%)	0.05
Reboiler-Condenser	
Weighted LMTD (K)	10
Salt extractive rectifier	
Number of Stages	20 - 60
Operating Pressure (kPa)	101.3
Distillate Ethanol Concentration (wt%)	99.5
Bottoms Ethanol Concentration (wt%)	0.05
Electrodialysis	
Operating Temperature (K)	313.15
Concentration of $CaCl_2$ in Concentrate (wt%)	40
Current Efficiency (%)	90
Spray Dryer	
Hot Gas Temperature (K)	923.15
Moist Gas Temperature (K)	473.15

For the salt extractive rectifier in Case II and Case III, the important parameters are the total number of stages and the $CaCl_2$ concentration profile. To optimize these parameters, initially the total number of stages is fixed, and then the calcium chloride concentration is optimized. Increasing the $CaCl_2$ concentration in the salt extractive rectifier can decrease the reboiler duty because of the improvement in the VLE, but can lead to an increase in salt recovery energy demand because of the increased $CaCl_2$ mass flow. Hence, the $CaCl_2$ concentration in the salt extractive rectifier has to be optimized to achieve a minimum of the sum of the energy requirements for the system. The mass and energy balance calculations for the electrodialyzer, and the spray dryer are separately performed using Microsoft Excel® 2003 and Mathcad® 13. The results are later incorporated in the overall simulation using the User Model feature of Aspen

Plus® 2006.5. After optimizing the calcium chloride concentration in the salt extractive rectifier for different total number of stages, an economic analysis is carried out to determine the optimal total number of stages.

Table 3-3. Input data and specified parameters for Case III – salt extractive process with direct vapor recompression for beer column

Input Data and Specified Parameters	Case III
Beer Column	
Number of Stages	15
Operating Pressure (kPa)	101.3
Bottoms Ethanol Concentration (wt%)	0.05
Compressor	
Outlet Pressure (kPa)	229.1
Reboiler-Condenser	
Weighted LMTD (K)	10
Salt extractive rectifier	
Number of Stages	20 - 50
Operating Pressure (kPa)	101.3
Distillate Ethanol Concentration (wt%)	99.5
Bottoms Ethanol Concentration (wt%)	0.05
Electrodialysis	
Operating Temperature (K)	313.15
Concentration of $CaCl_2$ in Concentrate (wt%)	40
Current Efficiency (%)	90
Spray Dryer	
Hot Gas Temperature (K)	923.15
Moist Gas Temperature (K)	473.15

Figure 3-3. Process flow scheme for Case III – salt extractive process with direct vapor recompression for beer column.

3.5 Results and Discussion

The distillate and bottoms composition for the salt extractive rectifier (Case II, Table 3-2) has been fixed. Therefore, the main parameters for the salt extractive rectifier are the total number of stages, the reflux (mass flow) and the concentration of salt in this reflux stream.

Initially, the total number of stages is fixed to optimize the reflux rate and concentration of salt in the reflux. The following discussion is for a total stage number of 35. It is necessary to at least eliminate the azeotrope so that fuel grade ethanol can be produced at all in a single salt extractive rectifier. This already occurs at about 2.9 wt% of $CaCl_2$ in the reflux. Above this concentration, the thermal energy demand of the salt extractive rectifier steeply declines with increasing $CaCl_2$ concentration in the reflux but this benefit levels out above about 9 wt% (Figure 3-4). The reason is that the distillation pinch point, the point of contact between the operating line and the VLE curve in a McCabe-Thiele diagram, shifts from the location at high ethanol content (tangent pinch) to the feed stage (feed pinch). This shift yields the principal benefit of the salt extractive approach above and beyond eliminating the azeotrope. Further increase in the $CaCl_2$ concentration in the reflux causes an increase in $CaCl_2$ mass flow (Figure 3-5) along with increasing energy demand for salt recovery (Figure 3-6) without significant added benefit. The overall combined energy demand, therefore, shows a minimum at about 9.3 wt% $CaCl_2$ in the reflux due to the competition between energy savings due to facilitated distillation, and energy demand for salt recovery (Figure 3-7). The above mentioned procedure to optimize the concentration of $CaCl_2$ in the reflux is repeated for different total number of stages. When the total number of stages is increased, initially, there is a significant reduction in the overall combined energy demand due to the reduction in the reflux rate and concentration of $CaCl_2$ in the reflux; however, this effect flattens out at higher total number of stages (Figure 3-8). A preliminary economic analysis indicated only marginal annual cost reduction above 50 stages. Hence, 50 stages are considered as economical, and the corresponding optimal concentration of $CaCl_2$ in the reflux is 8.5 wt%. The same procedure is repeated for the salt extractive rectifier in Case III, yielding an economical total stage number of 40, with an optimized calcium chloride concentration of 9.9 wt% in the reflux.
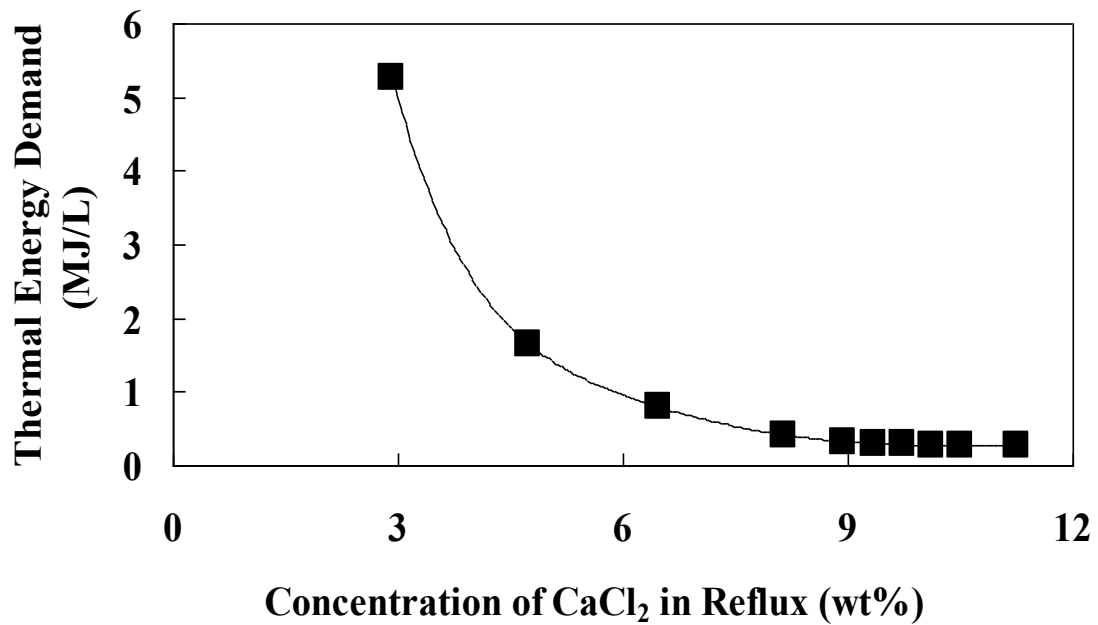
Figure 3-4. Influence of concentration of $CaCl_2$ in reflux on the thermal energy demand of the salt extractive rectifier (total number of stages =35).
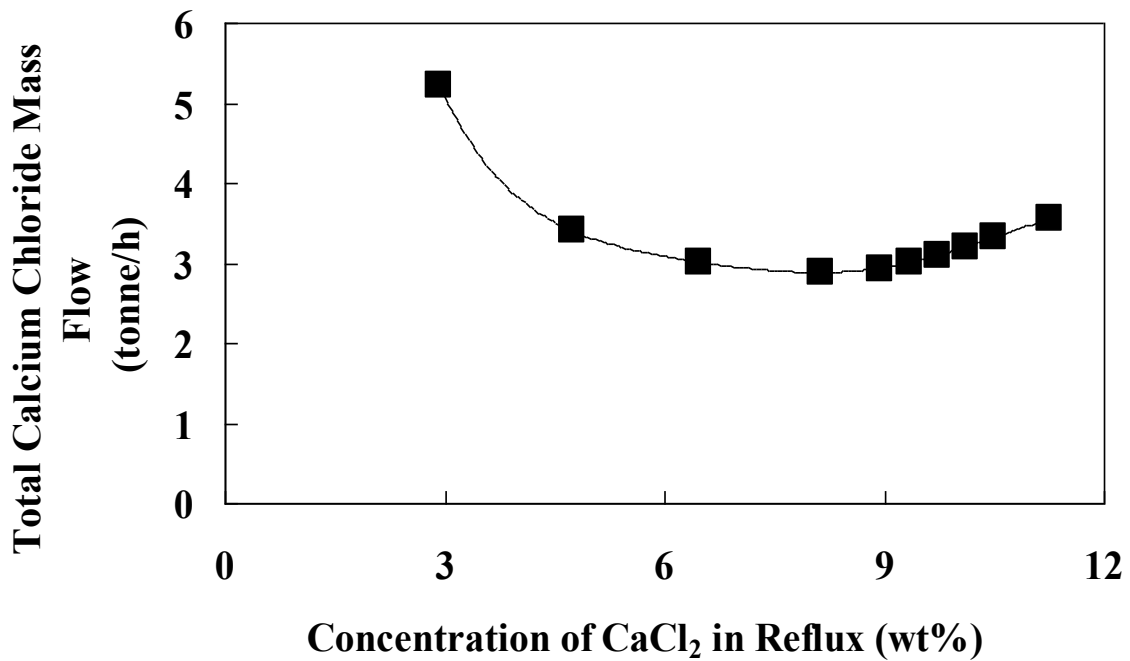
Figure 3-5. Influence of concentration of $CaCl_2$ in reflux on the total CaCl2 mass flow to the salt extractive rectifier (total number of stages =35).
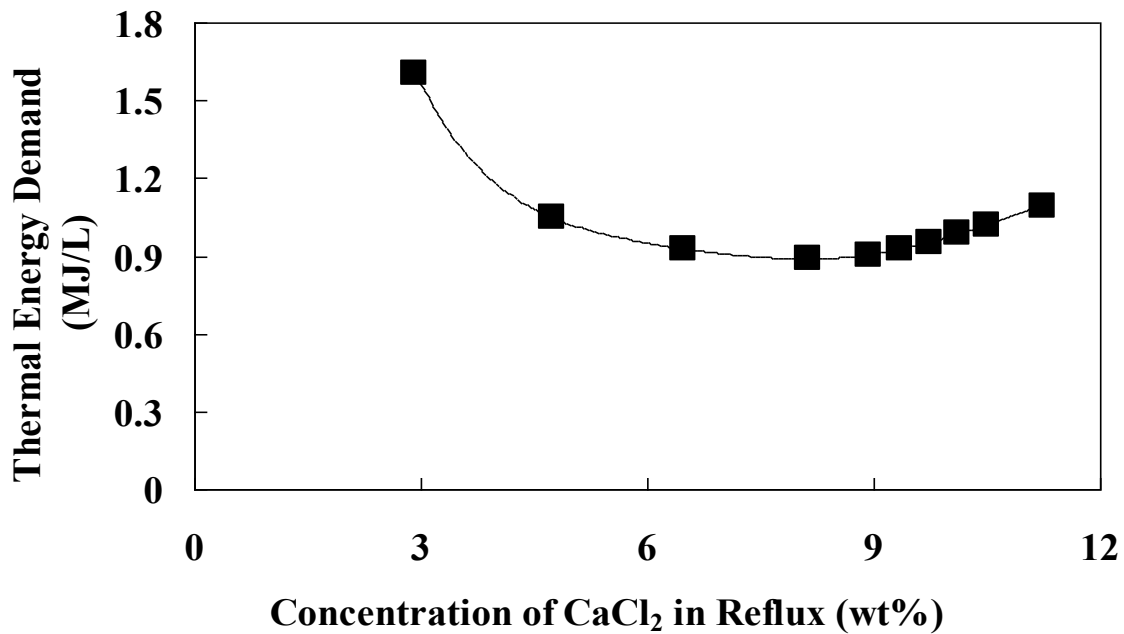
Figure 3-6. Influence of concentration of $CaCl_2$ in reflux on the thermal energy demand of the salt recovery units (total number of stages in the salt extractive rectifier =35).
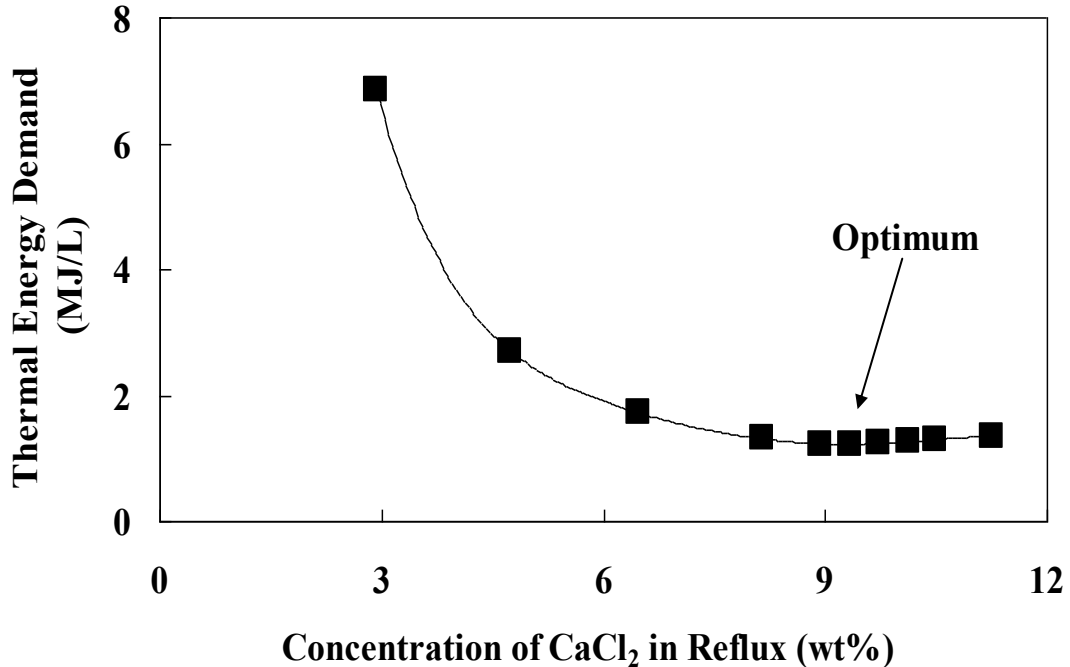
Figure 3-7. Influence of concentration of $CaCl_2$ in reflux on the total thermal energy demand of the salt extractive rectifier (total number of stages =35) and salt recovery units.
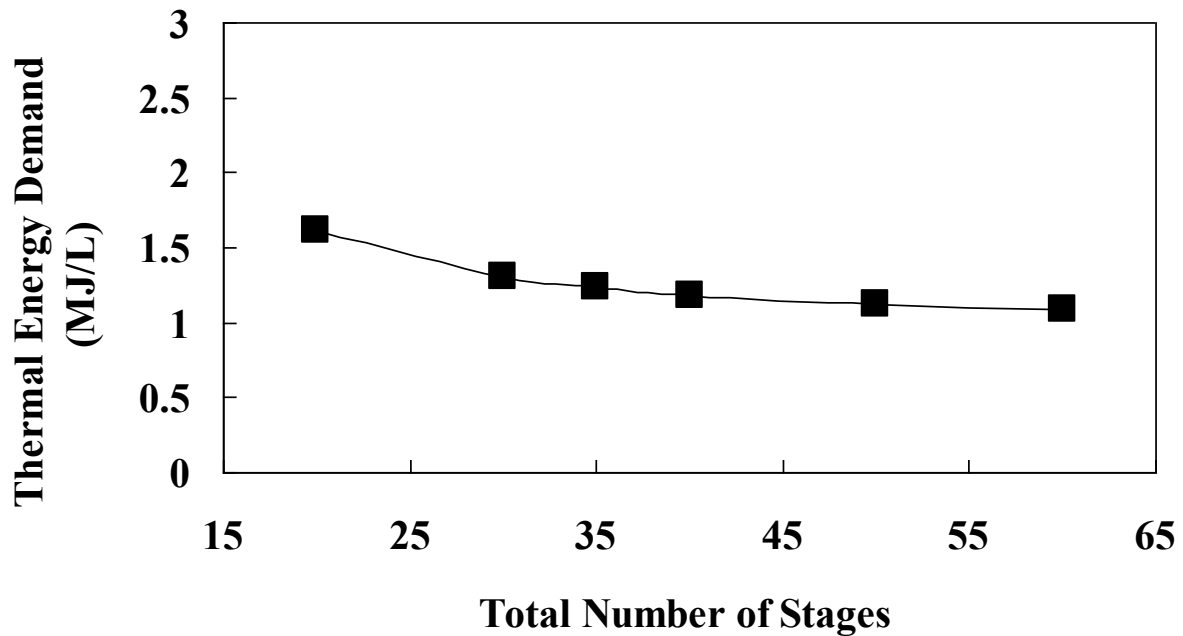
Figure 3-8. Influence of total number of stages in the salt extractive rectifier on the total thermal energy demand of the salt extractive rectifier and salt recovery units.

The results comparing the overall energy demand and process economics for the design cases are shown in Table 3-4. Both alternative design cases show substantial energy demand reduction when compared to the base case. Case III – salt extractive process with direct vapor recompression for beer column, provides an overall process energy demand reduction of 23.1%, while Case II – salt extractive process with double-effect beer columns, provides an overall process energy demand reduction of 12.8%. Case III shows higher energy demand reduction mainly due to the substantial energy demand reduction for the beer column through heat recovery by vapor recompression. Based on the overall process economics, Case III is the most economical process alternative with a total annual cost reduction on the order of MM$2.4, when compared to the base case.

71

Table 3-4 Comparison of thermal energy demand and total annual cost savings for the design cases

Design Variant[a]	Thermal Energy Demand (MJ/L)	Thermal Energy Demand Reduction (%)	Total Annual Cost Savings (MM$/year)	Total Annual Cost Savings (%)
Case I	9.2	--	--	--
Case II	8.1	12.8	1.6	8.1
Case III	7.1	23.1	2.4	12.4

[a] Case I: Base case, conventional distillation with molecular sieve based dehydration; Case II: Salt extractive process with double-effect beer columns; Case III: Salt extractive process with direct vapor recompression for beer column.

3.6 Conclusions and Outlook

In this study, two process designs implementing salt extractive distillation together with heat integrated distillation techniques of double-effect distillation and direct vapor recompression are investigated as possible alternatives to a base case comprising conventional distillation and molecular sieve based adsorption for recovering and purifying ethanol from the fermentation broth of a cellulosic fuel ethanol facility. Further, a systematic process simulation procedure is used to optimize the process conditions for salt extractive distillation, with salt recovery enabled by a novel scheme of electrodialysis and spray drying. While, both the design alternatives, Case II – salt extractive process with double-effect beer columns, and Case III – salt extractive process with direct vapor recompression for beer column, show significant thermal energy demand reduction and total annual cost savings, Case III is found to be the best economical alternative. A thermal energy savings potential of $5.7*10^{14}$ J (as natural gas HHV) per year with a total annual cost savings potential on the order of MM$2.4 per year can be estimated for producing 270 ML of fuel ethanol (99. 5 wt%) per year. An overall maximum energy savings potential of $1.3*10^{17}$ J or about 0.13 Quad (as natural gas HHV) per year could be realized for the targeted 60.6 GL of cellulosic biofuel to be produced in the U.S in 2022, if fermentation based cellulosic ethanol is used to achieve this target.

3.7 Literature Cited

1. Renewable Fuels Association (RFA). Available at: http://www.ethanolrfa.org. Accessed August 4, 2011.

2. Aden, A.; Ruth, M.; Ibsen, K.; Jechura, J.; Neeves, K.; Sheehan, J.; Wallace, B.; Montague, L.; Slayton, A.; Lukas, J. *Lignocellulosic Biomass to Ethanol Process Design and Economics Utilizing Co-current Dilute Acid Prehydrolysis and Enzymatic Hydrolysis for Corn Stover.NREL/TP-510-32438*; NREL: 2002.

3. Anex, R. P.; Kazi, F. K.; Fortman, J. A.; Hsu, D. D.; Aden, A.; Dutta, A.; Kothandaraman, G., Techno-economic comparison of process technologies for biochemical ethanol production from corn stover. *Fuel* 2010, 89, S20-S28.

4. Balat, M.; Balat, H.; Oz, C., Progress in bioethanol processing. *Progress in Energy and Combustion Science* 2008, 34, (5), 551-573.

5. Bezzo, F.; Piccolo, C., A techno-economic comparison between two technologies for bioethanol production from lignocellulose. *Biomass & Bioenergy* 2009, 33, (3), 478-491.

6. Cardona, C. A.; Sanchez, O. J., Fuel ethanol production: Process design trends and integration opportunities. *Bioresource Technology* 2007, 98, (12), 2415-2457.

7. Dwivedi, P.; Alavalapati, J. R. R.; Lal, P., Cellulosic ethanol production in the United States: Conversion technologies, current production status, economics, and emerging developments. *Energy for Sustainable Development* 2009, 13, 174-182.

8. Foust, T. D.; Aden, A.; Dutta, A.; Phillips, S., An economic and environmental comparison of a biochemical and a thermochemical lignocellulosic ethanol conversion processes. *Cellulose* 2009, 16, (4), 547-565.

9. Hamelinck, C. N.; van Hooijdonk, G.; Faaij, A. P. C., Ethanol from lignocellulosic biomass: techno-economic performance in short-, middle- and long-term. *Biomass & Bioenergy* 2005, 28, (4), 384-410.

10. Lynd, L. R., Overview and evaluation of fuel ethanol from cellulosic biomass: Technology, economics, the environment, and policy. *Annual Review of Energy and the Environment* 1996, 21, 403-465.

11. Nigam, P. S.; Singh, A., Production of liquid biofuels from renewable resources. *Progress in Energy and Combustion Science* 2011, 37, (1), 52-68.

12. Phillips, S.; Aden, A.; Jechura, J.; Dayton, D.; Eggeman, T. *Thermochemical ethanol via indirect gasification and mixed alcohol synthesis of lignocellulosic biomass, Technical report, NREL/TP-510-41168*; NREL: 2007.

13. Phillips, S. D., Technoeconomic analysis of a lignocellulosic biomass indirect gasification process to make ethanol via mixed alcohols synthesis. *Industrial & Engineering Chemistry Research* 2007, 46, (26), 8887-8897.

14. Zacchi, G.; Ohgren, K.; Rudolf, A.; Galbe, M., Fuel ethanol production from steam-pretreated corn stover using SSF at higher dry matter content. *Biomass & Bioenergy* 2006, 30, (10), 863-869.

15. Ladisch, M. R.; Mosier, N. S.; Kim, Y.; Ximenes, E.; Hogsett, D., Converting Cellulose to Biofuels. *Chemical Engineering Progress* 2010, 106, (3), 56-63.

16. *U.S. DOE 2006. Breaking the biological barriers to cellulosic ethanol: A joint research agenda, DOE/SC-0095, U.S. Department of Energy Office of Science and Office of Science and Office of Energy Efficiency and Renewable Energy. Available at: www.doegenomestolife.org/biofuels/. Accessed August 2, 2011*.

17. *Regulation of Fuels and Fuel Additives: 2011 Renewable Fuel Standards. EPA-HQ-OAR-2010-0133; FRL-9234-6*; Environmental Protection Agency: 2010.

18. Himmel, M. E.; Ding, S. Y.; Johnson, D. K.; Adney, W. S.; Nimlos, M. R.; Brady, J. W.; Foust, T. D., Biomass recalcitrance: Engineering plants and enzymes for biofuels production. *Science* 2007, 315, (5813), 804-807.

19. Mussatto, S. I.; Dragone, G.; Guimaraes, P. M. R.; Silva, J. P. A.; Carneiro, L. M.; Roberto, I. C.; Vicente, A.; Domingues, L.; Teixeira, J. A., Technological trends, global market, and challenges of bio-ethanol production. *Biotechnology Advances* 2010, 28, (6), 817-830.

20. Alzate, C. A. C.; Toro, O. J. S., Energy consumption analysis of integrated flowsheets for production of fuel ethanol from lignocellulosic biomass. *Energy* 2006, 31, (13), 2447-2459.

21. McAloon, A.; Taylor, F.; Yee, W.; Ibsen, K.; Wooley, R. *Determining the Cost of Producing Ethanol from Corn Starch and Lignocellulosic Feedstocks. NREL/TP-580-28893*; NREL: 2000.

22. Wingren, A.; Galbe, M.; Zacchi, G., Energy considerations for a SSF-based softwood ethanol plant. *Bioresource Technology* 2008, 99, (7), 2121-2131.

23. Zhang, S. P.; Marechal, F.; Gassner, M.; Perin-Levasseur, Z.; Qi, W.; Ren, Z. W.; Yan, Y. J.; Favrat, D., Process Modeling and Integration of Fuel Ethanol Production from Lignocellulosic Biomass Based on Double Acid Hydrolysis. *Energy & Fuels* 2009, 23, 1759-1765.

24. Côté, P.; Noël, G.; Moore, S., The Chatham demonstration: From design to operation of a 20 m^3/d membrane-based ethanol dewatering system. *Desalination* 2010, 250, (3), 1060-1066.

25. Griend, D. L. V. Ethanol Distillation Process. U.S. Patent 7,297,236 B1, Nov 20, 2007.

26. Kwiatkowski, J. R.; McAloon, A. J.; Taylor, F.; Johnston, D. B., Modeling the process and costs of fuel ethanol production by the corn dry-grind process. *Ind. Crops Prod.* 2006, 23, (3), 288-296.

27. Shapouri, H.; Gallagher, P. *USDA's 2002 Ethanol Cost-of-Production Survey. Agricultural Economic Report Number 841*; United States Department of Agriculture: Washington DC, July 2005.

28. Summers, D. R.; Ehmann, D. Enhanced V-Grid Trays Increase Column Performance. Presented at the AIChE Annual Meeting, Indianapolis, IN, November 2002.

29. Swain, R. L. B., Molecular Sieve Dehydrators: Why They Became the Industry Standard and How They Work. In *The Alcohol Textbook*, Fifth ed.; Ingeldew, W. M.; Kelsall, D. R.; Austin, G. D.; Kluhspies, C., Eds. Nottingham University Press: Thrumpton, U.K., 2009; pp 379-384.

30. Vane, L. M., Separation technologies for the recovery and dehydration of alcohols from fermentation broths. *Biofuels, Bioprod. Biorefin.* 2008, 2, (6), 553-588.

31. Madson, P. W.; Lococo, D. B., Recovery of volatile products from dilute high-fouling process streams. *Applied Biochemistry and Biotechnology* 2000, 84-6, 1049-1061.

32. Vane, L. M.; Alvarez, F. R., Membrane-assisted vapor stripping: energy efficient hybrid distillation-vapor permeation process for alcohol-water separation. *Journal of Chemical Technology and Biotechnology* 2008, 83, (9), 1275-1287.

33. Zacchi, G.; Axelsson, A., Economic-Evaluation of Preconcentration in Production of Ethanol from Dilute Sugar Solutions. *Biotechnology and Bioengineering* 1989, 34, (2), 223-233.

34. Lynd, L. R.; Grethlein, H. E., IHOSR/Extractive distillation for ethanol separation. *Chem. Eng. Prog.* 1984, 59-62.

35. Boukouvalas, C.; Markoulaki, E.; Magoulas, K.; Tassios, D., Recovery of near-Anhydrous Ethanol as Gasoline Additive from Fermentation Products. *Separation Science and Technology* 1995, 30, (11), 2315-2335.

36. Canales, E. R.; Marquez, F. E., Operation and Experimental Results on a Vapor Recompression Pilot-Plant Distillation Column. *Industrial & Engineering Chemistry Research* 1992, 31, (11), 2547-2555.

37. Collura, M. A.; Luyben, W. L., Energy-Saving Distillation Designs in Ethanol-Production. *Industrial & Engineering Chemistry Research* 1988, 27, (9), 1686-1696.

38. Eakin, D. E.; Donovan, J. M.; Cysewski, G. R.; Petty, S. E.; Maxham, J. V. *Preliminary Evaluation of Alternative Ethanol/Water Separation Processes. PNL-3823*; Pacific Northwest Laboratory: 1981.

39. Enweremadu, C.; Waheed, A.; Ojediran, J., Parametric study of an ethanol-water distillation column with direct vapour recompression heat pump. *Energy for Sustainable Development* 2009, 13, 96-105.

40. Larsson, M.; Zacchi, G., Production of ethanol from dilute glucose solutions - A technical-economic evaluation of various refining alternatives. *Bioprocess Engineering* 1996, 15, (3), 125-132.

41. Muhrer, C. A.; Collura, M. A.; Luyben, W. L., Control of Vapor Recompression Distillation-Columns. *Industrial & Engineering Chemistry Research* 1990, 29, (1), 59-71.

42. Oliveira, S. B. M.; Marques, R. P.; Parise, J. A. R., Modelling of an ethanol-water distillation column with vapour recompression. *International Journal of Energy Research* 2001, 25, (10), 845-858.

43. Thibault, J.; Haelssig, J. B.; Tremblay, A. Y., Technical and economic considerations for various recovery schemes in ethanol production by fermentation. *Industrial & Engineering Chemistry Research* 2008, 47, (16), 6185-6191.

44. Bell, C. J., Pressure staged distillation of ethanol/water can reduce energy costs. *Alternative Energy Sources IV* 1982, 4, (3), 411-418.

45. Furter, W. F., Salt effect in distillation : A technical review. *Chem. Eng. (Rugby, U. K.)* 1968, 46, (5), CE173-CE177.

46. Furter, W. F., Salt effect in distillation : A literature-review II. *Can. J. Chem. Eng.* 1977, 55, (3), 229-239.

47. Furter, W. F., Production of fuel-grade ethanol by extractive distillation employing the salt effect. *Sep. Purif. Methods* 1993, 22, (1), 1-21.

48. Furter, W. F.; Cook, R. A., Salt effect in distillation - a literature review. *Int. J. Heat Mass Transfer* 1967, 10, (1), 23-36.

49. Cook, R. A.; Furter, W. F., Extractive distillation employing a dissolved salt as separating agent. *Can. J. Chem. Eng.* 1968, 46, (2), 119-123.

50. Siklós, J.; Timár, L.; Ország, I.; Ratkovics, F., A simulation of the distillation of ethanol-water mixtures containing salts. *Hung. J. Ind. Chem.* 1982, 10, 309-316.

51. Cespedes, A. P.; Ravagnani, S. P., Modelado y simulación del proceso de destilacion extractiva salina de etanol. *Inf. Tecnol.* 1995, 6, (5), 17-20.

52. Ligero, E. L.; Ravagnani, T. M. K., Simulation of salt extractive distillation with spray dryer salt recovery for anhydrous ethanol production. *J. Chem. Eng. Jpn.* 2002, 35, (6), 557-563.

53. Ligero, E. L.; Ravagnani, T. M. K., Dehydration of ethanol with salt extractive distillation - A comparative analysis between processes with salt recovery. *Chem. Eng. Process.* 2003, 42, 543-552.

54. Schmitt, D.; Vogelpohl, A., Distillation of ethanol - water solutions in the presence of potassium acetate. *Sep. Sci. Technol.* 1983, 18, (6), 547-554.

55. Ravagnani, S. P.; Reis, P. R., Modelo de orden reducido aplicado a una columna de destilacion extractiva salina. *Inf. Tecnol.* 2000, 11, (2), 43-50.

56. Torres, J. L.; Grethlein, H. E.; Lynd, L. R., Computer simulation of the Dartmouth process for separation of dilute ethanol water mixtures. *Appl. Biochem. Biotechnol.* 1989, 20-1, 621-633.

57. Barba, D.; Brandani, V.; Digiacomo, G., Hyperazeotropic ethanol salted-out by extractive distillation - theoretical evaluation and experimental check. *Chem. Eng. Sci.* 1985, 40, (12), 2287-2292.

58. Llano-Restrepo, M.; Aguilar-Arias, J., Modeling and simulation of saline extractive distillation columns for the production of absolute ethanol. *Comput. Chem. Eng.* 2003, 27, (4), 527-549.

59. Pinto, R. T. P.; Wolf-Maciel, M. R.; Lintomen, L., Saline extractive distillation process for ethanol purification. *Comput. Chem. Eng.* 2000, 24, (2-7), 1689-1694.

60. Seader, J. D.; Henley, E. J., *Separation Process Principles*. Second ed.; Wiley: New York, 2006.

61. Sata, T., *Ion Exchange Membranes: Preparation, Characterization, Modification and Application*. Royal Society of Chemistry: Cambridge, U.K., 2004.

62. Strathmann, H., *Ion-Exchange Membrane Separation Processes*. First ed.; Elsevier: Amsterdam, The Netherlands, 2004.

63. Pfromm, P. H., Low effluent processing in the pulp and paper industry: Electrodialysis for continuous selective chloride removal. *Sep. Sci. Technol.* 1997, 32, (18), 2913-2926.

64. Masters, K., *Spray Drying Handbook*. Fourth ed.; George Godwin: London, 1985.

65. Oakley, D. E., Spray dryer modeling in theory and practice. *Drying Technol.* 2004, 22, (6), 1371-1402.

66. Renon, H.; Prausnitz, J. M., Local compositions in thermodynamic excess functions for liquid mixtures. *AIChE J.* 1968, 14, (1), 135-144.

67. Chau-Chyun, C.; Britt, H. I.; Boston, J. F.; Evans, L. B., Local composition model for excess Gibbs energy of electrolyte systems. Part I: Single solvent, single completely dissociated electrolyte systems. *AIChE J.* 1982, 28, (4), 588-596.

68. Chen, C. C.; Evans, L. B., A local composition model for the excess Gibbs energy of aqueous-electrolyte systems. *AIChE J.* 1986, 32, (3), 444-454.

69. Mock, B.; Evans, L. B.; Chen, C. C., Thermodynamic representation of phase-equilibria of mixed-solvent electrolyte systems. *AIChE J.* 1986, 32, (10), 1655-1664.

70. Redlich, O.; Kwong, J. N. S., On the thermodynamics of solutions. V. An equation of state. Fugacities of gaseous solutions. *Chem. Rev. (Washington, DC, U. S.)* 1949, 44, (1), 233-244.

71. Hussain, M. A. M.; Anthony, J. L.; Pfromm, P. H., Reducing the energy demand of corn-based fuel ethanol through salt extractive distillation enabled by electrodialysis. *AIChE Journal* 2011, doi:10.1002/aic.12577.

Chapter 4 - Concentration of CaCl$_2$ through electrodialysis to enable salt extractive distillation of bioethanol

4.1 Abstract

Salt extractive distillation with salt recovery enabled by a novel scheme of electrodialysis and spray drying can reduce the energy demand for recovering ethanol from a fermentation broth and purifying to fuel grade. Further electrodialytic concentration of CaCl$_2$ from already high diluate concentrations, expected in the salt recovery process when CaCl$_2$ is used as the salt separating agent in the salt extractive distillation of bioethanol, was carried out to determine the fundamental transport properties of an ion exchange membrane pair comprising commercially available membranes (NEOSEPTA CMX and AMX). The membrane pair transport characteristics, solute and osmotic permeabilities, current efficiency, and water transport number, are determined using the mass transport equations based on irreversible thermodynamics. The water transport number decreased with the increase in the concentration of the diluate and approached a limiting value. Based on the membrane pair transport properties under the experimental conditions studied, the maximum CaCl$_2$ concentration achievable in the concentrate is determined as 34.6 wt%, which is mainly limited by the water transport number.[c]

4.2 Introduction

The expanded Renewable Fuel Standard (RFS2), established under the Energy Independence and Security Act (EISA) of 2007, mandates the production of 136.3 GL/year of renewable fuels in 2022: 56.8 GL/year of corn-ethanol, 60.6 GL/year of second generation biofuels such as cellulosic ethanol, and 18.9 GL/year of advanced biofuels such as biomass-based diesel.[1] Currently, corn-ethanol is the most widely produced biofuel in the U.S.[1] Dry milling is currently the most widely used process in the U.S for producing fuel ethanol from corn by fermentation. Similar to corn-ethanol, fermentation can be used to produce fuel ethanol from cellulosic feedstock.[2-9] Recovering ethanol from fermentation broth and purifying it to fuel grade is difficult and energy intensive due to the dilute nature of the fermentation broth and the challenging water-ethanol vapor liquid equilibrium (VLE) with an azeotrope at about 96 wt% ethanol. Simple distillation cannot be used to distill ethanol above the azeotropic composition. The contemporary process used in the fuel ethanol industry to produce fuel ethanol is distillation close to the azeotropic composition followed by dehydration in a molecular sieve based adsorption unit.[10-13] The ethanol concentration in the fermentation broth varies from about 10 to 15 wt% for corn-ethanol[10, 11, 14-16] compared to about 3 to 6 wt% for cellulosic ethanol.[2-9] In case of corn-ethanol, recovering and purifying ethanol from fermentation broth requires about 70 % of the total steam generated in the dry milling plant.[17] While for cellulosic ethanol, the recovery and purification energy demand is much higher due the drastic increase in the distillation energy demand as the ethanol concentration in the fermentation broth decreases.[14, 18-20] Hence, it is essential to reduce the separation and purification energy demand to improve the possible economical and environmental advantages of bioethanol over fossil fuels.

The VLE of the water-ethanol system can be improved through dissolving a salt in the liquid phase to increase the relative volatility of ethanol.[21-24] In addition to "salting out" ethanol, the water-ethanol azeotrope may be eliminated.[21, 23, 25] For instance, starting with a binary mixture of water and ethanol containing 70 wt% ethanol, 99.6 wt % ethanol was distilled using potassium acetate as the salt separating agent requiring only a quarter of the energy needed to obtain 93 wt% ethanol (near azeotropic composition) by conventional distillation.[26] However, efficient recovery and reuse of the salt is crucial. Potassium acetate[25-33] and calcium chloride[27, 31, 34-36] have been investigated for water-ethanol separation utilizing the "salting out" effect. The use of the salt separating agent in a process with tightly closed water cycles such as the bioethanol

plant requires that the salt not impact other processing areas negatively. In this study, calcium chloride was selected for the following reasons: low cost, large "salting out" effect[27, 31] and compatibility with fermentation.

In a salt extractive distillation column, the salt is usually dissolved in the reflux stream and introduced at the top of the column. Since salt is non volatile and always remains in the liquid phase, a high purity distillate free of salt can be obtained. The salt moves downward and leaves the column along with the distillation column bottoms. Afterwards, the salt is recovered and purified from the distillation column bottoms for re-use in the top of the column. Therefore, two distinct steps are involved: salt extractive distillation and salt recovery/purification.

There are several experimental and theoretical studies[25-36] on utilizing the "salting out" effect for water-ethanol separation; however, most of them focus only on the salt extractive distillation step. Furthermore, the studies[21, 23, 28-30, 32-34] which include both steps of salt extractive distillation and salt recovery only consider evaporative and drying techniques for salt recovery. Since evaporative salt concentration/crystallization and solids drying techniques are energy intensive, reducing the energy requirement for recovering salt is essential. A combination of electrodialysis and spray drying can be advantageous for salt recovery. Electrodialysis is used to concentrate the salt solution by selectively separating the salt ions from the solution[37, 38] rather than evaporating water, which leads to lower energy demand than that of an evaporative process. Final recovery of dry salt is achieved in a spray dryer, which is widely used to directly convert a liquid feed containing salt into dry solid particles through drying with hot gas.[39, 40] Earlier conceptual studies by the authors for the salt extractive distillation of fuel ethanol, with salt recovery enabled by the novel scheme of electrodialysis and spray drying, showed significant energy savings for both corn-ethanol and cellulosic ethanol.[41, 42] To evaluate these studies for practical applications, it is necessary to investigate the electrodialytic concentration of $CaCl_2$ in the operating conditions prevalent during the salt extractive distillation of fuel ethanol.

One of the main industrial applications of electrodialysis is the preconcentration of sea water to produce NaCl,[37, 38, 43] and this process has been most extensively studied.[44-54] Further, electrodialytic concentration of several organic and inorganic salts,[55-67] and acids[68-71] has been investigated. However, there are only a few studies on the electrodialytic concentration of $CaCl_2$.[72-76] Moreover, these studies are focused on concentrating $CaCl_2$ from dilute solutions, as opposed to the expected requirement of concentrating $CaCl_2$ from solutions with initial $CaCl_2$

81

concentrations as high as 15 wt% obtained from the bottoms stream in the salt extractive distillation of fuel ethanol.[41] The main goal of this study is to investigate the fundamental transport properties of an ion exchange membrane pair comprised of commercially available ion exchange membranes (NEOSEPTA CMX and AMX) – solute and osmotic permeabilities, current efficiency, and water transport number, in high $CaCl_2$ concentrations expected in the salt extractive distillation process. The overall transport properties of the ion exchange membrane pair are determined using the mass transport equations based on irreversible thermodynamics relating the ionic and water fluxes across the ion exchange membrane pair to the overall driving forces in the electrodialytic concentration process.

4.3 Experimental Materials and Methods

4.3.1 Experimental Setup

In this study, a Deukum electrodialysis system (Deukum GmbH, Frickenhausen, Germany) with online data acquisition (LabVIEW 6.1) is used. The integrated rectifier has a maximum supply voltage and current of 65 V and 10 A, respectively. The electrodialysis stack is of sheet-flow type with an effective cross-sectional membrane surface area of 100 cm^2. NEOSEPTA standard grade ion exchange membranes (Table 4-1) are used. Figure 4-1 shows the cell arrangement with 7 cation exchange membranes and 6 anion exchange membranes. To block the calcium ions from reaching the electrode rinse solution (Na_2SO_4, 0.5 m) and forming calcium sulfate precipitate, NaCl solution (1 m) is circulated in the adjacent chambers of the electrode rinse chambers. Therefore, five cell pairs are available for the electrodialytic concentration process. Platinum wires are inserted in the first diluate (D1) and last concentrate chambers (C5) for measuring voltage.
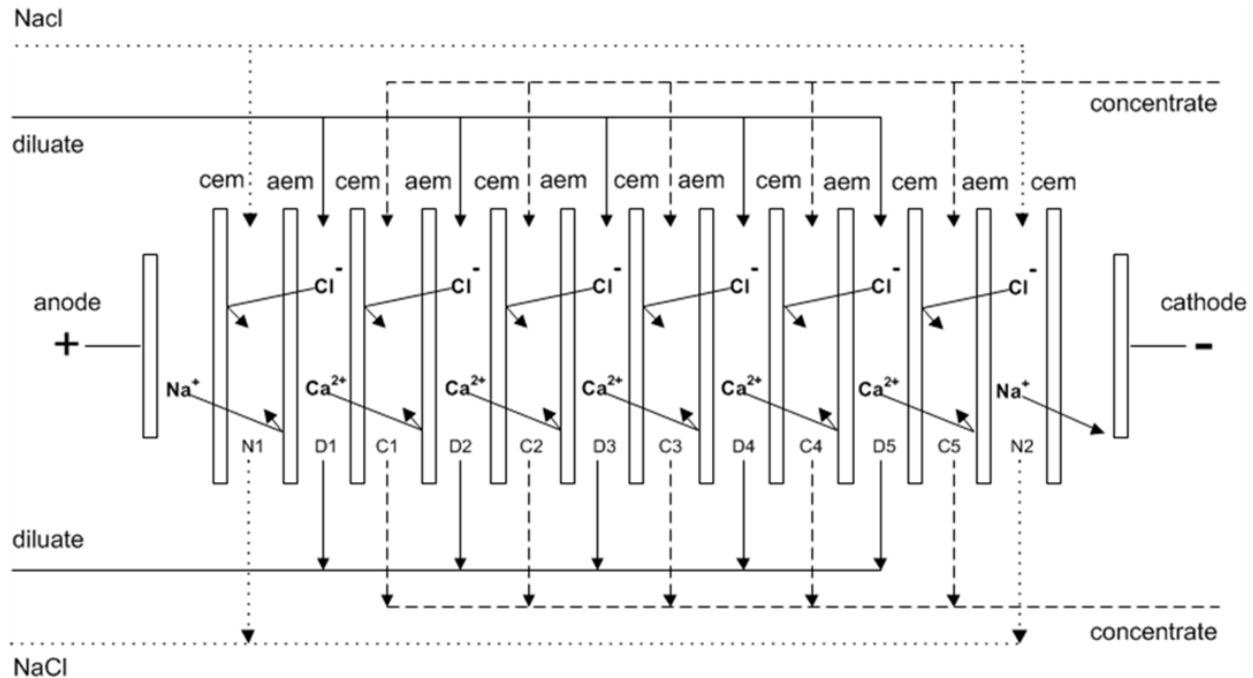
Figure 4-1. Schematic diagram of the electrodialysis stack.

4.3.2 Experimental Procedure

Before starting each experiment, the membranes are equilibrated in the feed solutions for at least 12 hours. All experiments are carried out in a continuous batch recirculation mode. The temperature of the feed tanks is maintained at $25\pm2^{\mathrm{o}}$ C through heat exchange with cooling water. Two different sets of experiments (Table 4-2) with and without applied current are carried out In the first set of experiments, the effect of concentration difference between the diluate and concentrate solutions on the solute diffusion and osmotic water transfer across the membranes is studied. In the second set of experiments, electrical current density and initial $CaCl_2$ concentration in the diluate are varied to study their effects on solute transport and electroosmotic water transport across the membranes. In addition, limiting current density experiments are performed wherein the limiting current density was not reached even at the maximum current supply (10 *A*; 1000 *A/m²*) of the rectifier due to the high concentration of the diluate solutions. Hence, the range of current densities investigated is safely below the limiting current density. To properly control temperature and avoid excessive heating, the upper limit for current density was selected at 500 *A/m²*. Samples are taken at regular time intervals during the course of the experiments for calcium analysis by Atomic Absorption Spectroscopy (AAS).

Table 4-1. Properties of ion exchange membranes (manufacturer data)

Ion Exchange Membrane	CEM	AEM
Manufacturer	ASTOM Corporation	ASTOM Corporation
Trade name	NEOSEPTA CMX	NEOSEPTA AMX
Type	Strongly acidic	Strongly basic
Electric Resistance at 25° C (Ω/cm^2)	3.0	2.4
Thickness (*mm*)	0.17	0.14

4.3.3 Mathematical Model for the Electrodialytic Process

Based on the application of irreversible thermodynamics to electrodialysis,[77-81] the overall salt and water fluxes occurring through an ion exchange membrane pair during electrodialysis can be written as follows:[77, 80, 81]

$$j_s = \frac{\eta i}{ZF} + p_s \Delta C \qquad \text{Equation 5-1}$$

$$j_w = \frac{t_w i}{F} - p_w \Delta C \qquad \text{Equation 5-2}$$

where j_s is the solute flux in *mol/m²s*; j_w, water flux, *mol/m²s*; η, current efficiency; Z, ion valence, *equivalent/mol*; F, Faraday constant, 96485 *A.s/equivalent*; t_w, water transport number, mol/F; p_s, solute permeability, *m/s*; p_w, osmotic water permeability, *m/s*; and ΔC, solute concentration difference between the diluate and concentrate, *mol/m³*. The above relations have been applied to describe the transport processes occurring during the electrodialytic concentration process for concentrations up to about 5M.[48, 51, 52, 54, 82]

Table 4-2. Experimental conditions for evaluating the transport properties of the ion exchange membranes

Experiment type		Current density, i (A/m^2)	Initial CaCl$_2$ concentration in diluate, C_{sdi} (mol/kg)	Initial CaCl$_2$ concentration in concentrate, C_{sci} (mol/kg)	Superficial velocity in diluate, V_s (cm/s)	Time, Δt (h)
Zero current	A1	--	1.15	0.04	2.8	6.0
	A2	--	2.07	0.03	2.5	5.9
	A3	--	3.75	0.06	2.3	3.1
	A4	--	5.88	0.07	2.3	3.0
Constant current	B1	250	1.07	0.02	3.5	5.6
	B2	375	1.16	0.03	2.9	4.5
	B3	500	1.13	0.04	3.5	4.5
	B4	250	1.61	0.04	3.8	5.9
	B5	375	1.66	0.04	4.0	4.5
	B6	500	1.72	0.04	3.0	4.5
	B7	250	2.34	0.04	2.1	5.8
	B8	375	2.26	0.04	2.4	5.7
	B9	500	2.27	0.04	2.2	4.6

Assuming well mixed conditions in the individual circuits and negligible solution leakage between the individual chambers in the electrodialysis stack, the mass balance equations for the solute and water in the concentrate and diluate circuits can be written as follows:

$$\frac{dN_{sc}}{dt} = -\frac{dN_{sd}}{dt} = j_s a_m n_{cell} \hspace{3cm} \text{Equation 5-3}$$

$$\frac{dN_{wc}}{dt} = -\frac{dN_{wd}}{dt} = j_w a_m n_{cell} \hspace{3cm} \text{Equation 5-4}$$

where N_{sc} and N_{sd} are the number of moles of solute in the concentrate and diluate circuits, respectively; N_{wc} and N_{wd} are the number of moles of water in the concentrate and diluate circuits, respectively; a_m, membrane surface area, m^2; and n_{cell}, number of cell pairs. Substituting Equation 5-1 and Equation 5-2, respectively, in Equation 5-3 and Equation 5-4 followed by integration yields the following equations:

$$\Delta N_{sc} = -\Delta N_{sd} = \frac{\eta i a_m n_{cell}}{ZF} t + p_s a_m n_{cell} \int_0^t \Delta C \, dt \hspace{2cm} \text{Equation 5-5}$$

$$\Delta N_{wc} = -\Delta N_{wd} = \frac{t_w i a_m n_{cell}}{F} t - p_w a_m n_{cell} \int_0^t \Delta C \, dt \hspace{2cm} \text{Equation 5-6}$$

where ΔN_{sc} and ΔN_{sd} are the total change in the number of moles of solute, respectively, in the concentrate and diluate circuits after a time interval Δt, and ΔN_{wc} and ΔN_{wd} are the total change in

the number of moles of water, respectively, in the concentrate and diluate circuits after a time interval Δt. The integral in Equation 5-5 and Equation 5-6 can be evaluated by using an empirical equation for the change in ΔC, solute concentration difference between diluate and concentrate, during the time interval Δt.

4.4 Results and Discussion

4.4.1 Zero Current Experiments

The time course of the change in ΔC, solute concentration difference between diluate and concentrate, during the time interval Δt can be expressed as a linear function of time t:[46, 69, 83]

$$\Delta C = \Delta C_i + mt \qquad \text{Equation 5-7}$$

where ΔC_i is the initial solute concentration difference between diluate and concentrate, and m is an empirical factor. Substituting Equation 5-7 and $i = 0$ in Equation 5-5 and Equation 5-6 and integrating yields the following equations for solute and water transfer under zero current conditions:

$$\Delta N_{sc} = -\Delta N_{sd} = p_s a_m n_{cell} \Delta C_i t + \frac{p_s a_m n_{cell} m}{2} t^2 \qquad \text{Equation 5-8}$$

$$\Delta N_{wc} = -\Delta N_{wd} = -p_w a_m n_{cell} \Delta C_i t - \frac{p_w a_m n_{cell} m}{2} t^2 \qquad \text{Equation 5-9}$$

The cumulative change in number of moles of solute and water in the concentrate circuit with time for the zero current experiments (A1-A4) is shown in Figure 4-2 and Figure 4-3, respectively. Since a straight line provides a good fit at the 95% confidence level for these plots, the quadratic term in Equation 5-8 and Equation 5-9 can be neglected, resulting in the following equations:

$$\Delta N_{sc} = -\Delta N_{sd} \approx p_s a_m n_{cell} \Delta C_i t \qquad \text{Equation 5-10}$$

$$\Delta N_{wc} = -\Delta N_{wd} \approx p_w a_m n_{cell} \Delta C_i t \qquad \text{Equation 5-11}$$

Hence, the solute and water permeabilities can be calculated from the slope of the straight lines in Figure 4-2 and Figure 5–3, respectively. The solute and osmotic permeabilities for different initial solute concentrations in the diluate remain almost constant as shown in Figure 4-4 and Figure 4-5 respectively. The following average values for the solute and osmotic permeabilities are obtained:

$$p_s = 2.01 \times 10^{-7} \pm 9.89 \times 10^{-9}\,\text{m/s} \qquad\qquad \text{Equation 5-12}$$

$$p_w = 4.13 \times 10^{-6} \pm 1.58 \times 10^{-7}\,\text{m/s} \qquad\qquad \text{Equation 5-13}$$

Figure 4-2. Net increase in the mass of $CaCl_2$ in the concentrate with time for different initial $CaCl_2$ concentrations (C_{sdi}) in the diluate for zero current experiments (A1-A4); ($\circ$): C_{sdi} = 1.15 mol/kg; ($\square$): C_{sdi} = 2.07 mol/kg; ($\times$) $\circ$: C_{sdi} = 3.75 mol/kg; (Δ): C_{sdi} = 5.88 mol/kg.
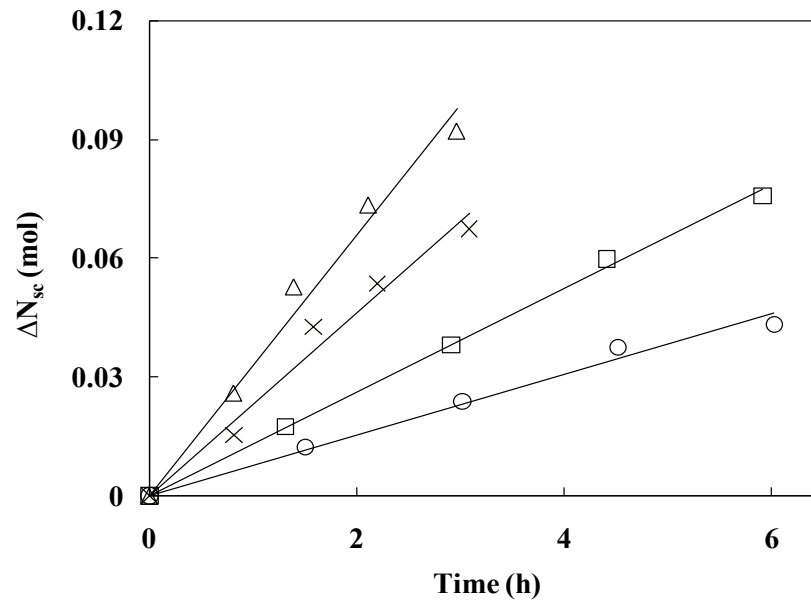
Figure 4-3. Net decrease in the mass of water in the concentrate with time for different initial CaCl$_2$ concentrations (C$_{sdi}$) in the diluate for zero current experiments (A1-A4); (○): C$_{sdi}$ = 1.15 mol/kg; (□): C$_{sdi}$ = 2.07 mol/kg; (×○): C$_{sdi}$ = 3.75 mol/kg; (Δ): C$_{sdi}$ = 5.88 mol/kg.

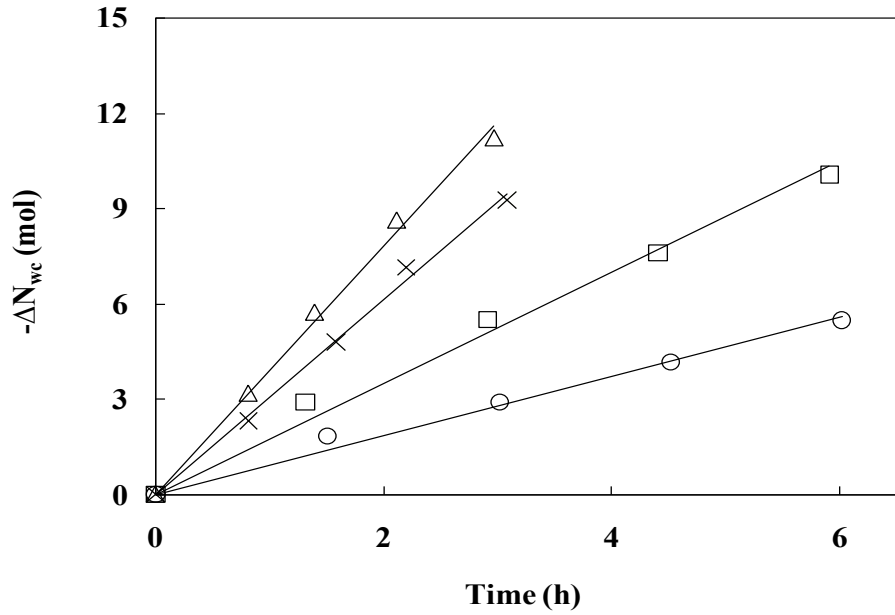Figure 4-4. Variation of the overall solute permeability of the membrane pair as a function of the initial CaCl$_2$ concentration in the diluate; solid line: average; dotted lines: upper and lower limits of the 95% confidence interval.
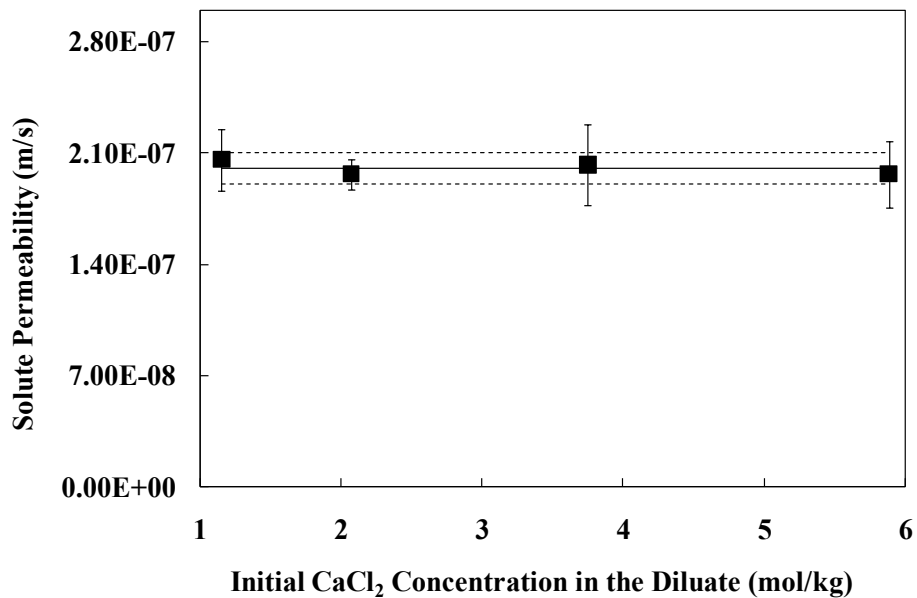
Figure 4-5. Variation of the overall osmotic permeability of the membrane pair as a function of the initial CaCl$_2$ concentration in the diluate; solid line: average; dotted lines: upper and lower limits of the 95% confidence interval.
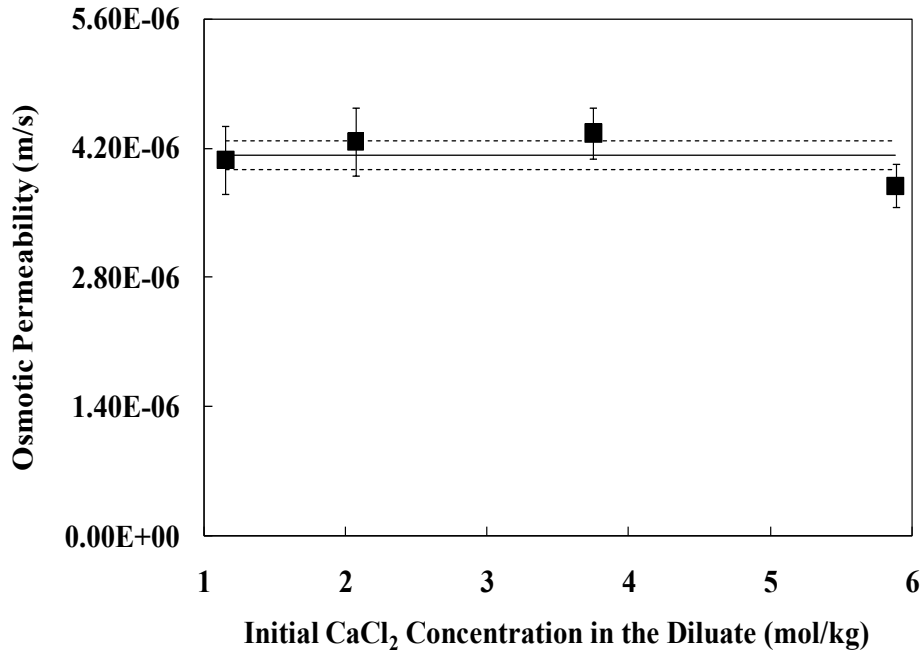
4.4.2 Constant Current Experiments

Substituting Equation 5-7 in Equation 5-5 and Equation 5-6 and integrating yields the following equations for solute and water transfer under constant current conditions:

$$\Delta N_{sc} = -\Delta N_{sd} = \frac{\eta i a_m n_{cell}}{ZF}t + p_s a_m n_{cell}\Delta C_i + \frac{p_s a_m n_{cell}m}{2}t^2 \qquad \text{Equation 5-14}$$

$$\Delta N_{wc} = -\Delta N_{wd} = \frac{t_w i a_m n_{cell}}{F}t - p_w a_m n_{cell}\Delta C_i t - \frac{p_w a_m n_{cell}m}{2}t^2 \qquad \text{Equation 5-15}$$

The cumulative change in number of moles of solute and water in the concentrate circuit with time for the constant current experiments (B1-B3) is shown in Figure 4-6 and Figure 4-7 respectively. A straight line provides a good fit at the 95% confidence level for these plots; same is the case for the other constant current experiments (B4-B9) as illustrated in Figure B-1 - Figure B-4.

Therefore, the quadratic term in Equation 5-14 and Equation 5-15 can be neglected, resulting in the following equations:

89

$$\Delta N_{sc} = -\Delta N_{sd} \approx \left[\frac{\eta i a_m n_{cell}}{ZF} + p_s a_m n_{cell} \Delta C_i \right] t \qquad \text{Equation 5-16}$$

$$\Delta N_{wc} = -\Delta N_{wd} \approx \left[\frac{t_w i a_m n_{cell}}{F} - p_w a_m n_{cell} \Delta C_i \right] t \qquad \text{Equation 5-17}$$

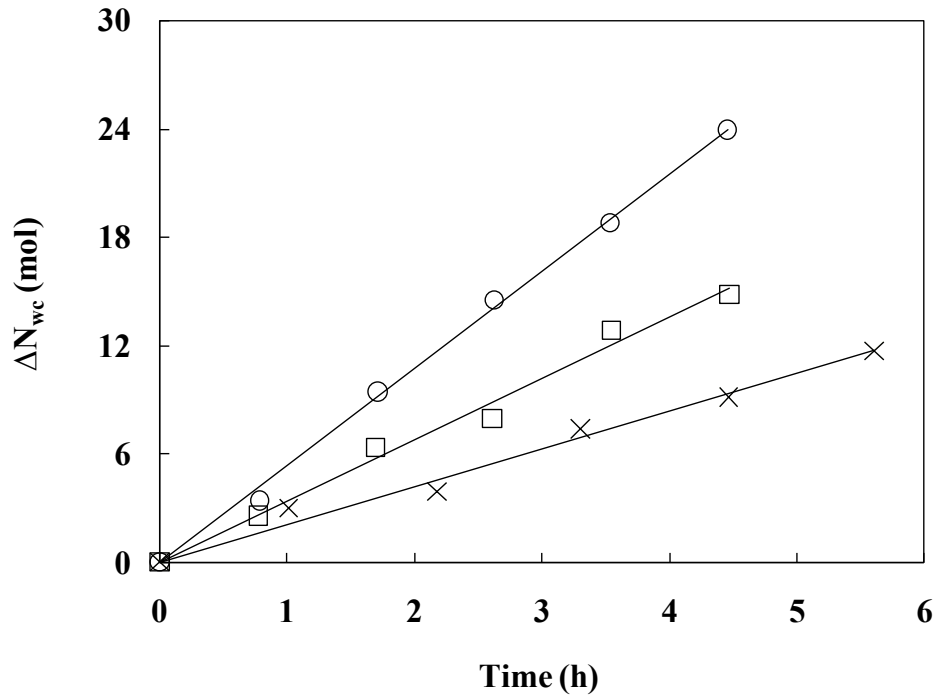Figure 4-6. Net increase in the mass of CaCl$_2$ in the concentrate with time for an initial CaCl$_2$ concentration in the diluate, C$_{sdi}$ ≈ 1.1 mol/kg at different current densities (i); ×○: i = 250 A/m^2; □: i = 375 A/m^2; ○: i = 500 A/m^2.
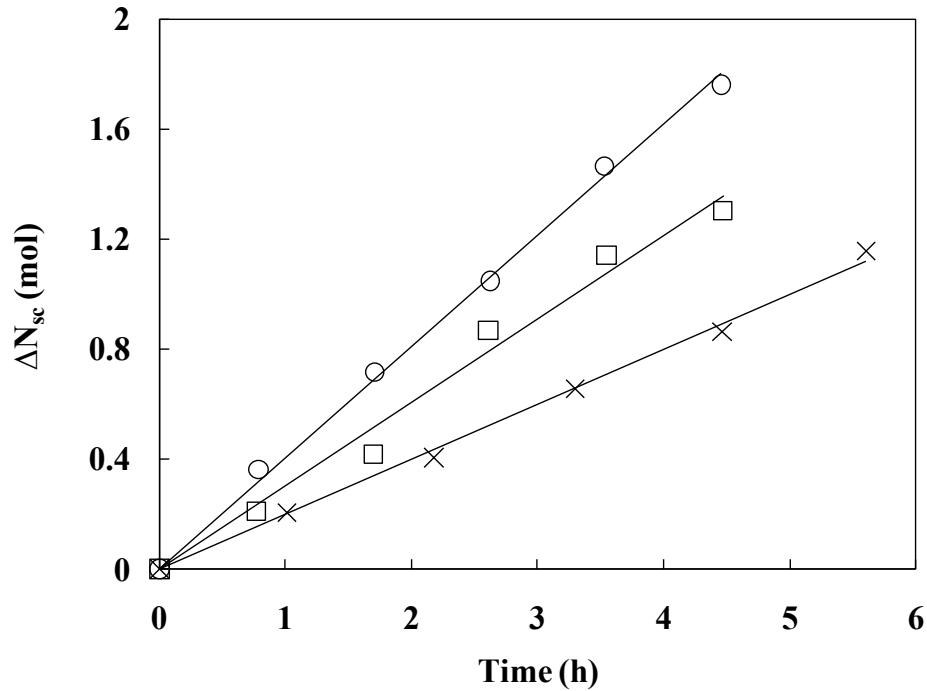
Figure 4-7. Net increase in the mass of water in the concentrate with time for an initial $CaCl_2$ concentration in the diluate, $C_{sdi} \approx 1.1$ mol/kg at different current densities (i); $\times\circ$: i = 250 A/m^2; $\square$: i = 375 A/m^2; $\circ$: i = 500 A/m^2.

Therefore, the current efficiency and water transport number can be calculated from the slope of the straight lines in ΔN_{sc} vs.t and ΔN_{wc} vs.t plots respectively, after substituting the values for the solute and osmotic permeabilities. Current density has almost negligible influence on the current efficiency (Figure B-5 - Figure B-7) and the water transport number (Figure B-8 - Figure B-10) at different initial solute concentrations in the diluate. Also, current efficiency remains almost constant with the increase in the initial solute concentration in the diluate (Figure 4-8). But, the water transport number decreases with the increase in the initial solute concentration in the diluate (Figure 4-9). The water transport number characterizes the electroosmotic water transfer through the ion exchange membranes due to the passage of electric current. Electroosmotic water transfer can be considered as a sum of two contributions: hydration water of the migrating ions and free water dragged by the migrating ions.[54, 84-89] The first contribution is due to the tightly bound water molecules in the hydration shell of the ions while the second contribution is due to the free water molecules in the solution dragged along with the

hydrated ions. When the initial solute concentration in the diluate increases, the internal solution concentration in the ion exchange membrane increases due to the electrolyte penetration resulting in the decrease of the water content in the ion exchange membranes. Therefore, the movement of the free water molecules dragged by the hydrated ions is restricted, while only the hydration water molecules tightly bound to the ions could pass through. Hence, the water transport number decreases with the increase in the initial solution concentration in the diluate and tends toward a limiting value corresponding to the hydration number of $CaCl_2$. Similar results have been obtained for other salts such as NaCl and LiCl in various studies.[47, 54, 82, 84, 85]
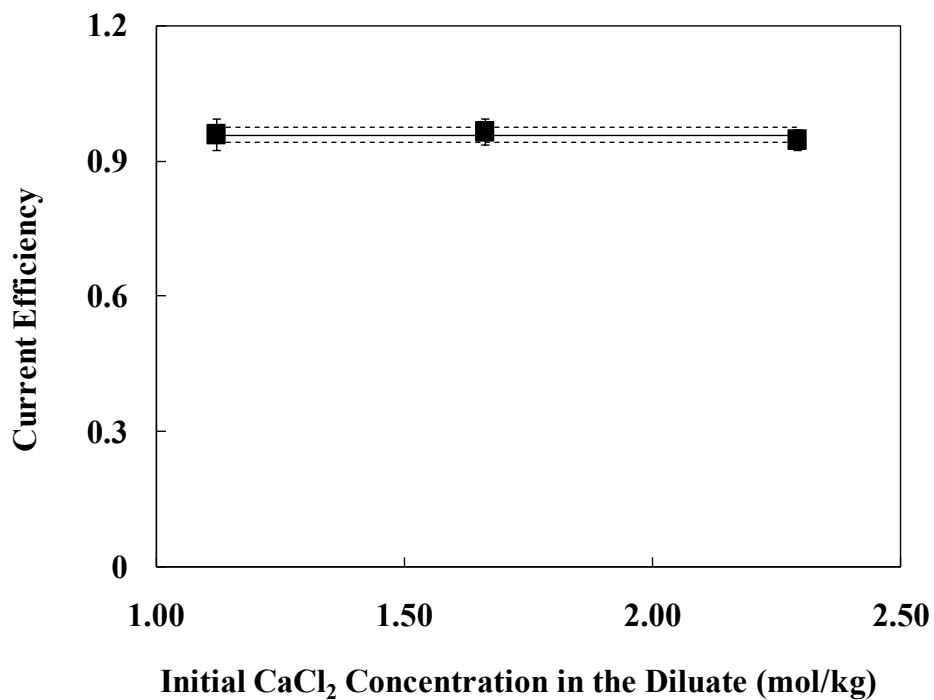

Figure 4-8. Variation of the overall current efficiency (η) of the membrane pair as a function of the initial $CaCl_2$ concentration in the diluate; solid line: average; dotted lines: upper and lower limits of the 95% confidence interval.
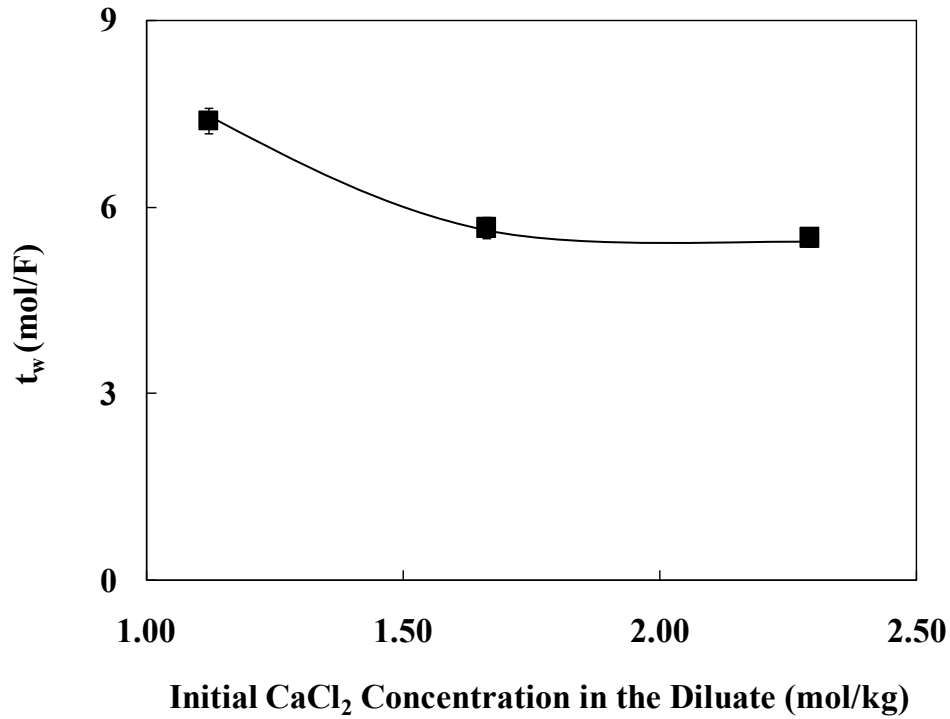
Figure 4-9.Variation of the overall water transport number (t_w) of the membrane pair as a function of the initial CaCl$_2$ concentration in the diluate.

Once the overall transport properties of the cation and anion exchange membranes – solute permeability, osmotic permeability, current efficiency, and water transport number, are evaluated, the concentration of CaCl$_2$ in the concentrate (C_{sc}^*, mol. fraction) of the electrodialytic concentration process can be calculated as follows:

$$C_{sc}^* = \frac{j_s}{j_s + j_w} = \frac{\frac{\eta i}{ZF} - p_s \Delta C}{\left[\frac{\eta}{Z} + t_w\right]\frac{i}{F} + [p_w - p_s]\Delta C}$$

Equation 5-18

When ΔC, solute concentration difference between the diluate and concentrate, tends to zero, and the water transport number reaches the limiting value, the maximum concentration of CaCl$_2$ in the concentrate is achieved. The maximum achievable concentration of CaCl$_2$ in the concentrate is 0.079 mol. fraction (34.6 wt %).

The specific electrical energy requirement of electrodialysis for removing and concentrating the salt can be calculated as follows:

$$E = \frac{V_{cp}ZF}{3600M\eta}$$
<div align="right">Equation 5-19</div>

where E is the specific energy demand in *kWh/kg*; V_{cp}, voltage drop per cell pair, *V*; and *M*, molecular weight of the salt, *g/mol*. This does not include the energy required for the electrode reactions. The specific energy demand increases with current density due to the increase in cell voltage. The highest specific energy requirement at the experimental conditions studied is 0.379 *kWh/kg* at 500 A/m^2 and the lowest specific energy requirement is 0.138 *kWh/kg* at 250 A/m^2. The energy requirement must be balanced against the capital expense for installed membrane area. Operating at higher electrical current density allows reduction of the installed membrane area; thereby, reducing capital cost while simultaneously increasing the specific operating cost per mass of salt recovered.

4.5 Conclusions and Outlook

Electrodialytic concentration of $CaCl_2$ from high diluate concentrations, expected in the salt extractive distillation of fuel ethanol with salt recovery enabled by a novel scheme of electrodialysis and spray drying, is carried out to determine the fundamental transport properties of an ion exchange membrane pair comprising NEOSEPTA CMX and AMX. The membrane pair transport characteristics, solute and osmotic permeabilities, current efficiency, and water transport number, are determined using the mass transport equations based on irreversible thermodynamics. Solute and osmotic permeabilities, and current efficiency remained essentially constant in the range of initial diluate concentrations and current densities studied. Water transport number decreased with the increase in the concentration of the diluate, and approached a limiting value due to the restriction of free water molecules dragged by the hydrated ions through the ion exchange membrane pair.

After determining the transport properties of the membrane pair, the concentration of $CaCl_2$ in the concentrate is calculated using the mass transport equations. The maximum $CaCl_2$ concentration achievable in the concentrate is 34.6 wt%, which is mainly limited by the water transport number. The basic transport properties of the membrane pair evaluated from the experiments serve to enable process design and optimization for concepts involving calcium chloride in salt extractive distillation.

4.6 Literature Cited

1. Renewable Fuels Association (RFA). Available at: http://www.ethanolrfa.org. Accessed August 4, 2011.

2. Aden, A.; Ruth, M.; Ibsen, K.; Jechura, J.; Neeves, K.; Sheehan, J.; Wallace, B.; Montague, L.; Slayton, A.; Lukas, J. *Lignocellulosic Biomass to Ethanol Process Design and Economics Utilizing Co-current Dilute Acid Prehydrolysis and Enzymatic Hydrolysis for Corn Stover.NREL/TP-510-32438*; NREL: 2002.

3. Alzate, C. A. C.; Toro, O. J. S., Energy consumption analysis of integrated flowsheets for production of fuel ethanol from lignocellulosic biomass. *Energy* 2006, 31, (13), 2447-2459.

4. Hamelinck, C. N.; van Hooijdonk, G.; Faaij, A. P. C., Ethanol from lignocellulosic biomass: techno-economic performance in short-, middle- and long-term. *Biomass & Bioenergy* 2005, 28, (4), 384-410.

5. Lynd, L. R., Overview and evaluation of fuel ethanol from cellulosic biomass: Technology, economics, the environment, and policy. *Annual Review of Energy and the Environment* 1996, 21, 403-465.

6. McAloon, A.; Taylor, F.; Yee, W.; Ibsen, K.; Wooley, R. *Determining the Cost of Producing Ethanol from Corn Starch and Lignocellulosic Feedstocks. NREL/TP-580-28893*; NREL: 2000.

7. Wingren, A.; Galbe, M.; Zacchi, G., Energy considerations for a SSF-based softwood ethanol plant. *Bioresource Technology* 2008, 99, (7), 2121-2131.

8. Zacchi, G.; Ohgren, K.; Rudolf, A.; Galbe, M., Fuel ethanol production from steam-pretreated corn stover using SSF at higher dry matter content. *Biomass & Bioenergy* 2006, 30, (10), 863-869.

9. Zhang, S. P.; Marechal, F.; Gassner, M.; Perin-Levasseur, Z.; Qi, W.; Ren, Z. W.; Yan, Y. J.; Favrat, D., Process Modeling and Integration of Fuel Ethanol Production from Lignocellulosic Biomass Based on Double Acid Hydrolysis. *Energy & Fuels* 2009, 23, 1759-1765.

10. Griend, D. L. V. Ethanol Distillation Process. U.S. Patent 7,297,236 B1, 2007.

11. Kwiatkowski, J. R.; McAloon, A. J.; Taylor, F.; Johnston, D. B., Modeling the process and costs of fuel ethanol production by the corn dry-grind process. *Ind. Crops Prod.* 2006, 23, (3), 288-296.

12. Swain, R. L. B., Molecular Sieve Dehydrators: Why They Became the Industry Standard and How They Work. In *The Alcohol Textbook*, Fifth ed.; Ingeldew, W. M.; Kelsall, D. R.; Austin, G. D.; Kluhspies, C., Eds. Nottingham University Press: Thrumpton, U.K., 2009; pp 379-384.

13. Vane, L. M., Separation technologies for the recovery and dehydration of alcohols from fermentation broths. *Biofuels, Bioprod. Biorefin.* 2008, 2, (6), 553-588.

14. Côté, P.; Noël, G.; Moore, S., The Chatham demonstration: From design to operation of a 20 m^3/d membrane-based ethanol dewatering system. *Desalination* 2010, 250, (3), 1060-1066.

15. Shapouri, H.; Gallagher, P. *USDA's 2002 Ethanol Cost-of-Production Survey. Agricultural Economic Report Number 841*; United States Department of Agriculture: Washington DC, July 2005.

16. Summers, D. R.; Ehmann, D. Enhanced V-Grid Trays Increase Column Performance. Presented at the AIChE Annual Meeting, Indianapolis, IN, November 2002.

17. Meredith, J., Understanding Energy Use and Energy Users in Contemporary Ethanol Plants. In *The Alcohol Textbook*, Fourth ed.; Jacques, K. A.; Lyons, T. P.; Kelsall, D. R., Eds. Nottingham University Press: Thrumpton, U.K., 2003; pp 355-361.

18. Madson, P. W.; Lococo, D. B., Recovery of volatile products from dilute high-fouling process streams. *Applied Biochemistry and Biotechnology* 2000, 84-6, 1049-1061.

19. Vane, L. M.; Alvarez, F. R., Membrane-assisted vapor stripping: energy efficient hybrid distillation-vapor permeation process for alcohol-water separation. *Journal of Chemical Technology and Biotechnology* 2008, 83, (9), 1275-1287.

20. Zacchi, G.; Axelsson, A., Economic-Evaluation of Preconcentration in Production of Ethanol from Dilute Sugar Solutions. *Biotechnology and Bioengineering* 1989, 34, (2), 223-233.

21. Furter, W. F., Salt effect in distillation : A technical review. *Chem. Eng. (Rugby, U. K.)* 1968, 46, (5), CE173-CE177.

22. Furter, W. F., Salt effect in distillation : A literature-review II. *Can. J. Chem. Eng.* 1977, 55, (3), 229-239.

23. Furter, W. F., Production of fuel-grade ethanol by extractive distillation employing the salt effect. *Sep. Purif. Methods* 1993, 22, (1), 1-21.

24. Furter, W. F.; Cook, R. A., Salt effect in distillation - a literature review. *Int. J. Heat Mass Transfer* 1967, 10, (1), 23-36.

25. Cook, R. A.; Furter, W. F., Extractive distillation employing a dissolved salt as separating agent. *Can. J. Chem. Eng.* 1968, 46, (2), 119-123.

26. Siklós, J.; Timár, L.; Ország, I.; Ratkovics, F., A simulation of the distillation of ethanol-water mixtures containing salts. *Hung. J. Ind. Chem.* 1982, 10, 309-316.

27. Cespedes, A. P.; Ravagnani, S. P., Modelado y simulación del proceso de destilacion extractiva salina de etanol. *Inf. Tecnol.* 1995, 6, (5), 17-20.

28. Ligero, E. L.; Ravagnani, T. M. K., Simulation of salt extractive distillation with spray dryer salt recovery for anhydrous ethanol production. *J. Chem. Eng. Jpn.* 2002, 35, (6), 557-563.

29. Ligero, E. L.; Ravagnani, T. M. K., Dehydration of ethanol with salt extractive distillation - A comparative analysis between processes with salt recovery. *Chem. Eng. Process.* 2003, 42, 543-552.

30. Lynd, L. R.; Grethlein, H. E., IHOSR/Extractive distillation for ethanol separation. *Chem. Eng. Prog.* 1984, 59-62.

31. Ravagnani, S. P.; Reis, P. R., Modelo de orden reducido aplicado a una columna de destilacion extractiva salina. *Inf. Tecnol.* 2000, 11, (2), 43-50.

32. Schmitt, D.; Vogelpohl, A., Distillation of ethanol - water solutions in the presence of potassium acetate. *Sep. Sci. Technol.* 1983, 18, (6), 547-554.

33. Torres, J. L.; Grethlein, H. E.; Lynd, L. R., Computer simulation of the Dartmouth process for separation of dilute ethanol water mixtures. *Appl. Biochem. Biotechnol.* 1989, 20-1, 621-633.

34. Barba, D.; Brandani, V.; Digiacomo, G., Hyperazeotropic ethanol salted-out by extractive distillation - theoretical evaluation and experimental check. *Chem. Eng. Sci.* 1985, 40, (12), 2287-2292.

35. Llano-Restrepo, M.; Aguilar-Arias, J., Modeling and simulation of saline extractive distillation columns for the production of absolute ethanol. *Comput. Chem. Eng.* 2003, 27, (4), 527-549.

36. Pinto, R. T. P.; Wolf-Maciel, M. R.; Lintomen, L., Saline extractive distillation process for ethanol purification. *Comput. Chem. Eng.* 2000, 24, (2-7), 1689-1694.

37. Sata, T., *Ion Exchange Membranes: Preparation, Characterization, Modification and Application*. Royal Society of Chemistry: Cambridge, 2004.

38. Strathmann, H., *Ion-Exchange Membrane Separation Processes*. First ed.; Elsevier: Amsterdam, The Netherlands, 2004.

39. Masters, K., *Spray Drying Handbook*. Fourth ed.; George Godwin: London, 1985.

40. Oakley, D. E., Spray dryer modeling in theory and practice. *Drying Technol.* 2004, 22, (6), 1371-1402.

41. Hussain, M. A. M.; Anthony, J. L.; Pfromm, P. H., Reducing the energy demand of corn-based fuel ethanol through salt extractive distillation enabled by electrodialysis. *AIChE Journal* 2011, doi:10.1002/aic.12577.

42. Hussain, M. A. M.; Pfromm, P. H., Reducing the energy demand of cellulosic ethanol through salt extractive distillation enabled by electrodialysis. *Separation Science and Technology (In review)* 2011.

43. Strathmann, H., Electrodialysis, a mature technology with a multitude of new applications. *Desalination* 2010, 264, (3), 268-288.

44. Casas, S.; Bonet, N.; Aladjem, C.; Cortina, J. L.; Larrotcha, E.; Cremades, L. V., Modelling Sodium Chloride Concentration from Seawater Reverse Osmosis Brine by Electrodialysis: Preliminary Results. *Solvent Extraction and Ion Exchange* 2011, 29, (3), 488-508.

45. Kobuchi, Y.; Terada, Y.; Tani, Y. In *The first salt plant in the middle east using electrodialysis and ion exchange membranes*, Sixth International Symposium on Salt, Toronto, Canada, 1983; Toronto, Canada, 1983; pp 541-555.

46. Moresi, M.; Fidaleo, M., Optimal strategy to model the electrodialytic recovery of a strong electrolyte. *Journal of Membrane Science* 2005, 260, (1-2), 90-111.

47. Schoeman, J. J.; vanStaden, J. F., Electro-osmotic pumping of sodium chloride solutions. *Journal of Membrane Science* 1997, 132, (1), 1-21.

48. Shkirskaya, S. A.; Protasov, K. V.; Berezina, N. P.; Zabolotskii, V. I., Composite Sulfonated Cation-Exchange Membranes Modified with Polyaniline and Applied to Salt Solution Concentration by Electrodialysis. *Russian Journal of Electrochemistry* 2010, 46, (10), 1131-1140.

49. Sreenivasarao, K.; Patsiogiannis, F.; Hryn, J. N. In *Concentration and precipitation of NaCl and KCl from salt cake leach solutions by electrodialysis*, Light metals, Warrendale, PA, 1997; Warrendale, PA, 1997; pp 1153-1158.

50. Tanaka, Y., Regularity in ion-exchange membrane characteristics and concentration of sea water. *Journal of Membrane Science* 1999, 163, (2), 277-287.

51. Tanaka, Y., Ion-Exchange Membrane Electrodialysis for Saline Water Desalination and Its Application to Seawater Concentration. *Industrial & Engineering Chemistry Research* 2011, 50, (12), 7494-7503.

52. Tanaka, Y.; Ehara, R.; Itoi, S.; Goto, T., Ion-exchange membrane electrodialytic salt production using brine discharged from a reverse osmosis seawater desalination plant. *Journal of Membrane Science* 2003, 222, (1-2), 71-86.

53. Yamane, R.; Ichikawa, M.; Mizutani, Y.; Onoue, Y., Concentrated Brine Production from Sea Water by Electrodialysis Using Ion Exchange Membranes. *Industrial & Engineering Chemistry Process Design and Development* 1969, 8, (2), 159-&.

54. Zabolotskii, V. I.; Protasov, K. V.; Sharafan, M. V., Sodium chloride concentration by electrodialysis with hybrid organic-inorganic ion-exchange membranes: An investigation of the process. *Russian Journal of Electrochemistry* 2010, 46, (9), 979-986.

55. Audinos, R., Optimization of Solution Concentration by Electrodialysis - Application to Zinc-Sulfate Solutions. *Chemical Engineering Science* 1983, 38, (3), 431-439.

56. Audinos, R.; Paci, S., Water Transport during the Concentration of Waste Zinc-Sulfate Solutions by Electrodialysis. *Desalination* 1987, 67, 523-545.

57. Boniardi, N.; Rota, R.; Nano, G.; Mazza, B., Analysis of the sodium lactate concentration process by electrodialysis. *Separations Technology* 1996, 6, (1), 43-54.

58. Cheryan, M.; Chukwu, U. N., Electrodialysis of acetate fermentation broths. *Applied Biochemistry and Biotechnology* 1999, 77-9, 485-499.

59. de Groot, M. T.; Bos, A. A. C. M.; Lazaro, A. P.; de Rooij, R. M.; Bargeman, G., Electrodialysis for the concentration of ethanolamine salts. *Journal of Membrane Science* 2011, 371, (1-2), 75-83.

60. Fidaleo, M.; Moresi, M., Modelling the electrodialytic recovery of sodium lactate. *Biotechnology and Applied Biochemistry* 2004, 40, 123-131.

61. Fidaleo, M.; Moresi, M., Modeling of sodium acetate recovery from aqueous solutions by electrodialysis. *Biotechnology and Bioengineering* 2005, 91, (5), 556-568.

62. Fidaleo, M.; Moresi, M., Assessment of the main engineering parameters controlling the electrodialytic recovery of sodium propionate from aqueous solutions. *Journal of Food Engineering* 2006, 76, (2), 218-231.

63. Moresi, M.; Fidaleo, M., Application of the Nernst-Planck approach to model the electrodialytic recovery of disodium itaconate. *Journal of Membrane Science* 2010, 349, (1-2), 393-404.

64. Rockstraw, D. A.; Scamehorn, J. F.; Orear, E. A., An Integrated Electrodialysis Evaporation Process for the Treatment of Aqueous Process Streams Containing Electrolytes. *Journal of Membrane Science* 1990, 52, (1), 43-56.

65. Thampy, S. K.; Narayanan, P. K.; Chauhan, D. K.; Trivedi, J. J.; Indusekhar, V. K.; Ramasamy, T.; Prasad, B. G. S.; Rao, J. R., Concentration of Sodium-Sulfate from Pickle Liquor of Tannery Effluent by Electrodialysis. *Separation Science and Technology* 1995, 30, (19), 3715-3722.

66. Hakushi, T.; Azumi, T.; Takashima, S., Studies on ion exchange membranes (VI). Measurement of the dynamic transport of ion-exchange membranes by the electrodialytic concentration method. *Himeji Kogyo Daigaku Kenkyu Hokoku* 1965, 18, 69-75.

67. Grebenyuk, V. D.; Penkalo, I. I.; Fedorova, I. A., Effect of certain factors on the process of extreme concentration of salts during electrodialysis. *Khimiya i Tekhnologiya Vody* 1984, 6, (5), 399-401.

68. Andres, L. J.; Riera, F. A.; Alvarez, R., Recovery and concentration by electrodialysis of tartaric acid from fruit juice industries waste waters. *Journal of Chemical Technology and Biotechnology* 1997, 70, (3), 247-252.

69. Aziz, N.; Rohman, F. S.; Othman, M. R., Modeling of batch electrodialysis for hydrochloric acid recovery. *Chemical Engineering Journal* 2010, 162, (2), 466-479.

70. Habe, H.; Shimada, Y.; Fukuoka, T.; Kitamoto, D.; Itagaki, M.; Watanabe, K.; Yanagishita, H.; Sakaki, K., Two-stage electrodialytic concentration of glyceric acid from fermentation broth. *Journal of Bioscience and Bioengineering* 2010, 110, (6), 690-695.

71. Luo, G. S.; Pan, S.; Liu, J. G., Use of the electrodialysis process to concentrate a formic acid solution. *Desalination* 2002, 150, (3), 227-234.

72. Bobrinskaya, G. A.; Lebedinskaya, G. A.; Tolov, Y. A., Electrolytic desalting of water after lime coagulation purification. *Khimiya i Tekhnologiya Vody* 1981, 3, (4), 349-351.

73. Hakushi, T.; Dohno, R.; Azumi, T.; Takashima, S., Studies on ion exchange membranes. XXIII. The electrodialytic concentration of various chloride solutions using ion exchange membranes. *Himeji Kogyo Daigaku Kenkyu Hokoku* 1973, 26, 75-79.

74. Hirayama, K.; Hanada, F.; Sata, T.; Mizutani, Y. In *Analysis of Properties of Advanced Ion-Exchange Membranes: Neosepta CIMS and ACS-2*, Seventh Symposium on Salt, 1993; 1993; pp 53-58.

75. Nishiwaki, T., Concentration of Electrolytes with an Electromembrane Process Prior to Evaporation. In *Industrial Processing with Membranes*, Lacey, R. E.; Loeb, S., Eds. Wiley: New York, 1972.

76. Smagin, V. N.; Chukhin, V. A.; Kharchuck, V. A., Technological Account of Electrodialysis Apparatus for Concentration. *Desalination* 1983, 46, (May), 283-290.

77. Garrido, J., Transport coefficients in desalting processes by electrodialysis. *Desalination* 2011, 265, (1-3), 274-278.

78. Hwang, S. T., Nonequilibrium thermodynamics of membrane transport. *Aiche Journal* 2004, 50, (4), 862-870.

79. Kedem, O., The role of volume flow in electrodialysis. *Journal of Membrane Science* 2002, 206, (1-2), 333-340.

80. Tanaka, Y., Irreversible thermodynamics and overall mass transport in ion-exchange membrane electrodialysis. *Journal of Membrane Science* 2006, 281, (1-2), 517-531.

81. Zabolotskii, V. I.; Shudrenko, A. A.; Gnusin, N. P., Transport characteristics of ion-exchange membranes during concentration of electrolytes by electrodialysis. *Elektrokhimiya* 1988, 24, (6), 744-750.

82. Demin, A. V.; Zabolotskii, V. I., Model verification of limiting concentration by electrodialysis of an electrolyte solution. *Russian Journal of Electrochemistry* 2008, 44, (9), 1058-1064.

83. Moresi, M.; Fidaleo, M., Electrodialytic desalting of model concentrated NaCl brines as such or enriched with a non-electrolyte osmotic component. *Journal of Membrane Science* 2011, 367, (1-2), 220-232.

84. Berezina, N.; Gnusin, N.; Dyomina, O.; Timofeyev, S., Water Electrotransport in Membrane Systems - Experiment and Model Description. *Journal of Membrane Science* 1994, 86, (3), 207-229.

85. Berezina, N. P.; Kononenko, N. A.; Dyomina, O. A.; Gnusin, N. P., Characterization of ion-exchange membrane materials: Properties vs structure. *Advances in Colloid and Interface Science* 2008, 139, (1-2), 3-28.

86. Breslau, B. R.; Miller, I. F., A Hydrodynamic Model for Electroosmosis. *Industrial & Engineering Chemistry Fundamentals* 1971, 10, (4), 554-&.

87. Lakshminarayaniah, N., *Transport Phenomena in Membranes*. Academic Press: New York, 1969.

88. Okada, T., Theory for water management in membranes for polymer electrolyte fuel cells - Part 1. The effect of impurity ions at the anode side on the membrane performances. *Journal of Electroanalytical Chemistry* 1999, 465, (1), 1-17.

89. Okada, T.; Xie, G.; Gorseth, O.; Kjelstrup, S.; Nakamura, N.; Arimura, T., Ion and water transport characteristics of Nafion membranes as electrolytes. *Electrochimica Acta* 1998, 43, (24), 3741-3747.

Chapter 5 - Conclusions and recommendations

5.1 Conclusions

One of the main challenges when a biochemical conversion route is employed to produce bioethanol is the dilute nature of the fermentation broth. Recovering ethanol from fermentation broth and purifying to fuel grade is difficult and energy intensive because of the dilute nature of the fermentation broth and the challenging water-ethanol vapor liquid equilibrium (VLE) with an azeotrope at about 96 wt% ethanol. Significant energy savings could be realized when salt extractive distillation is used to recover ethanol from the fermentation broth and directly purify to fuel grade. However, recovery of the salt used in the salt extractive distillation is highly energy intensive when the most widely investigated techniques of evaporative salt concentration/crystallization and solids drying are used. In this study, a novel combination of electrodialysis and spray drying was investigated for reducing the salt recovery energy demand.

Conceptual integration of the salt extractive distillation enabled by electrodialysis in the fermentation broth-water separation trains of corn-ethanol and cellulosic ethanol facilities was investigated towards reducing the separation energy demand. Process simulation and economic analysis was carried out with Aspen Plus® 2006.5 and Aspen Icarus Process Evaluator® 2006.5, respectively.

5.1.1 Initial conceptual process design

In case of corn-ethanol there is already a large amount of installed capital. So, the focus of the conceptual process design was on retrofitting salt extractive distillation enabled by electrodialysis in the fermentation broth-ethanol separation train of a contemporary corn-ethanol facility. In a contemporary corn-ethanol facility, recovery of ethanol from the fermentation broth and further purification to fuel grade is achieved by three distillation columns (beer column, rectifier, and side stripper) and final water removal by molecular sieve based adsorption. Purification of the beer column distillate to near azeotropic composition in a rectifier, and final water removal in the molecular sieve units is considered as the base case. In the salt extractive process, the concentration of calcium chloride in the reflux to the salt extractive distillation column was identified as the main parameter, and it was optimized to achieve the minimal overall energy demand of salt extractive distillation and salt recovery. Retrofitted salt extractive

distillation resulted in an energy demand reduction of 28.5% for producing fuel ethanol from an assumed beer column distillate, when the state of the art rectification/adsorption process (base case) is compared to the salt extractive rectification with salt recovery

In case of cellulosic ethanol, completely new process designs for salt extractive distillation were considered since the production technology for cellulosic ethanol is only in the developmental stages. Two conceptual process designs implementing salt extractive distillation together with heat integrated distillation techniques of double-effect distillation and direct vapor recompression were investigated as possible alternatives to a base case comprising conventional distillation and molecular sieve based adsorption for recovering and purifying ethanol from the fermentation broth of a cellulosic ethanol facility. Further, a systematic process simulation procedure was used to optimize the process conditions for salt extractive distillation, with salt recovery enabled by electrodialysis and spray drying. Both the design alternatives, salt extractive process with double-effect beer columns, and salt extractive process with direct vapor recompression for beer column, showed significant energy demand reduction. Salt extractive process with direct vapor recompression for beer column showed the highest energy demand reduction of 23.1% when compared to the base case.

5.1.2 Electrodialysis experiments

Concentration of calcium chloride through electrodialysis was experimentally studied to determine the fundamental transport properties of an ion exchange membrane pair comprising commercially available ion exchange membranes (NEOSEPTA CMX and AMX).– solute and osmotic permeabilities, current efficiency, and water transport number. Solute and osmotic permeabilities, and current efficiency remained essentially constant in the range of initial diluate concentrations and current densities studied. Water transport number decreased with the increase in the concentration of the diluate, and approached a limiting value due to the restriction of free water molecules dragged by the hydrated ions through the ion exchange membrane pair. The maximum calcium chloride concentration achievable in the concentrate is 34.6 wt%, which is mainly limited by the water transport number.

5.1.3 Economic Analysis

The experimentally derived parameters for electrodialysis to concentrate calcium chloride were incorporated in the initial conceptual process designs to carry out the final economic analysis.

In case of corn-ethanol, retrofitted salt extractive distillation resulted in an energy demand reduction of about 20% for producing fuel ethanol from the beer column distillate when the state of the art rectification/adsorption process (base case) is compared to the salt extractive distillation with salt recovery enabled by electrodialysis. A thermal energy savings potential of $5.2*10^{13}$ J (as natural gas HHV) per year with a total annual cost savings potential on the order of MM$0.5 per year can be estimated for producing 151.4 ML of fuel ethanol (99.5 wt%) per year.

In case of cellulosic ethanol, salt extractive distillation with direct vapor recompression provided the highest energy savings of about 22% when compared with the base case comprising conventional distillation and molecular sieve based adsorption for recovering and purifying ethanol from the fermentation broth. A thermal energy savings potential of $5.4*10^{14}$ J (as natural gas HHV) per year with a total annual cost savings potential on the order of MM$2.4 per year can be estimated for producing 270 ML of fuel ethanol (99. 5 wt%) per year.

When salt extractive distillation enabled by electrodialysis is implemented in the fermentation broth-ethanol separation trains of the corn and cellulosic ethanol facilities, an overall maximum energy savings potential of $1.5*10^{17}$ J or about 0.14 Quad (as natural gas HHV) per year could be realized for the targeted 56.8 GL of corn-ethanol and 60.6 GL of cellulosic ethanol to be produced in the U.S in 2022.

5.2 Recommendations

5.2.1 Process design

In this study, recovering ethanol from the fermentation broth and purifying to fuel grade is only considered for reducing the energy demand, not the overall bioethanol production process. Recovering ethanol from the fermentation broth and purifying to fuel grade represents a significant portion of the overall energy demand of the bioethanol production process. Since the salt extractive distillation process showed significant energy savings, the next step would be to investigate the impact of the integration of the salt extractive distillation process on the several processing steps involved in the overall bioethanol production. The fermentation broth-ethanol

separation train is typically interconnected with other units in the bioethanol plant, such as fermenters and stillage processing units, through heat integration and recycle streams. Hence, further opportunities for energy demand reduction through heat integration can be investigated. When co-locating corn-ethanol and cellulosic ethanol facilities, salt extractive process enabled by electrodialysis can be investigated to integrate the fermentation broth-ethanol separation trains of both facilities towards reducing the overall energy demand.

One of the main issues that has to be addressed before implementing salt extractive distillation is the corrosion due to salt solutions. Special construction material such as stainless steel or a more corrosion-resistant material may be necessary or increased corrosion rates may have to be considered in the distillation column design.[1, 2] Other general issues of salt extractive distillation related to solids handling, feeding and dissolving salt in the reflux stream, potential decrease in plate efficiency, and foaming inside the column[3-5] should also be considered.

5.2.2 Electrodialysis

When electrodialysis is used to concentrate salt solutions, the maximum achievable salt concentration in the concentrate is mainly determined by the water transport number. Besides increasing the concentration of the diluate to decrease the water transport number, the ion exchange membranes with reduced water content can be used to achieve lower water transport numbers.[6] Reducing the water capacity of the ion exchange membranes through chemical modification could achieve this goal.[7-9] Hence, modified ion exchange membranes with low water content could be explored to concentrate calcium chloride towards application in salt extractive distillation of bioethanol.

5.2.3 Literature Cited

1. Barba, D.; Brandani, V.; Digiacomo, G., Hyperazeotropic ethanol salted-out by extractive distillation - theoretical evaluation and experimental check. *Chem. Eng. Sci.* 1985, 40, (12), 2287-2292.

2. Seader, J. D.; Henley, E. J., *Separation Process Principles*. Second ed.; Wiley: New York, 2006.

3. Cook, R. A.; Furter, W. F., Extractive distillation employing a dissolved salt as separating agent. *Can. J. Chem. Eng.* 1968, 46, (2), 119-123.

4. Furter, W. F., Salt effect in distillation : A technical review. *Chem. Eng. (Rugby, U. K.)* 1968, 46, (5), CE173-CE177.

5. Furter, W. F., Production of fuel-grade ethanol by extractive distillation employing the salt effect. *Sep. Purif. Methods* 1993, 22, (1), 1-21.

6. Larchet, C.; Auclair, B.; Nikonenko, V., Approximate evaluation of water transport number in ion-exchange membranes. *Electrochimica Acta* 2004, 49, (11), 1711-1717.

7. Shkirskaya, S. A.; Protasov, K. V.; Berezina, N. P.; Zabolotskii, V. I., Composite Sulfonated Cation-Exchange Membranes Modified with Polyaniline and Applied to Salt Solution Concentration by Electrodialysis. *Russian Journal of Electrochemistry* 2010, 46, (10), 1131-1140.

8. Zabolotskii, V. I.; Protasov, K. V.; Sharafan, M. V., Sodium chloride concentration by electrodialysis with hybrid organic-inorganic ion-exchange membranes: An investigation of the process. *Russian Journal of Electrochemistry* 2010, 46, (9), 979-986.

9. Kotov, V. V.; Peregonchaya, O. V.; Selemenev, V. F., Electrodialysis of binary electrolyte mixtures with membranes modified by organic species. *Russian Journal of Electrochemistry* 2002, 38, (8), 927-929.

Appendix A - Economic analysis

Aspen Icarus Process Evaluator[®] 2006.5 was used to estimate all process equipment cost except for molecular sieve units and the electrodialyzer. In this study, the costs (US$ basis) were updated using CEPCI – Chemical Engineering Plant Cost Index, and are reported on 2011 first quarter basis.[d] Molecular sieve equipment cost was estimated using the scaling and installation factors taken from Aden et al.,[1] while the electrodialyzer equipment cost was estimated using the following equations:

$C_{EDZ} = C_P + C_S$	Equation A-1
$C_P = 1.5 \; x \, C_S$	Equation A-2
$C_S = 1.5 \; x \, (2M_A) \, x \, C_M$	Equation A-3
$M_A = \dfrac{ZFn_s}{\eta i_{cd}}$	Equation A-4

where C_{EDZ} is the electrodialyzer installed equipment cost, C_P and C_S are the peripheral and stack costs, respectively, M_A is the overall membrane area required for each ion exchange membrane type (m^2), Z is the ion valence (*equivalent/mol*), F is the Faraday constant (96485 *As/equivalent*), n_s is the salt removal rate (*mol/s*), η is the electrical current efficiency and i_{cd} is the operating current density (A/m^2). The following values were used:

$C_M = \$100/m^2$

$\eta = 0.9$

$i_{cd} = 300 \; A/m^2$

To calculate the annual operating costs (C_O), a plant operation time of 8400 *h/year*,[d] and the following utility costs were used: steam – \$17.08/*ton*, cooling water – \$0.07/*ton*, process water – \$0.53/*ton*, electricity – \$0.07/*kWh*, and natural gas – \$5.7/*GJ* (\$6/*MM Btu*).[2,3]

The total annualized cost (*TAC*) was calculated using the following equations:

$TAC = C_O + ACCR \; x \, TIC$	Equation A-5
$ACCR = \dfrac{i(1+i)^n}{(1+i)^n - 1}$	Equation A-6

---

[d] For corn-ethanol (chapter 2), the following values were used: cost – 2010 second quarter basis, plant operation time – 7920 *h/year*.

where *ACCR* is the annual capital charge ratio, *TIC* is the total installed equipment cost, *i* is the interest rate, and *n* is the plant life (years). The following values were used:

$i = 0.1$

$n = 10$ years (general plant life)

$n = 5$ years (for membrane replacement cost)

Finally, the total annual cost savings (*TACS*) was calculated using the following equation:

$$TACS = TAC_{Case-I} - TAC_{Case-II/III}$$

<div align="right">Equation A-7</div>

A.1 Literature Cited

1. Aden, A.; Ruth, M.; Ibsen, K.; Jechura, J.; Neeves, K.; Sheehan, J.; Wallace, B.; Montague, L.; Slayton, A.; Lukas, J. *Lignocellulosic Biomass to Ethanol Process Design and Economics Utilizing Co-current Dilute Acid Prehydrolysis and Enzymatic Hydrolysis for Corn Stover.NREL/TP-510-32438*; NREL: 2002.

2. Kwiatkowski, J. R.; McAloon, A. J.; Taylor, F.; Johnston, D. B., Modeling the process and costs of fuel ethanol production by the corn dry-grind process. *Ind. Crops Prod.* 2006, 23, (3), 288-296.

3. Peters, M. S.; Timmerhaus, K. D.; West, R. E., *Plant design and economics for chemical engineers*. 5th ed.; McGraw Hill: New York, 2003.

Appendix B - Experimental plots for electrodialytic concentration of calcium chloride

The following figures are referenced in Chapter 4 – Electrodialytic concentration of $CaCl_2$ through electrodialysis to enable salt extractive distillation of bioethanol.
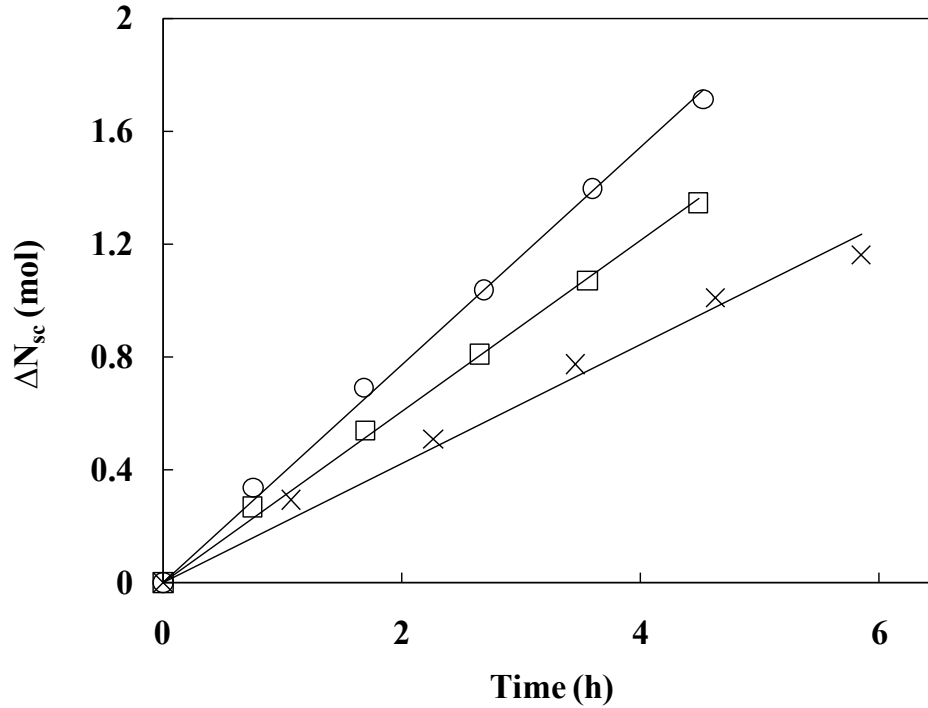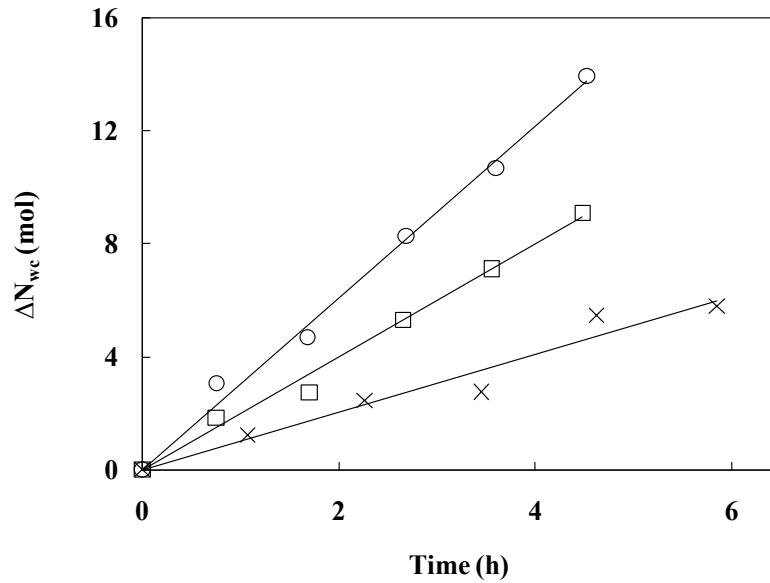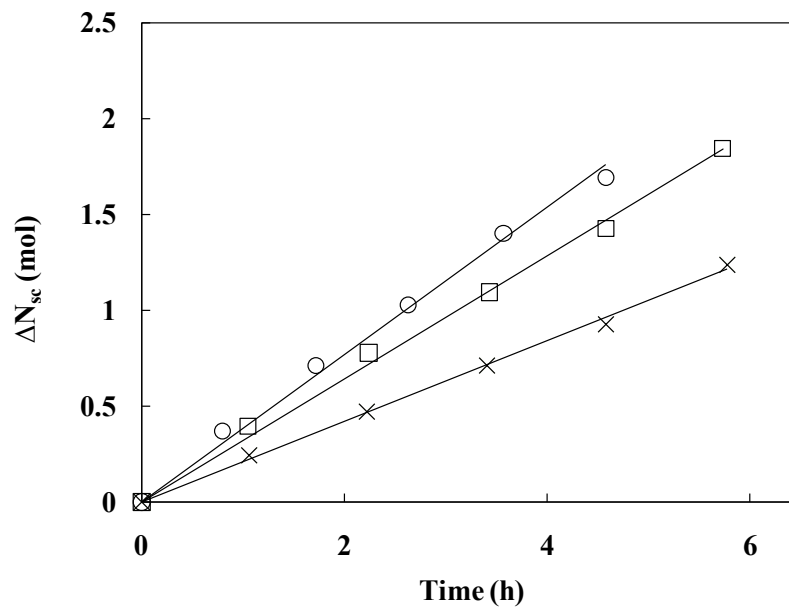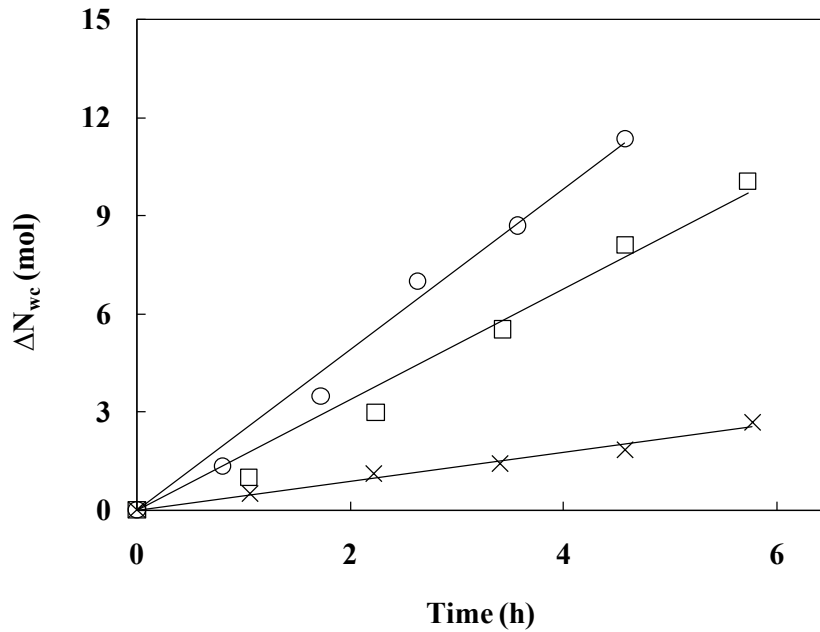

Figure B-1. Net increase in the mass of $CaCl_2$ in the concentrate with time for an initial $CaCl_2$ concentration in the diluate, $C_{sdi} \approx 1.7$ mol/kg at different current densities (i); ×∘: i = 250 A/m^2; □: i = 375 A/m^2; ∘: i = 500 A/m^2.

Figure B-2. Net increase in the mass of water in the concentrate with time for an initial $CaCl_2$ concentration in the diluate, $C_{sdi} \approx 1.7$ mol/kg at different current densities (i); $\times \circ$: i = 250 A/m^2; $\square$: i = 375 A/m^2; $\circ$: i = 500 A/m^2.

Figure B-3. Net increase in the mass of $CaCl_2$ in the concentrate with time for an initial $CaCl_2$ concentration in the diluate, $C_{sdi} \approx 2.3$ mol/kg at different current densities (i); $\times \circ$: i = 250 A/m^2; $\square$: i = 375 A/m^2; $\circ$: i = 500 A/m^2.

Figure B-4. Net increase in the mass of water in the concentrate with time for an initial $CaCl_2$ concentration in the diluate, $C_{sdi} \approx 2.3$ mol/kg at different current densities (i); $\times\circ$: i = 250 A/m^2; $\square$: i = 375 A/m^2; $\circ$: i = 500 A/m^2.
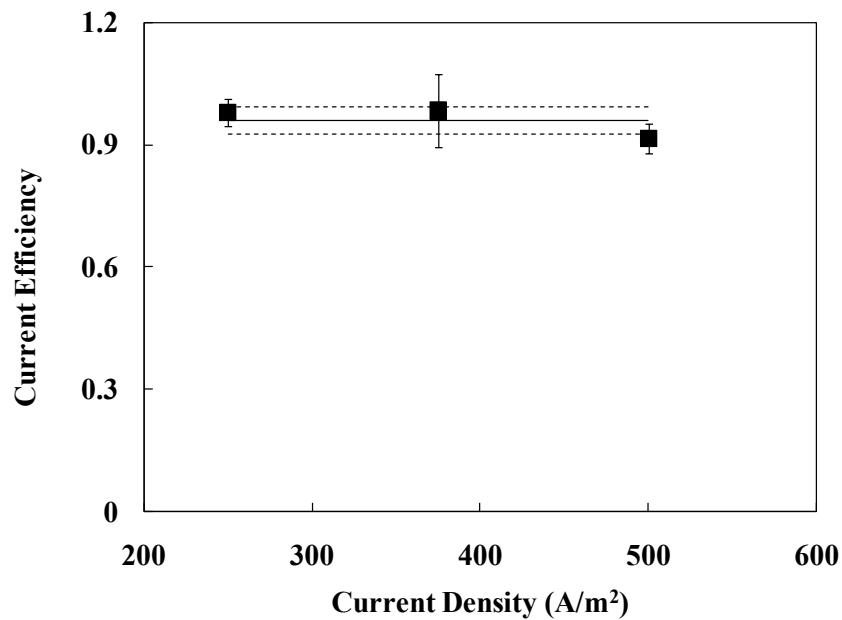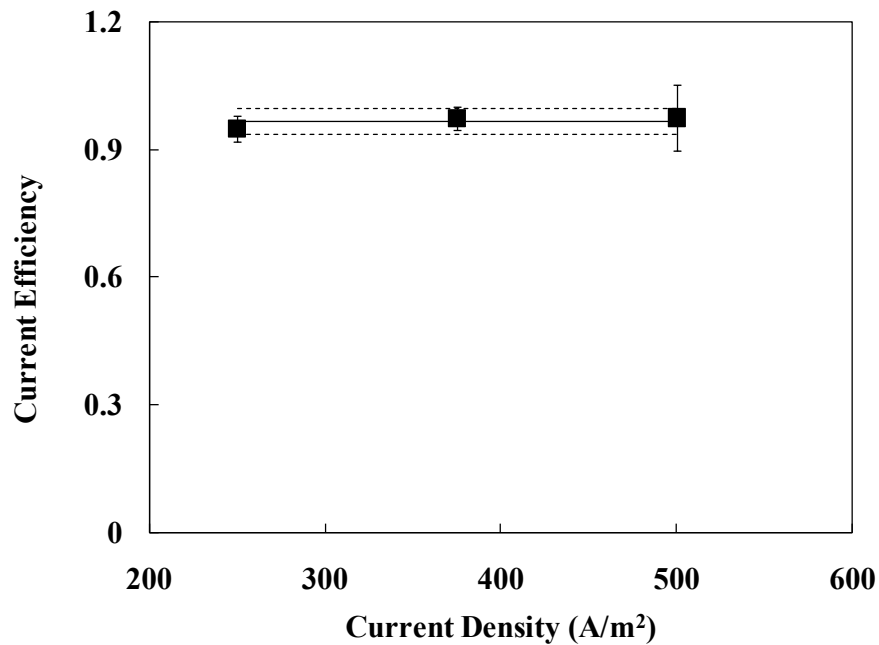

Figure B-5. Variation of the overall current efficiency (η) of the membrane pair at different current densities (initial $CaCl_2$ concentration in the diluate, $C_{sdi} \approx 1.1$ mol/kg); solid line: average; dotted lines: upper and lower limits of the 95% confidence interval.
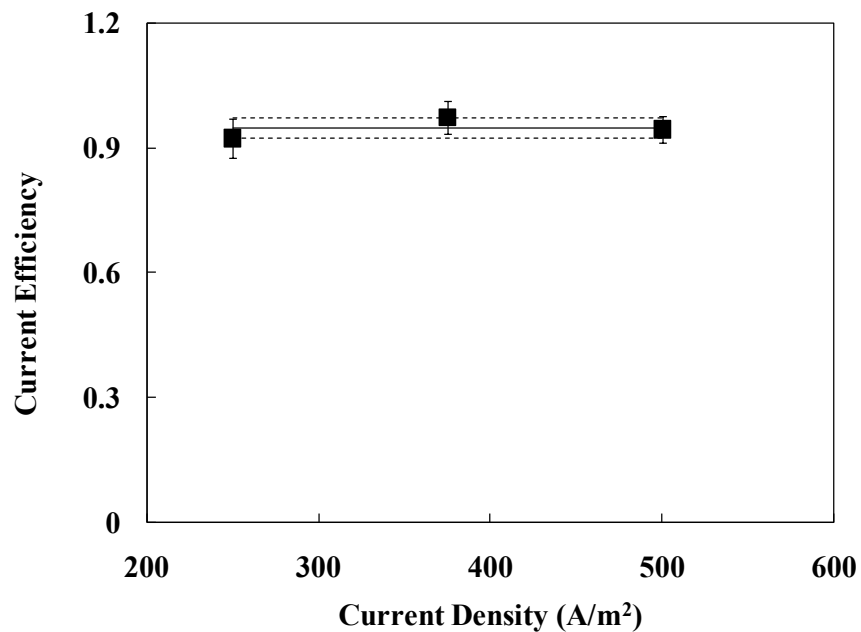
Figure B-6. Variation of the overall current efficiency (η) of the membrane pair at different current densities (initial $CaCl_2$ concentration in the diluate, $C_{sdi} \approx 1.7$ mol/kg); solid line: average; dotted lines: upper and lower limits of the 95% confidence interval.

Figure B-7. Variation of the overall current efficiency (η) of the membrane pair at different current densities (initial $CaCl_2$ concentration in the diluate, $C_{sdi} \approx 2.3$ mol/kg); solid line: average; dotted lines: upper and lower limits of the 95% confidence interval.
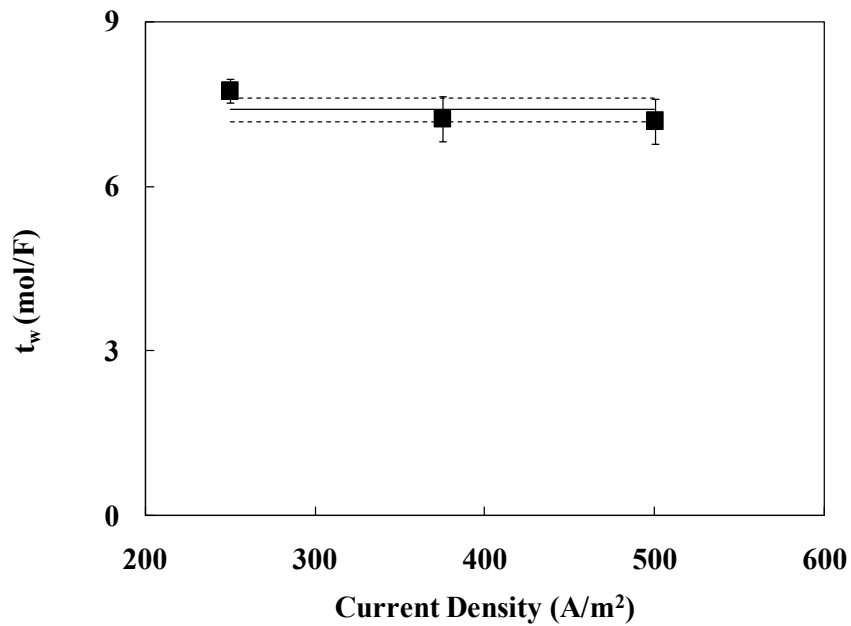
113

Figure B-8. Variation of the overall water transport number (t_w) of the membrane pair at different current densities (initial $CaCl_2$ concentration in the diluate, $C_{sdi} \approx 1.1$ mol/kg); solid line: average; dotted lines: upper and lower limits of the 95% confidence interval.
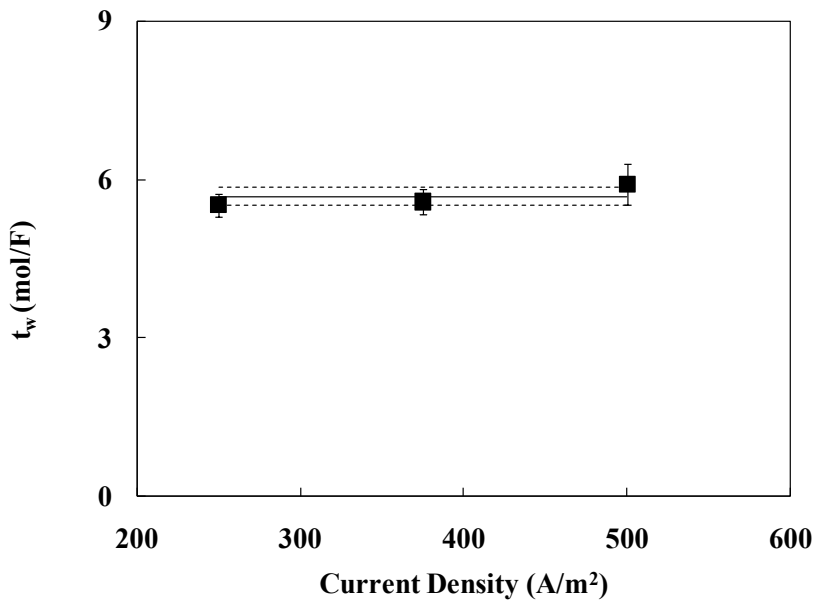

Figure B-9. Variation of the overall water transport number (t_w) of the membrane pair at different current densities (initial $CaCl_2$ concentration in the diluate, $C_{sdi} \approx 1.7$ mol/kg); solid line: average; dotted lines: upper and lower limits of the 95% confidence interval.

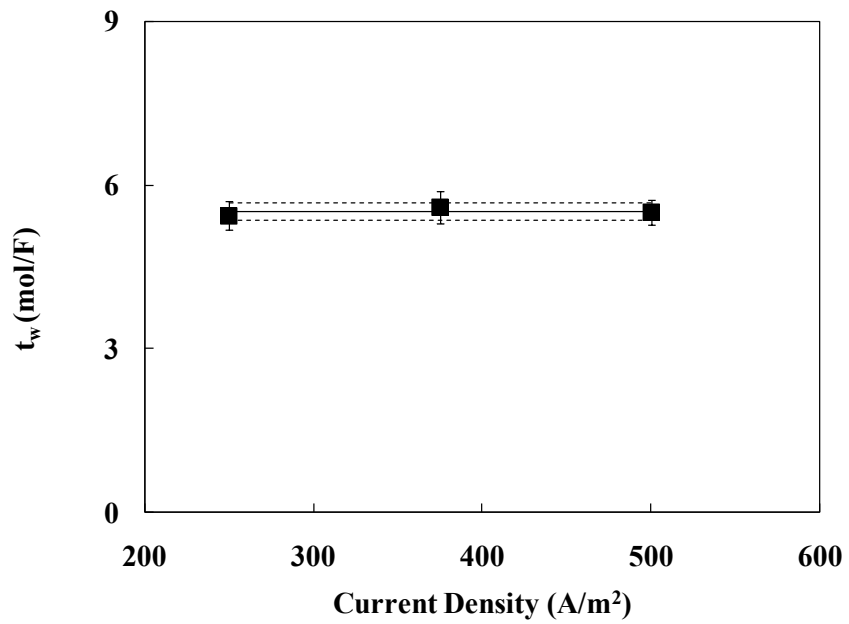Figure B-10. Variation of the overall water transport number (t_w) of the membrane pair at different current densities (initial $CaCl_2$ concentration in the diluate, $C_{sdi} \approx 2.3$ mol/kg); solid line: average; dotted lines: upper and lower limits of the 95% confidence interval.